Design and Testing of Fiber Reinforced Self Compacting Concrete

AHMED ALYOUSIF

Submitted to the
Institute of Graduate Studies and Research
in partial fulfillment of the requirements for the Degree of

Master of Science
in
Civil Engineering

Eastern Mediterranean University
August 2010
Gazimağusa, North Cyprus

Approval of the Institute of Graduate Studies and Research

Prof. Dr. Elvan Yılmaz
Director (a)

I certify that this thesis satisfies the requirements as a thesis for the degree of Master of Science in Civil Engineering.

Asst. Prof. Dr. Mürüde Çelikağ
Chair (a), Department of Civil Engineering

We certify that we have read this thesis and that in our opinion it is fully adequate in scope and quality as a thesis for the degree of Master of Science in Civil Engineering.

Assoc. Prof. Dr. Özgür Eren
Supervisor

Examining Committee

1. Assoc. Prof. Dr. Khaled Marar

2. Assoc. Prof. Dr. Özgür Eren

3. Asst. Prof. Dr. Mustafa Ergil

ABSTRACT

Many countries are producing self-compacting concrete (SCC) that has many advantages compared to conventional concrete. To improve tensile strength of concrete and produce fiber reinforced concrete (FRC), steel fibers are added. Although FRC is being produced in N. Cyprus for a long time, SCC is a new product for the construction industry. Therefore, combination of SCC and FRC would bring many benefits.

This study was composed of three parts. The first part was based on the design of SCC and FR-SCC with locally available materials of N. Cyprus in addition to chemical additives. The second part was based on studying the effects of using different percentages of steel fibers on SCC by testing the fresh properties of SCC and FR-SCC matrix such as slump flow, J-ring L-box, V-funnel and column segregation. The third part was dealing with the comparison of hardened properties of SCC and FR-SCC mixes such as compressive strength, splitting tensile strength, flexural strength, impact energy, surface abrasion resistance, and depth of water penetration, density, absorption, voids content, chloride ion permeability and ultrasonic pulse velocity tests. The results have shown that the addition of fibers improves the compressive strength, splitting tensile strength, impact energy, and depending on the w/c ratio and admixture content better workability can be obtained for FR-SCC.

Keywords: Fiber reinforced self-compacting concrete, J-Ring, T50, Impact energy, Surface abrasion.

ÖZ

Günümüzde birçok ülkede kendinden yerleşen beton (KYB) kullanılmaktadır ve bu betonun normal betonlaragöre avantajları bulunmaktadır. Betonun gerilme dayanımını artırmak için betona çelık lifler eklenebilir. Kuzey Kıbrıs Türk Cumhuriyeti'nde lif kullanımı artmasına rağmen kendinden yerleşen betonun kullanımı henüz yaygınlaşmamıştır. Bu çalışma sayesinde çelik lifli kendinden yerleşen betonun (ÇLKYB) KKTC'de kullanımı da teşvik edilmiş olacaktır.

Bu çalışma üç kısıma ayrılmıştır. Birinci kısım; kendinden yerleşen betonun tasarımına dayanır. Kimyasal katkılara ek olarak K. Kıbrıs'taki yerel malzemelerin kullanılması esas alınarak tasarım yapılmıştır. İkinci kısımda ise KYB'da kullanılan farklı miktarlardaki çelik liflerin slump, J ring, L-box, V-funnel ve kolon segregasyonu gibi özelliklerine olan etkilerine bakılmıştır. Üçüncü kısımda ise KYB ve KYÇLB'un basınç mukavemeti, aşınma dayanımı, su basıncı altında geçirgenliği, yoğunluk, su emme, boşluk oranı, hızlı su geçirgenliği, ve ultrasonic hız deneyleri yapılmıştır.

Yapılan deney sonuçlarına göre ise çelik liflerin KYB'na eklenmesiyle betonun basınç dayanımı, çekme dayanımı, tokluk enerjisi ve yüzey aşınma dayanımı gibi pekçok özelliklerini iyileştirdiği görülmüştür. Ayrıca su/çimento oranı ve kimyasal katkı miktarı ayarlanması ile işlenebilirlik kontrol altına alınmıştır.

AnahtarKelimeler: Çelik lifli kendinden yerleşen beton, J-ring, T50, Tokluk enerjisi, Yüzey aşınması.

To my father and to my mother

To my young lady Haefa and my little princess Iman

ACKNOWLEDGMENTS

I owe my deepest gratitude to my supervisor, Assoc. Prof. Dr. Özgür Eren, whose inspiration, motivation, guidance and support from the beginning to the end of this study enabled me to develop an understanding of the subject.

I would like to thank Prof. Dr. Saad Altaan from Civil Engineering Department at Mosul University, for his help during my study.

I would like to disclose my special thanks to Asst. Prof. Dr. Mustafa Ergil and Asst. Prof. Dr. Adham Mackieh for their help throughout the statistical analysis of this study.

I am grateful to Materials of Construction Laboratory staff at EMU, Mr. Ogün Kılıç and Mr. Mevlüt Çetin for their great efforts during the experimental part of this thesis.

I am indebted to the whole department of Civil Engineering at EMU for being a home away from home and to many of my colleagues for supporting me, especially to Yousef Baalousha, Alireza Rezaei, Ahmed Zaid, Mohammad Badran, Faruk Ibišević and Alireza Bajgiran.

Lastly, it is an honor for me to thank my dear parents, my wife, my brother and my sisters for their everlasting love, support, patient and encouragement throughout my life; this dissertation is simply impossible without them.

TABLE OF CONTENTS

LIST OF TABLES

LIST OF FIGURES

LIST OF PHOTOS

LIST OF SYMBOLS

ACI	American Concrete Institute
ASTM	American Society for Testing and Materials
BS EN	British European Standards
cp	Centipoise
dB (A)	A-weighted Decibels
df	Degree of freedom
FR-SCC	Fiber Reinforced Self-Compacted Concrete
l/d	Length/diameter ratio, fiber aspect ratio
RCPT	Rapid Chloride Permeability Test
RILEM	*Reunion Internationale des Laboratoires et Experts des Materiaux, Systemes de Construction et Ouvrages* (French: International Union of Laboratories and Experts in Construction Materials, Systems, and Structures)
SCC	Self-Compacting Concrete
sd	Standard deviation
SF	Silica fume
SFRC	Steel Fiber Reinforced Concrete
UPV	Ultrasonic Pulse Velocity

Chapter 1

INTRODUCTION

1.1 General

Self-compacting concrete (SCC) was first introduced in Japan during 1980's, since then it has been the subject to numerous investigations in order to achieve the desired properties of modern concrete structures. At the same time the producers of additives have developed more and more sophisticated plasticizers and stabilizers tailor-made for the precast and the ready-mix industry (Okamura & Ouchi, 2003; Kordts & Grube, 2003).

Self-compacting concrete (SCC) is highly flowable and rheologically stabile that does not require vibration for placing and compaction. It is able to flow under its own weight, completely filling formwork and achieving full compaction, it has excellent applicability even in the presence of congested reinforcement. Such concrete should have a relatively low yield value to ensure high flow ability, a moderate viscosity to resist segregation and bleeding, and must maintain its homogeneity during transportation, placing and curing to ensure adequate structural performance and long term durability (ACI 237, 2007; Ferrara et al., 2007). The successful development of SCC must ensure a good balance between deformability and stability (Aggarwal et al., 2008).

The addition of fibers into self-compacting concrete may take advantage of extending the possibility of field application of SCC (Grünewald & Walraven, 2001). The replacement of conventional concrete totally or partially with fibers will improve the construction process. Using the reinforcement bars in the construction of concrete structures has a considerable economic impact on the cost of construction (Cunha et al., 2008). It is likely to reduce the energy consumption, better working environment, with reduced noise and health hazard (Ferrara et al., 2007), however fibers are known to significantly affect the workability of concrete (Grünewald & Walraven, 2001). Designing a proper FR-SCC is not an easy task. Several investigations were carried out in order to obtain the proportions of FR-SCC (Felekoğlu et al., 2007). In order to improve and develop the ability of SCC and FR-SCC to flow and to be able to maintain its workability within the addition of steel fibers, superplasticizer was used.

Okamura and Ouchi have reported that the coarse and fine aggregate contents can be kept constant to obtain the self-compatibility easier by adjusting the water/cement ratio and the superplasticizer dosage only (Okamura & Ouchi, 1999; Felekoğlu et al., 2007).

1.2 Statement of the Problem

Self-compacting concrete has an impact on concrete placement and construction economics. On the other hand it is known that self-compacting concrete (SCC) is a new emerging technology and it is not standardized yet. Therefore, it was necessary to develop a mix design method for proportioning the SCC with locally available materials of N. Cyprus.

1.3 Objectives of This Study

The objectives are:

1. To provide concise literature survey about the characteristics, physical and mechanical properties of self-compacting concrete and fiber reinforced self-compacting concrete.
2. To design SCC and FR-SCC with locally available materials of N. Cyprus in addition to chemical additives.
3. To provide more information about the effects of amount of steel fibers and superplasticizer on fresh properties of SCC like workability and hardened properties such as compressive strength, splitting tensile strength, flexural strength, impact energy, surface abrasion resistance, depth of water penetration as well as density, absorption, voids content, chloride ion penetration, surface abrasion resistance and ultrasonic pulse velocity tests.
4. To study the properties of fresh SCC and FR-SCC such as flowability, passingability and segregation resistance.
5. To study the properties of hardened SCC and FR-SCC such as compressive strength, splitting tensile strength, flexural strength, impact energy, depth of water penetration as well as density, absorption, voids content, chloride ion penetration, surface abrasion resistance and ultrasonic pulse velocity test.

1.4 Works Done

In order to achieve the aims and objectives explained above, the followings were done:

1. A review of available publications was undertaken to assess previous work in this field.
2. Lectures on “fiber reinforced concrete”, “cement replacement materials”, “repair and maintenance of concrete” were attended.
3. Standards such as British European Standards (BS EN) and American Society for Testing and Materials (ASTM) were used to make and perform the experiments in this investigation.
4. Experiments in order to investigate the physical and mechanical properties such as workability, compressive strength, splitting tensile strength, flexural strength, impact energy, depth of water penetration, density, absorption, voids content, chloride ion penetration, surface abrasion resistance and ultrasonic pulse velocity tests were carried out.
5. Tow apparatuses were fabricated from metal and PVC named J-ring used to check the passing ability of the SCC and FR-SCC mixes and column segregation used to check the segregation resistance of SCC and FR-SCC mixes.

1.5 Achievements

The achievements are:

1. Mix design proportioning for SCC with locally available materials of N. Cyprus and the proportioning are as following:
    - Cement: 400 kg/m^3
    - Silica fume content: 75 kg/m^3
    - Water/Powder ratio: 0.40
    - Fine/Coarse aggregates ratio: 1.12

- Superplasticizer: 1.25% of cement content

2. The mix design proportioning for FR-SCC by adjusting the amount of superplasticizer in the mixes.
3. Some physical and mechanical properties of aggregates were evaluated.
4. The effect of different amounts of steel fibers on fresh properties such as flowability, passingability, segregation resistance were obtained and evaluated.
5. The effect of different amounts of steel fibers on hardened properties such as compressive strength, splitting tensile strength, flexural strength, impact energy, surface abrasion resistance, depth of water penetration, density, absorption, voids content, chloride ion penetration, surface abrasion resistance and ultrasonic pulse velocity tests were obtained and evaluated.
6. A correlation among the results were statistically studied and the followings were found:
    - There is a directly proportional linear regression relationship between compressive strength and splitting tensile Strength.
    - There is a directly proportional linear regression relationship between compressive strength and depth of water penetration.
    - There is a polynomial (2^{nd} order) regression relationship between compressive strength and ultrasonic pulse velocity.
    - There is a polynomial (2^{nd} order) regression relationship between compressive strength and absorption.
    - There is a polynomial (2^{nd} order) regression relationship between compressive strength and voids content.

- There is a directly proportional linear regression relationship between compressive strength and impact energy.
- There is an inverse linear regression relationship between compressive strength and surface abrasion resistance.
- There is a directly proportional relationship between chloride ion penetration and depth of water penetration.
- There is a directly proportional linear regression relationship between voids content and absorption.
- There is an inverse linear regression relationship between surface abrasion and impact energy.

1.6 Guide to Thesis

Chapter 2 is a literature survey on self-compacting concrete (SCC), fiber reinforced concrete (FRC) and fiber reinforced self-compacting concrete (FR-SCC).

Chapter 3 deals with experimental details as well as the properties of materials used. Methodology as characterized in mix proportions, mixing procedure, casting of specimens, curing method and test specimens are explained. Also determination of fresh and hardened concrete are explained in details.

Chapter 4 deals with results, discussions and analysis of the results.

Chapter 5 deals with conclusions and further recommendations.

References and appendices are as well attached at the back pages.

Chapter 2

LITERATURE REVIEW

2.1 Self-Compacting Concrete (SCC)

2.1.1 Definition of Self-Compacting Concrete

Self-compacting concrete (SCC) is "highly flowable, non-segregating concrete that can spread into place, fill in the formwork and encapsulate the reinforcement without any mechanical consolidation'' (ACI 237, 2007, p.2). It is made with conventional concrete materials and in order to maintain the workability in some cases a viscosity-modifying admixture (VMA) is used.

Initially, High performance concrete (HPC) name was used in Japan during the late 80's, and then the name was changed to self-compacting concrete (Ouchi, 1998) to avoid confusion with high performance concrete (HPC), which is a normal concrete based on the use of low water/cement ratio to achieve higher strength and to enhance the durability properties. Since then, SCC was born and it has been accepted worldwide (Daczko & Vachon, 2006).

Self-compacting concrete has been described with various definitions in recent years (Vachon & Daczko, 2002). Most of the definitions share the following common points (Daczko & Vachon, 2006):

- SCC is fluid enough to fill the forms without any vibration;

- SCC remains workable and homogenous during and after placement;
- SCC is able to flow through congested reinforcement, if necessary.

In the literature, SCC is known also as self-compacting concrete, self-placing concrete and self-leveling concrete (ACI 237, 2007).

2.1.2 History of SCC

The use of SCC was developed in the last two decades and has become widely accepted in the world. It was developed to enhance the durability properties of the concrete which was the main topic and the main concern at that time in Japan. Then researches started the investigation about this problem and one of their findings that were affecting the durability of concrete structures was the improper consolidation of the fresh concrete due to unskilled labor on the jobsite.

In the mid of 1980's, proposal about the concept of a high durability concrete with no consolidation to achieve full compaction was prepared. In the following years, the conception was refined and guidelines for the use of SCC were published to permit the use of local raw materials in Japanese. However it should be noted that concrete with no consolidation energy or vibration was used before in the late 70's and 80's, either to increase placing rate or to allow placing in hard to reach or highly reinforced sections (Daczko & Vachon, 2006; Collepardi, 2003).

Okamura published for the first time on SCC in 1989 at the Second East-Asia and Pacific Conference on Structural Engineering and Construction (EASEC-2) (Ozawa et al., 1989). Then many researchers worked on SCC in the first half of the 90's. As a result, many countries like Sweden, the Netherlands, Korea, Thailand, and Canada started their own researches in the mid of 90's in an effort to evaluate the potential

benefits SCC that can bring to the construction industry (Daczko & Vachon, 2006; Skarendahl, 1998; Walraven, 1998; Byun et al., 1998; Tangtermsirikul, 1998; Khayat & Aitcin, 1998). Recommendations and guidelines for the use of SCC were developed through cooperative work in Europe by the late 90's (Association Francaise de Genie Civil, 2000; BE96-3801, 1996; EFNARC, 2002).

Many large construction companies also started using this technology, not only for increasing the durability potential, but also for logistic reasons. The results showed that SCC could be used in construction in a shorter time and less post-demolding operations than conventional concrete (Daczko & Vachon, 2006).

SCC has recently been used in concrete repair applications, including the repair of bridge abutments and pier caps, tunnel sections, parking garages, and retaining walls, where it ensured adequate filling of congested areas and provided high surface quality (finishability) (Jacobs & Hunkeler, 2001; Khayat & Morin, 2002).

Since the early development of SCC in Japan, this new invention has been used in several countries in cast-in-place and precast applications (RILEM 174-SCC, 2000).

The use of SCC in world generally and in North America specially has grown enormously, particularly in the precast industry, where it has been used regularly in the production at precast plants in the United States since 2000. The majority of such concrete has been used to produce precast elements for parking garage structures and architectural panels. The estimated volume of SCC in the precast industry in the United States was 135,000 m^3 in the year 2000; it increased to 1.8 million m^3 in the year 2003 (ACI 237, 2007). In 2002, 40% of precast factories in the United States

had used SCC, and in some cases, new plants are currently being built around the idea of using SCC Technology. On the other hand, the use of SCC in the ready mixed concrete industry is still in its beginning in the United States (Vachon & Daczko, 2002).

In N. Cyprus, self-compacting property is being used for producing foam concrete (mortar) for the last 5-10 years. This foam mortar is made by using foaming agent, cement, chemical admixture and sometimes natural sand. Mainly it is applied for leveling slab on grades in order to increase thermal resistance and reduce the dead weight of the buildings. Self-compacting concrete which is made of fine and coarse aggregates, cement, and chemical admixture is not yet produced by any of the concrete production plants.

2.1.3 Advantages of SCC

Due to its very attractive properties in the fresh state as well as after hardening and long term properties, the use of self-compacting concrete (SCC) increased worldwide. However, this type of concrete needs a more advanced mix design than traditional vibrated concrete and a more careful quality assurance with more testing and checking. It will replace the manual compaction of fresh concrete with a modern semi-automatic placing technology (BE96-3801, 2000).

Properly proportioned and placed SCC can result in both economic and technological benefits for the end user. The in-place cost savings, performance enhancements, or both, are the driving forces behind the use of SCC. Specifically, SCC can provide the following benefits (ACI 237, 2007):

- Reduction in site manpower and equipment will lead to saving of purchasing and maintaining the equipment, also this will inquire less need for screeding because of the better surface finishability (self-levelling characteristic).
- Faster construction through higher rate of casting or placing;
- Improved durability and reliability of concrete structures and eliminate some of the potential for human error.
- Reduced noise level;
- Providing a safer working environment and decreasing worker injuries (Walraven, 2003);
- By using a well-proportioned SCC mixture with adequate handling and placing technique will provide smooth surfaces free of honeycombing and signs of bleeding.

2.1.4 Fresh properties of SCC

The specific fresh properties of self-compacting concrete as compared to conventional concrete are obviously connected to what can be described as the self-compactability. This property is in mechanism terms related to the rheology of fresh concrete, while in the terms of handling in practice is related to workability parameters (RILEM 174-SCC, 2000). These characteristics are further elaborated on and defined as following:

- **Rheology:** "refers to the science of deformation, and flow of matter is fundamental to understanding the flow of fresh SCC." (ACI 237, 2007, p.9).
- **Workability:** The ease, with which concrete mixes can be mixed, placed and compacted as completely as possible while using the lowest possible

water/cement ratio. Workability of SCC is defined as filling ability, passing ability, and stability (ACI 237, 2007).

- The **filling ability** is the ability of SCC to flow in the formwork by its own weight without any effort.
- The **passing ability** is the ability of the concrete to pass through narrow places with reinforcement easily only by its own weight.
- **Stability** of concrete describes the ability of a material to maintain the uniformity (ACI 237, 2007).

2.1.5 Testing Fresh SCC

Before SCC is produced and used, the mix has to be designed and tested to be sure that the mix fulfills the demands regarding among others workability, segregation and passing ability.

The main characteristics of SCC that have to be checked are:

- Filling ability;
- Passing ability;
- Segregation resistance or stability ; and
- Surface quality and finishing ability (ACI 237, 2007).

2.1.5.1 Slump Flow Test

The slump flow test is used to determine the horizontal free-flow of SCC in the absence of obstructions. The procedure is based on standards (ASTM C 1611, 2005), with an adjustment for determining the slump of conventional concrete. The test is easy to use either at the laboratory or on the site. It is a most common used test to check the filling ability of SCC. It can measure two parameters: the flow spread

which indicates the free, unrestricted deformability and the flow time T50 which indicates the rate of deformation within a defined flow distance (De Schutter, 2005). Slump flow test apparatus is detailed in Figure 1.

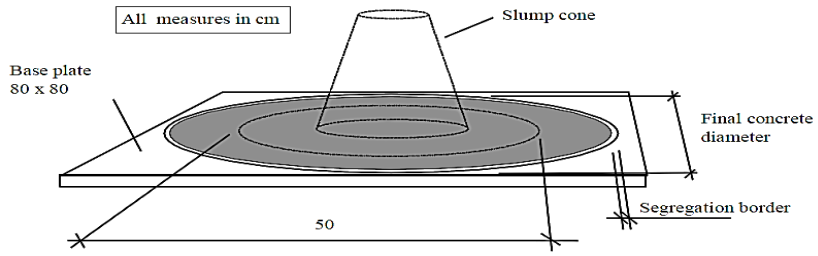

Figure 1: Slump Flow test apparatus
Source: (BE96-3801, 2000)

A common range of slump flow for SCC is 450 to 760 mm. The higher the slump flow, the further the SCC can travel under its own weight, and the faster it can fill a form or mold (ACI 237, 2007).

2.1.5.2 Visual Stability Index Test

The visual stability index (VSI) test involves the visual inspection of the SCC slump flow spread resulting from using the slump flow test. This test provides a procedure to determine the stability by evaluating the relative stability of batches of SCC mixtures (Daczko & Kurtz, 2001; ACI 237, 2007).

As defined in Table 1, a VSI rating of 0 or 1 is an indication that the SCC mixture is stable and can be appropriate for the planned use. A VSI rating of 2 or 3 indicates possible segregation potential and action must be taken by adjusting the mixture to ensure stability. This test is subjective because it is determined visually. VSI rating is perfect quality control method for producing SCC, but it should not be used for acceptance or rejection of a mix. The VSI test is suitable for SCC mixtures that have

a tendency to bleed. If not, this test is less useful in recognizing a mixture's tendency to segregate (ACI 237, 2007; ASTM C 1611, 2005).

Table 1: Visual stability index (VSI) rating of SCC mixtures

VSI value	**Criteria**
0 = highly stable	No evidence of segregation in slump flow spread
1= stable	No mortal halo of aggregate pile in the slump flow spread
2 = unstable	A slight mortar halo < 10 mm or aggregate pile or both, in the slump flow spread
3 = highly unstable	Clearly segregating by evidence of a large mortar halo >10 mm or a large aggregate pile in the center of the concrete spread, or both.

Source: (Daczko & Kurtz, 2001)

2.1.5.3 T50 Test

The rate of flow of a SCC mixture is subjective by its viscosity. This test is useful to measure viscosity of SCC in the laboratory. The procedure of this test is same as for slump flow test. The time that takes the SCC mixture to reach a diameter of 500 mm from the time the mold is first raised is known as T50 and it provides a relative measure of the unconfined flow rate of the concrete mixture (ACI 237, 2007).

"A longer T50 time indicates a mixture with a higher viscosity; the opposite is true for a shorter T50 time. A T50 time of 2 seconds or less typically characterizes a SCC with a low viscosity, and a T50 time of greater than 5 seconds is generally considered a high- viscosity SCC mixture" (ACI 237, 2007, p.25).

2.1.5.4 J-ring Test

The passing ability of self-consolidating concrete can be determined by J-Ring test. This test method is limited to concrete with nominal maximum size of aggregate of up to 25 mm (ASTM 1621, 2006).

The J-ring test aims to examine both the filling ability and the passing ability of SCC. The J-ring test is used to characterize the ability of SCC to pass through reinforcing steel (Bartos et al., 2002; Sonebi & Batros, 1999). The J-ring test can measure three factors: flow spread, flow time T50 and blocking step. The J-ring flow spread indicates the restricted deformability of SCC due to blocking effect of reinforcement bars and the flow time T50 indicates the rate of deformation within a defined flow distance. The test is easy to perform either at a concrete plant or on a job site. The higher the J-ring slump flow, the further the SCC can be transportable through a reinforcing bar under its own weight, and the faster it can fill a steel-reinforced form or mold (ACI 237, 2007). J-ring apparatus details are shown in Figure 2.

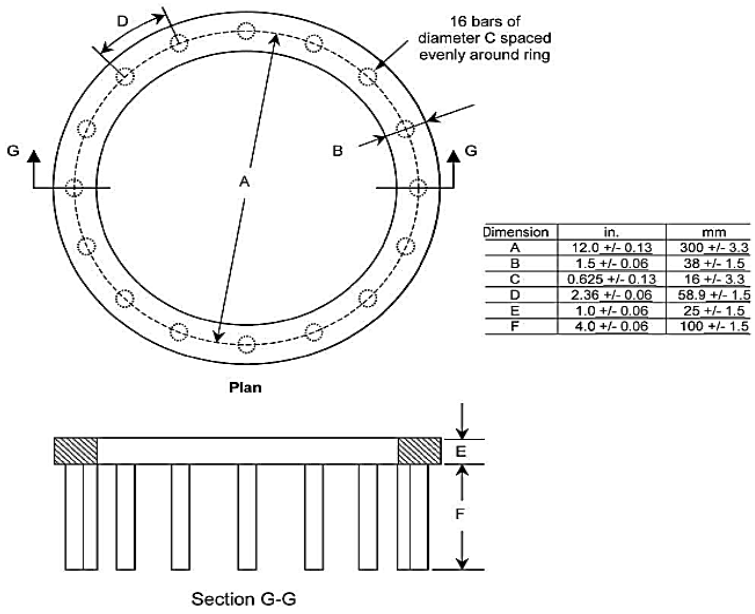

Dimension	in.	mm
A	12.0 +/- 0.13	300 +/- 3.3
B	1.5 +/- 0.06	38 +/- 1.5
C	0.625 +/- 0.13	16 +/- 3.3
D	2.36 +/- 0.06	58.9 +/- 1.5
E	1.0 +/- 0.06	25 +/- 1.5
F	4.0 +/- 0.06	100 +/- 1.5

Figure 2: J-ring apparatus details
Source: (ASTM 1621, 2006)

2.1.5.5 L-box Test

The passing ability of SCC can be investigated by this method. “It measures the reached height of fresh SCC after passing through the specified gaps of steel bars and

flowing within a certain flow distance, with this reached height, the passing or blocking behavior of SCC can be estimated" (De Schutter, 2005). The test method is suitable to be carried out in the laboratory.

The minimum ratio of the height in the horizontal section relative to the vertical section is considered to be 0.8, if the SCC flows as freely as water, it will be completely horizontal, and the ratio will be equal to 1.0,Therefore,the nearer this ratio to 1.0, the better the flow potential of the SCC mixture. This is an indication of passing ability, or the degree to which the passage of SCC through the bars is restricted. Coarse aggregate behind the reinforcing bars (blocking) and segregation at the end of the horizontal section can be detected visually. SCC mixtures with either of these characteristics should be re-proportioned to ensure stability of the mixture (ACI 237, 2007).

L-box apparatus details are shown in Figure 3.

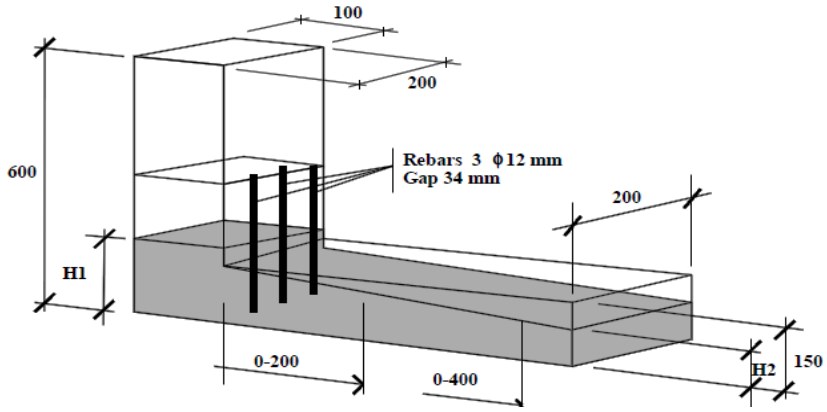

Figure 3: L-box apparatus details
All measures in (mm)
Source: (BE96-3801, 2000)

2.1.5.6 V-funnel Test

This test is used to determine the filling ability of SCC mixes and the method is limited to concrete with nominal maximum size of aggregate of up to 20 mm (Shetty, 2005).

The V-funnel flow time is the time needed for SCC to pass a narrow opening (De Schutter, 2005). It can also be used to check the resistance of the SCC mixture for segregation. V-funnel apparatus details are shown in Figure 4. Normal criteria for the test are 6 seconds to 12 seconds (De Schutter, 2005).

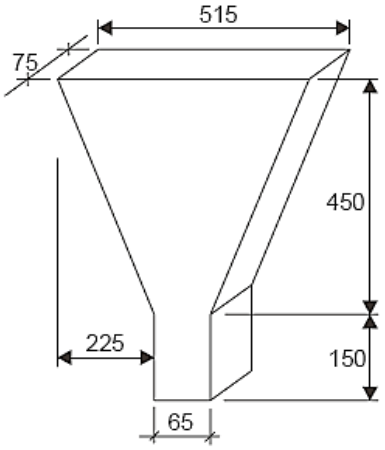

Figure 4: V-funnel apparatus details
All measures in (mm)
Source: (De Schutter, 2005)

2.1.5.7 Column Segregation Test

The static segregation of self-consolidating concrete can be determined by this method by quantifying the coarse aggregate content in the top and bottom parts of a cylindrical specimen (ASTM C 1610, 2006).

It can also measure the stability of SCC mixtures and this test method should be used to develop stable SCC mixtures and determine suitability for a particular application (ACI 237, 2007). The following equation is used to determine the probable percentage of segregation (ASTM C 1610, 2006). SCC is generally considered to be acceptable if the percentage of segregation is less than 10% (ACI 237, 2007). Figure 5 details the column segregation mold apparatus that is used to measure the

percentage of probable segregation of SCC. Figure 6 is a collector plate that is used for the test of column segregation.

The equation that is used to determine the static segregation percentage is given as:

$$S = 2\left[\frac{(CA_B - CA_T)}{(CA_B + CA_T)}\right] * 100, if\ CA_B > CA_T$$

$$S = 0, \quad if\ CA_B \leq CA_T$$

Where:

S = *static segregation in percent*

CA_T = *mass of coarse aggregate in the top section of the column*

CA_B = *mass of coarse aggregate in the bottom section of the column.*

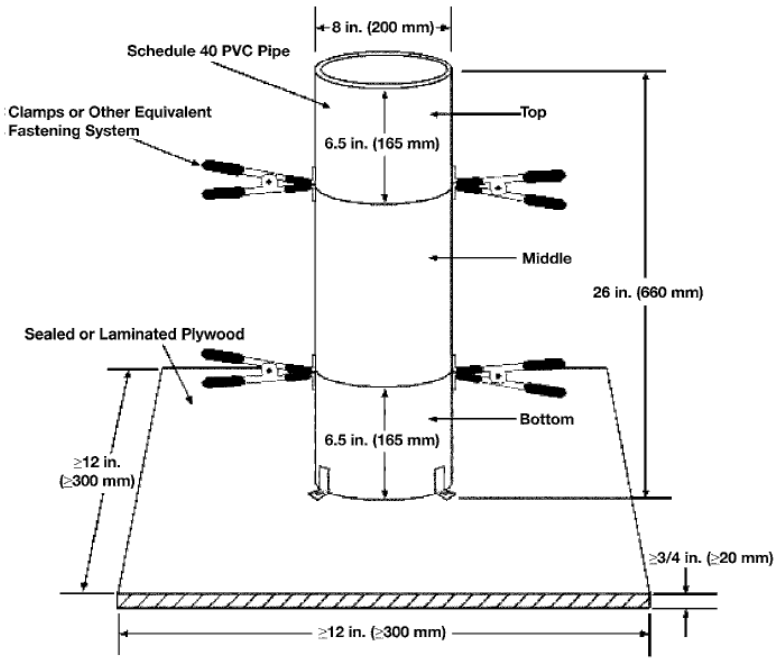

Figure 5: Column mold apparatus details
Source: (ASTM C 1610, 2006)

2.1.5.8 Other Tests

Some other test methods have been accomplished to measure the characteristics of SCC. Table 2 summarizes a list of these tests found in the literature (RILEM 174-SCC, 2000).

Table 2: Test methods to measure characteristics of SCC

Test Name	**Category**	**Characteristic**	**What test measures**
Flow cone V-shaped funnel Orimet	Confined flow	Filling ability	Flow rate
L-box	Confined flow	Passing and filling ability	Mow rate and distance
Surface settlement test	Confined flow	Resistance to segregation	Settlement of SCC surface
Rapid segregation test using penetration apparatus	Confined flow	Resistance to segregation	Segregation of aggregates
Wet sieving test	Confined flow	Resistance to segregation	Segregation of aggregates and measurement of laitance
Hardened examination	Static condition	Resistance to segregation	Distribution of coarse aggregate
Surface quality and finish evaluation	Confined flow	Surface quality and finishability	Observation of surface quality
K-slump	Confined flow	Segregation resistance	Flow rate
Rheometers: IBB Two-point test BTRHEOM BML	Rotational rheometer	Filling ability	Rheology
Slump meter	Rotational rheometer	Filling ability	Torque to turn truck mixer

Source: (ACI 237, 2007)

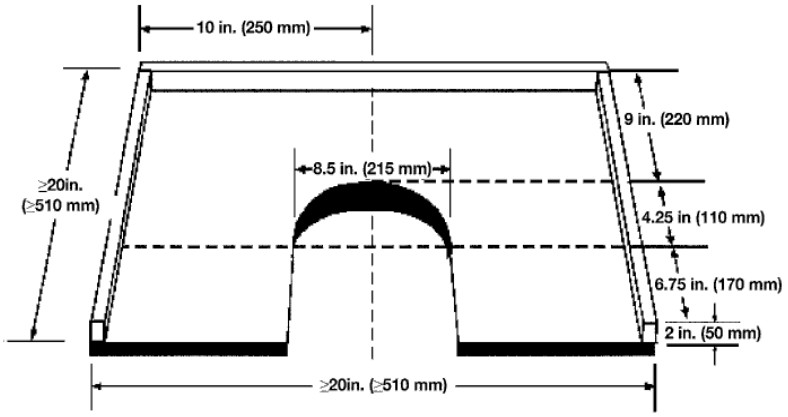

Figure 6: Detail of collector plate
Source: (ASTM C 1610, 2006)

2.1.6 Hardened Properties of SCC

2.1.6.1 Strength and Stiffness

The compressive strength of self-compacting concrete in practice is higher than the strength of normal vibrated concrete with same water/cement ratios. There is significant change in stiffness of SCC comparing with normal concrete. The relation between splitting tensile strength and compressive strength has been reported to be equal for SCC and normal concrete (RILEM 174-SCC, 2000).

The relation between strength gained from drilled cores and the one obtained from cubes has been found higher for SCC than normal concrete (RILEM 174-SCC, 2000).

For columns, the deference between the strength in the top and the strength in bottom part has been reported to be considerably less for SCC than normal vibrated concrete. It has also been reported in the literature that for walls, similar strength has been found for SCC and normal concrete for the top and the bottom part of the wall. By using Schmidt hummer, the surface hardness and the quality of the surface has been found to be much better for SCC than normal concrete (RILEM 174-SCC, 2000).

2.1.6.2 Bond to Reinforcement

SCC is highly flowable concrete that can fill the members to be casted with no vibration. The high flowability with the cohesiveness reduces the bleeding, segregation and improves degree of consolidation of the concrete before hardening. Otherwise under the lower half of horizontal embedded reinforcement and under the ribs of vertically positioned bars there will be a risk for increasing of porous cement paste, and this would obstruct the bond with the reinforcement. Same effect will be gained if there is no deformation capacity in the concrete to fully encapsulate the reinforcement bars (RILEM 174-SCC, 2000).

2.1.6.3 Shrinkage and Creep

Shrinkage and Creep like the other properties of concrete are depending on many factors. Studies have shown that the shrinkage will be higher in SCC while other studies mentioned the opposite (RILEM 174-SCC, 2000).

Comparing with the normal characteristics of normal concrete with the same strength it has been found that the creep of SCC and normal concrete was similar if the strength at loading was constant (RILEM 174-SCC, 2000).

Some studies (Bui Khanh & Montgomery, 1999) have reported that, the use of limestone with suitable fineness materials will reduce the shrinkage of SCC.

2.1.6.4 Transport and Durability Properties of SCC

The behavior of SCC for transport capacity of gases and liquids is similar for the shrinkage and creep. Lower and higher transport capacity has been found for self-compacting comparing with normal concrete. Some researchers reported that, this lower transport capacity is because of the avoidance of vibration and the use of high volume of fine particles (Rougeau et al., 1999; Tang et al., 1999). The durability

properties like reduction in carbonation, reduction of chloride penetration and water permeability are furthermore explained in the literature (RILEM 174-SCC, 2000). Generally, the type and the amount of the filler used to produce SCC are strongly influencing the durability properties of this type of concrete. The good freezing thawing behavior is because of producing SCC with lower air voids and it somehow considered being better than the normal vibrated concrete in this matter (RILEM 174-SCC, 2000).

2.1.7 Mix Design of SCC

A concrete mix can only be classified as self-compacting concrete if it has the following characteristics;

- Filling ability
- Passing ability
- Resistance to segregation

The approach to achieve these characteristics is shown in flowchart given in Figure 7. The use of limited and well graded coarse aggregate will provide the passing ability and the increasing of paste volume with the decrease of water/powder ratio with the presence of superplasticizer will provide the flowing ability and the resistance for segregation (RILEM 174-SCC, 2000).

Various methods exist for designing SCC and generally divided into step design. The first step is ‘continuous’ which covers the water, additives, cement and filling materials with the size of the particles less than 0.1 mm. The second step is ‘particle’ which covers the coarse aggregate and the fine aggregate (Gaimster & Dixon, 2003).

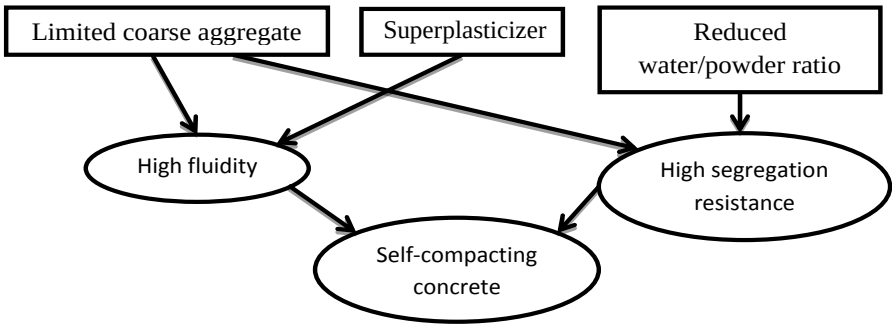

Figure 7: General flowchart approach to achieving SCC
Source: (Ouchi et al., 1998)

There is no standard mix design for the producing of SCC. Water/binder ratios are usually less than 0.5 and mixes have a lower coarse aggregate content and higher paste content comparing with conventional mixtures. Admixtures and concrete additions such as fly ash and silica fume contribute to enhance both the workability and segregation resistance. A study about the mix components and proportions from laboratory and in situ investigations showed that there were many differences in mix proportions; many aspects were common to a majority of mixes as it can be seen in the Table 3 below. Table 4 shows the suggested powder content with the desired slump flow diameter.

Table 3: Common factors for design of SCC

Property	**Comments**
Water content	150 – 200 kg/m^3
Admixtures	Superplasticizer: used to increase workability. Mainly naphthalene or melamine formaldehyde based. Viscosity modifiers: used to control segregation in mixes with higher water/binder ratios. Cellulose or polysaccharide 'biopolymer'.
Binders	Typically in range 450-600 kg/m^3. Fly Ash, GGBS, commonly used to improve cohesion. Silica Fume and Limestone filler also commonly used.
Fine Aggregate	Between (710 – 900) kg/m^3
Aggregates	Between (750 – 920) kg/m^3, both gravels and crushed rock used. Up to 20 mm nominal size is common. Lightweight SCC has also been produced.
Workability measurement	Numerous tests used to asses fresh properties (see 2.1.4)

Source: (RILEM 174-SCC, 2000; Gaimster & Dixon, 2003)

Table 4: Suggested powder content ranges

	Slump flow of < 550 mm	**Slump flow of 550 to 650 mm**	**Slump flow of >650 mm**
Powder content kg/m^3	355 to 385	385 to 445	445 plus

Source: (ACI 237, 2007, p.18)

As normal vibrated concrete, trial mixes should be done for SCC to adjust the proportions especially when calculating the superplasticizer content and the filler amount (Gaimster & Dixon, 2003).

Workability tests should be checked after using above given parameters and the results should be compared with the standards. If results obtained are not within the ranges, adjustments for the proportions should be made.

2.1.8 Production and Placing of SCC

Aggregates: Aggregate should be provided from same source without any variations in size, shape and moisture content.

Mixing: Any appropriate mixer can be used; generally, the time of mixing is longer than for normal vibrated concrete. The time of adding the admixture is very important. A system should be followed for better results and this system can be established during trial mixtures. In the beginning, the trail mixes may be under the risk of failing especially in the fresh properties of SCC. Therefore it is suggested that every batch must be tested until the final SCC mix is obtained. Then, visual inspection could be used (Shetty, 2005).

Formwork: The formwork that is used for SCC can be designed in different sizes and shapes. In order to get the target fluidity stability of SCC, the formwork should

be designed carefully because it directly affects the fresh characteristics of SCC (ACI 237, 2007).

"Formwork should be watertight (non-leaking) and grout-tight when placing SCC, especially when the mixture has relatively low viscosity" (ACI 237, 2007, p.21), It is necessary to design the formwork for water tightness more than conventional formwork in order to prevent honeycombs and surface defects.

Since SCC is highly flowable, the formwork pressure will be higher comparing with normal vibrated concrete, particularly when the rate of casting is high.

"Filling the form is accomplished by a pump attached to the bottom of the form; formwork pressure is about twice as high when filling from the top without pressure" (ACI 237, 2007, p.21).

The results of a research on form pressure showed that "SCC exerts equal or less pressure than conventional concrete with 200 to 260 mm slump that is vibrated" (ACI 237, 2007).

Placing: As for normal conventional concrete formwork has to be in good conditions to prevent leakage for SCC. Although it is easier to place SCC than ordinary concrete, the following instructions are to be followed to reduce the risk of segregation;

- "Limit the vertical free fall distance to 5 meters,
- Limit the height of pour lifts (layers) to 500 mm and

- Limit the permissible distance of horizontal flow from point of discharge to 10 meters" (Shetty, 2005, p.577).

Curing: If there is no bleeding or very little bleeding; SCC shows faster drying and may cause more plastic shrinkage cracking. Consequently, initial curing should be started as soon as possible. Otherwise the SCC must be successfully covered with polyethylene sheet. Because of the high content of powder, the plastic shrinkage or creep in SCC can be more than ordinary concrete mixes. There are disagreements on the above statement. These parameters should be well-thought-out during designing and specifying SCC. It should also be noted that early curing is required for SCC.

2.1.9 Environmental Aspects of SCC

2.1.9.1 Working Environment

The improvement of the working environment is one of the most important factors in the development of SCC. Normal concrete construction work has a high working environmental effect consisting generally of noise, vibration, mechanical loading and damages from accidents caused by delaying reinforcement bars, cables and other problems. In many countries the typical concrete worker has troubles in continuing working until retirement because of the high working environment load. In many places the loading is also seen as being severe enough to encourage authorizing like the following (RILEM 174-SCC, 2000):

- Reduce the working time for the worker for a specific load during a shift.
- Improvement of the working environment in concrete construction for the need of a human and society, on the other hand it is also a necessity in order to secure employment of interested and skillful people to concrete construction as well as to get desired productivity.

- Evaluation of the potential of enhancing the working environment by using SCC has been necessary in the development of the technology.

By using SCC instead of vibrated concrete, the reduction of noise for a worker subjected to during casting is 8 - 10 dB (A) which means that 90% reduction of noise is obtained.

"The vibration from handheld vibrators is inducing blood-circulating disturbances commonly known as white fingers." (RILEM 174-SCC, 2000, p.92).

"The mechanical loading from handling pokers with their hoses is eliminated through the use of SCC, and the risk of accidents at the workplace is reduced with less cables, transformers etc. which will make less noise making communication by talking possible" (RILEM 174-SCC, 2000, p.92).

2.1.9.2 Environmental Impact and Sustainability

There are a number of factors that reduce the environmental impact during construction when SCC is used. The most important are:

- "Less noise for building site neighbors.
- Less cement used for a specific function (higher strength leading to lower concrete volume or lower cement content per volume).
- Less energy consumption during construction" (RILEM 174-SCC, 2000, p.92).

Using waste resources like filling materials and recycled aggregates are quite good for SCC as for vibrated concrete. The risk of using admixtures for environment is

low for both SCC and vibrated concrete, likely for the risk of health hazards during handling. By using the new generation of admixtures for SCC the environment and medical impact is reduced (RILEM 174-SCC, 2000).

"Factors that positively affect the strive towards sustainable construction is the reduction of cement (clinker) consumption and the foreseen longer service life due to the improved durability based on improved microstructure" (RILEM 174-SCC, 2000, p.92).

2.1.10 Economical Aspects of SCC

There is a feeling that the cost of SCC is quite higher comparing with the equivalent normal strength or high strength concrete. It has been reported that the cost of materials of SCC is about 10 to 15 percent higher. By considering the components of costs such as cost of compaction, finishing, and labor etc., then SCC is definitely not a costly concrete for the same strength (Shetty, 2005).

2.2 Steel Fiber Reinforced Concrete (SFRC)

2.2.1 Definition of Steel Fiber Reinforced Concrete

Steel fiber reinforced concrete (SFRC) can be defined as "concrete made with hydraulic cement containing fine or fine and coarse aggregate and discontinuous discrete steel fibers" (ACI 544.1, 1996, p.7). The fibers can be produced from natural material like asbestos, sisal, cellulose or maybe a manufactured product such as glass, steel, carbon and polymer (Neville & Brooks, 2008).

The development of fiber reinforced concrete started in the early 1960's. Nowadays the available materials in the market include steel fiber, glass fibers, and carbon fibers, natural organic and mineral (wood, sisal, jute, bamboo, coconut and

rockwool) fibers, polypropylene fibers and synthetic fibers like kevlar, nylon and polyester (ACI 544.1, 1996).

Fibers act as crack arrestors, restricting the development of cracks and thus transforming an inherently brittle matrix, i.e., Portland cement with its low tensile and impact resistances, into a strong composite with superior crack resistance, improved ductility and distinctive post cracking behavior prior to failure (Somayaji, 2001).

The quantity of fibers used is small, typically 1 to 5 percent by volume, and to reduce them effective as reinforcement the tensile strength, elongation at failure and modulus of elasticity of the fibers need to be substantially higher the corresponding properties of the matrix (Neville & Brooks, 2008).

2.2.2 Types of Steel Fibers

Fibers are in various sizes and shapes. Round steel fibers made up of low-carbon steel or stainless steel, having diameters in the range of 0.25 mm to 1 mm. Flat steel fibers, produced by shearing sheet or flattening round wire and are available in thicknesses ranging from 0.15 mm to 0.41 mm. Crimped and deformed steel fibers are available both in full length or crimped at the ends only. A typical volume fraction of steel fibers is 0.25% to 1.5% (of the volume of concrete) (Somayaji, 2001). Detailed sketches of some of steel fiber types are as shown in Figure 8.

2.2.3 Physical Properties of SFRC

The important properties of fiber reinforcement concrete are the strength, stiffness and the ability of the fibers to bond with the concrete mix. Bond is dependent on the aspect ratio of the fiber. Typical aspect ratios range from about 20 to 100, while length dimensions range from 6.4 to 76 mm (ACI 544.1, 1996). The aspect ratio

defines the length (l) divided by its diameter (d). It is also called as equivalent fiber diameter (l/d). Typical properties of steel fibers are given in Table 5 (Illston & Domone, 2001).

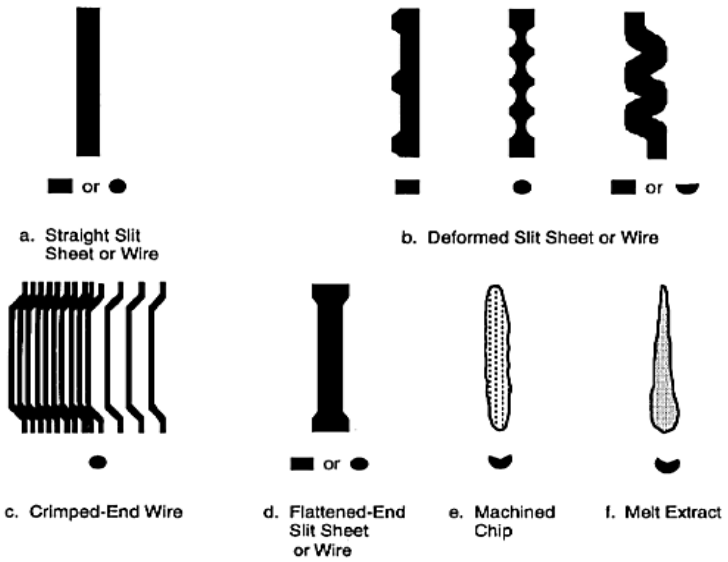

Figure 8: Steel fiber types with different geometric properties
Source: (ACI 544.1, 1996)

2.2.4 Mechanical Properties of SFRC

2.2.4.1 Tensile Strength of SFRC

Splitting tensile of mortar reinforced with steel fiber was reported to be about 2.5 times that of the unreinforced mortar when 3 percent fiber by volume was used and 2 times when 1.5 percent was used. On the other hand it was found the direct tensile strength of mortar reinforced with 1.5 percent of steel fibers is about 1.4 times that of unreinforced materials (ACI 544.1, 1996).

2.2.4.2 Dynamic (Impact) Strength of SFRC

The dynamic strength for various types of loading was 20 to 30 times greater for fiber reinforced than for plain concrete. The greater energy requirements to strip or pull out the fiber provide the impact strength and resistance to spalling and fragmentation (ACI 544.1, 1996; Taylor, 1991).

Table 5: Typical properties of cement-based matrices and fibers

Material or fiber	Relative density	Diameter or thickness (microns)	Length (mm)	Elastic modulus (GPa)	Tensile strength (MPa)	Volume in composite (%)
Mortar matrix	1.8-2.0	300-5000	-	10-30	1-10	85-97
Concrete matrix	1.8-2.4	10000-20000	-	20-40	1-4	97-99.5
Aromatic	1.45	10-15	5-continuous	70-130	2900	1-5
polyamides						
(aramides)						
Asbestos	2.55	0.02-30	5-40	164	200-1800	5-15
Carbon	1.16-1.95	7-18	3-continuous	30-390	600-2700	3-5
Cellulose	1.5	20-120	0.5-5.0	10-50	300-1000	5-15
Glass	2.7	12.5	10-50	70	600-2500	3-7
Polyacrylonitrile	1.16	13-104	6	17-20	900-1000	2-10
Polyethylene:						
Pulp	0.91-0.97	1-20	1	-	-	3-7
HDPE filament	0.96	900	3-5	5	200	2-4
High modulus	0.96	20-50	Continuous	10-30	>400	5-10
Polypropylene:						
Monofilament	0.91	20-100	5-20	4	-	0.1-0.2
Chopped film	0.91	20-100	5-50	5	300-500	0.1-1.0
Continuous nets	0.91-0.93	20-100	Continuous	5-15	300-500	5-10
Polyvinyl alcohol (PVA, PVOH)	1-3	3-8	2-6	12-40	700-1500	2-3
Steel	7.86	100-600	10-60	200	700-2000	0.5-2.0

Source: (Illston & Domone, 2001)

2.2.4.3 Compressive Strength of SFRC

The compressive strength is directly related to presence of voids, and for well compacted fiber concrete. The compressive strength generally does not vary beyond ± 10%, although increases up to 20% have also been observed. The size of aggregate, presence of admixture and fiber aspect ratio all influence the compressive strength only in so far as they affect the degree of compaction achieved. The reduction in compressive sometimes observed with fiber mortar appears to be due to the sand content (Swamy, 1975; ACI 544.1, 1996).

2.2.4.4 Flexural Tensile Strength of SFRC

The flexural strength depends on the volume and aspect ratio of fibers. Steel fibers up to 4 percent by volume have been found to increase the first crack, flexural strength of concrete up to 2.5 times the strength of unreinforced composite (ACI 544.1, 1996).

The major factors affecting the flexural strength are the volume fraction and the length/diameter (aspect) ratio of the fibers where an increase in both of those parameters leading to higher flexural strength (Hannant, 1978). Normally it is known that the flexural strength increases linearly with volume and length/diameter (aspect) ratio of the fibers (Eren, 1999).

Poorly aligned fibers can give greatly reduced strength as shown in Figure 9 but, if care is taken to align the wires uniaxially, flexural strength up to 30 MPa can be achieved (Hannant, 1978).

2.2.4.5 Toughness and Ductility of SFRC

There are various ways of defining and quantifying toughness of SFRC. Flexural toughness may be defined as the area under the load-deflection curve in flexure, which is the total energy absorbed prior to complete separation of the specimen. The total energy absorbed as measured by the area under the load-deflection curve before complete separation of a beam is at least 10-40 times higher for fiber reinforced concrete than for the plain concrete. Studies have shown that, the primary parameters influencing toughness are the type, volume percentage, aspect ratio, nature of deformation, and orientation of the fiber itself (ACI 544.1, 1996).

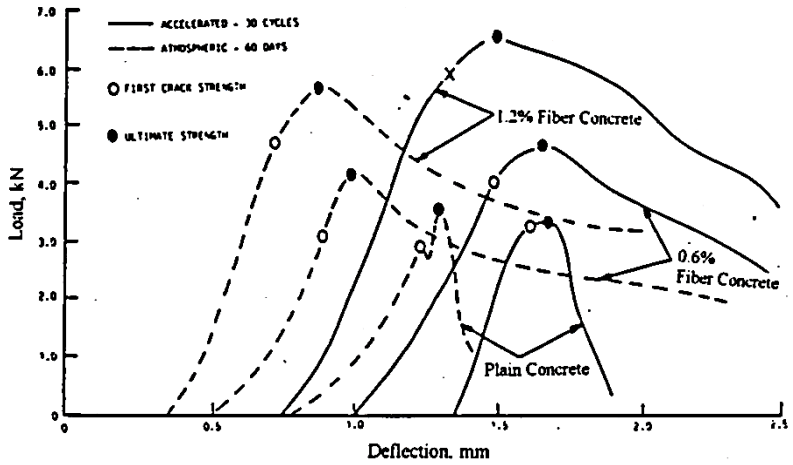

Figure 9: Flexural Load-Deflection curve of concrete specimens with and without fiber reinforced after 60 days or 30 cycle's exposure

Source: (Hannant, 1978)

2.2.4.6 Fatigue Behavior of SFRC

Data on fatigue behavior of SFRC is rare. Experimental studies show that, for a given type of fiber, there is a significant increase in flexural fatigue strength with increasing percentage of steel fibers. It has been shown that the addition of fibers to conventionally reinforced beams increases the fatigue life and decreases the crack width under fatigue loading. It has also been shown that, the fatigue strength of conventionally reinforced beams made with SFRC increases (ACI 544.1, 1996).

2.2.4.7 Creep Behavior of SFRC

Compression-creep tests carried out over a loading period of 12 months showed that, the addition of steel fibers does not significantly reduce the creep strains of the composite. This behavior for creep is consistent with the low volume concentration of fiber when compared with an aggregate volume of approximately 70% (ACI 544.4, 1988).

2.2.5 Fresh properties of SFRC

Steel fiber reinforced concrete may be very stiff in fresh state. Long thin fibers (l/d>100) tend to mat together while short stubby fibers (l/d<50) cannot interlock and can be dispersed by vibration (Gambhir, 1990).

A particular fiber type, orientation and percentage of fibers, the workability of the mix decreased as the size and quantity of aggregate particles greater than 5 mm increased; the presence of aggregate particles less than 5 mm in size had little effect on the compacting characteristics of the mix (Chanh, 2005).

The workability of fiber reinforced concrete is also influenced by maximum size of aggregate. As the size of aggregate increases it becomes more difficult to achieve uniform fiber dispersion, since the fibers are bunched into mortar fraction which can move freely past the fibers during compaction. To obtain a better dispersion the coarse aggregate content is kept lower than to 10 mm.

2.2.6 Durability of SFRC

One of the major problems related with the use of steel fibers is their durability in concrete structures. Corrosion of steel fibers may lead to loss of their ability to arrest, control cracks propagation and also to contribute the load capacity of the structural element at service and ultimate load conditions. The fiber volume is usually very small, and the expansive forces due to corrosion are so small that spalling does not occur. On a structural element involved both steel fibers and reinforcement bars, the expansive forces due to corrosion in the steel bars are far more critical than those due to corrosion of fibers themselves. Hence, steel reinforcing bars can provide a far greater risk to corrosion than steel fibers, and in elements containing steel fibers, spalling is rarely observed although staining may occur. In good quality concrete,

fiber corrosion does not penetrate into the concrete, and that it is confined to fibers that exposed at the surfaces (break away in time). In very aggressive environment, it is possible to use stainless steel fibers which are totally resistant to corrosion (Swamy & Stavrides, 1979).

2.3 Fiber Reinforced Self-Compacting Concrete (FR-SCC)

2.3.1 Introduction

The elimination of vibration for the compaction of fresh concrete makes the use of self-compacting concrete (SCC) beneficial in terms of cost reduction and improvement of the work environment. Furthermore, due to its intrinsic low porosity, SCC usually has high performance properties also in terms of mechanical behavior and durability. These properties could even be elevated improved if steel fibers are incorporated, thus obtaining fiber reinforced self-compacting concrete (FR-SCC) (Torrijos et al., 2007).

The addition of fibers into self-compacting concrete may take advantage of its high performance in the fresh state for uniformly dispersal within the matrix as well as many advantages like the improvement in the economic efficiency of the construction process, increased speed of construction, reduction or suitably focused rearrangement of labor resources, costs and energy consumption, better working environment, with reduced noise and health hazards, also the contribution toward the automation and reliability of quality control (Ferrara et al., 2007).

The use of fibers might extend the possible fields of application of SCC. Fibers are produced in a wide range of materials, at different shapes, with divergent properties concerning their affinity to paste or water. Some types of fibers are fragile, flexible

or stiff, cylindrically, rectangular or irregular shaped. They are known to affect the workability and the flow characteristics of plain concrete essentially. The degree to which workability decreases does depend on the type and content of fibers used, on the matrix in which they are embedded and the properties of the constituents of the matrix on their own. A high content of fibers is difficult to distribute uniformly; a good distribution, however, is required to achieve optimum benefits of the fibers. Manufactures try to improve the pull-out resistance of the fibers by deforming or crimping them, giving them a surface texture that increases the roughness, and bend or enlarge the ends to improve the anchorage capacity (Grünewald & Walraven, 2001).

Steel fibers and micro-filler materials are widely used in the construction industry. These materials enhance the performance of self-compacting concrete, consisting of very fine powder. Studies proved that these materials improve the quality of the concrete both in fresh and hardened states. As the volume of the micro-filler materials increases, the distance between the large sizes aggregates also increases, reducing the internal friction of the concrete. As the blockage of the large aggregates is prevented, the flow and workability properties of the fresh concrete are improved. The developed volumetric water-to-powder ratio method enables the use of binding materials effectively and provides a tool for optimization, as well as new areas for research on the interaction between the microstructure and mechanical properties of the concrete (Sengul et al., 2006).

2.3.2 Mix Design of FR-SCC

A fiber reinforced self-compacting concrete should be extremely workable concrete without bleeding or segregation. The slump loss should also be well controlled. To

satisfy those requirements, materials had to be carefully selected and their proportion optimized (Miao et al., 2003).

The mix design of self-compacting concrete includes fine materials such as cement, fine aggregates and limestone powder, as well as pozzolanic materials such as fly ash and silica fume. Viscosity modifying agents and plasticizers, based on polycarboxylate ether complex, naphthalene sulphonates or melamine sulphonates, are further added to the mixtures, depending on the properties of the targeted workability. The aim of the mixture design is to obtain the desired workability and segregation resistance. This mixture should be able to flow around the steel reinforcement and should not segregate or clump. For this reason, the water/powder ratio and aggregate gradation should be controlled, and effective admixtures should be used during the production of self-compacting concrete (Sengul et al., 2006).

2.3.3 Durability Design Consideration of FR-SCC

In conventional mixture design, concrete workability is decided by the water amount and the compressive strength, whereas the durability is decided by the water-to-cement ratio (ACI 211.1, 1991). The workability can be improved by increasing the water amount and the strength can be increased by increasing the cement content. However, too much cement paste will cause large slump loss and bleeding as well as segregation; moreover, the hydration of the cement will cause chemical shrinkage, and the shrinkage rate or expansion rate is in direct proportion with the water and the cement amounts. Besides, ordinary concrete contains water at least 20% of the concrete volume, and hence drying shrinkage cannot be avoided. Thus the durability of concrete is destroyed, due to disintegration and crack formation. To avoid these problems, a concrete mixture designed with low water amount and low cement content is suggested (Chih-Ta et al., 2009).

Durability design should be considered for improving both the fresh and hardened stages of the concrete and should finally extend their service life. First and foremost the concrete mix design should have a very low water amount so as to minimize the shrinkage rate or the expansion rate of concrete, Then, the concrete must be designed to satisfy the construction needs such as low slump concrete (e.g. roller compacted concrete) or high slump concrete (e.g. self-compacting concrete, high performance concrete), type of construction work, and the required final finished result. In the plastic stage, the fresh concrete is designed to prevent the occurrence of plastic shrinkage cracks due to excess water evaporation from the concrete surface. A certain amount of steel fiber should be included in the concrete mix to absorb energy and in the case of crack formation, to stop their propagating. The addition of pozzolanic materials is necessary to help the self-healing of cracks if they are generated. A strict standard operation procedure for mixture proportion, material selection, trial batch, quality control, and curing are required to lower the possibility of crack formation (Chih-Ta et al., 2009).

Chapter 3

EXPERIMENTAL STUDIES

3.1 Introduction

Self-compacting concrete (SCC) and fiber reinforced self-compacting concrete (FR-SCC) mixes were composed of blast-furnace slag cement, silica fume, crushed limestone (fine, medium, and coarse) aggregates, and high range water reducing admixture (superplasticizer) and steel fibers. Just after mixing, slump flow tests (VSI and T50), J-ring, V-funnel and column segregation tests were performed on fresh concretes. Various tests, namely, compressive strength, splitting tensile strength, flexural strength, impact energy, depth of water penetration, density, absorption, voids content, chloride ion penetration, surface abrasion resistance and ultrasonic pulse velocity tests were done on hardened SCC and FR-SCC.

3.2 Materials and Mixes Used

3.2.1 Cement and Silica Fume

Throughout this study, blast furnace slag cement (BFSC), and silica fume (SF) were supplied from a single batch and were stored in a dry place. Silica fume used was a commercially available by-product of silicon metal and ferrosilicon alloys. It was used as an addition to the cement so as to improve the concrete properties both in fresh and hardened states. Silica fume was added at 18.75 percent by weight of cement. Details of the compositions and properties of BFSC and SF are given in Table 6.

Table 6: Details of the compositions and properties of blast-furnace slag cement (BFSC) and silica fume (SF)

Property	**Cement**	**Silica fume**
SiO_2 (%)	29.15	82.2
Al_2O_3 (%)	7.34	0.50
Fe_2O_3 (%)	2.42	0.42
CaO (%)	50.04	1.55
MgO (%)	3.99	0.00
SO_3 (%)	1.97	3.03
CI (%)	0.01	-
C_3A (%)	3.0 – 4.5	-
Dissolved impurities (%)	0.27	-
L.O.I. (Loss of Ignition) %	1.65	5.66
Fineness-Blaine (cm2/gr)	3340	-
W/c (%)	29.9	-
Setting time (minutes)		
Initial	218	-
Final	303	-
Le Chatelier(mm)	0.67	-
Specific weight (gr/cm3)	2.96	2.29
Compressive Strength (MPa)		
2 days	9.2	-
7 days	20.2	-
28 days	38.0	-

3.2.2 Aggregates

The maximum size of coarse aggregate was about 14 mm. All aggregates used were crushed limestone, with high amount of dust and limestone powder, and their properties are shown in Table 7. The fine and coarse aggregate grading was complying with the standards (ASTM C 33, 2008). Sieve analysis results of aggregates are detailed in Table 8. The grading curve, according to the standards (ASTM C 33, 2008) for fine and coarse aggregates, is as shown in Figure 10.

Table 7: The properties of fine and coarse aggregates

Properties	**Relevant Standards**	**Fine Aggregate**	**Coarse Aggregate**
Relative Density (SSD)	(ASTM C 127, 2007) (ASTM C 128, 2007)	2.66	2.68
water absorption (% of dry mass)		2.56	0.8
Dust content (%)	(ASTM C 117, 2004)	16.7	4.5

Table 8: Sieve analysis results of fine and coarse aggregate

Sieve sizes (mm)	Percentage passing (by weight)	
	Fine aggregate	Coarse aggregate
37.5	100	100
25	100	100
19	100	100
12.5	100	88
9.5	100	61
4.75	100	8
2.36	88	3
1.18	74	-
0.600	42	-
0.300	21	-
0.150	5	-
0.075	1	-

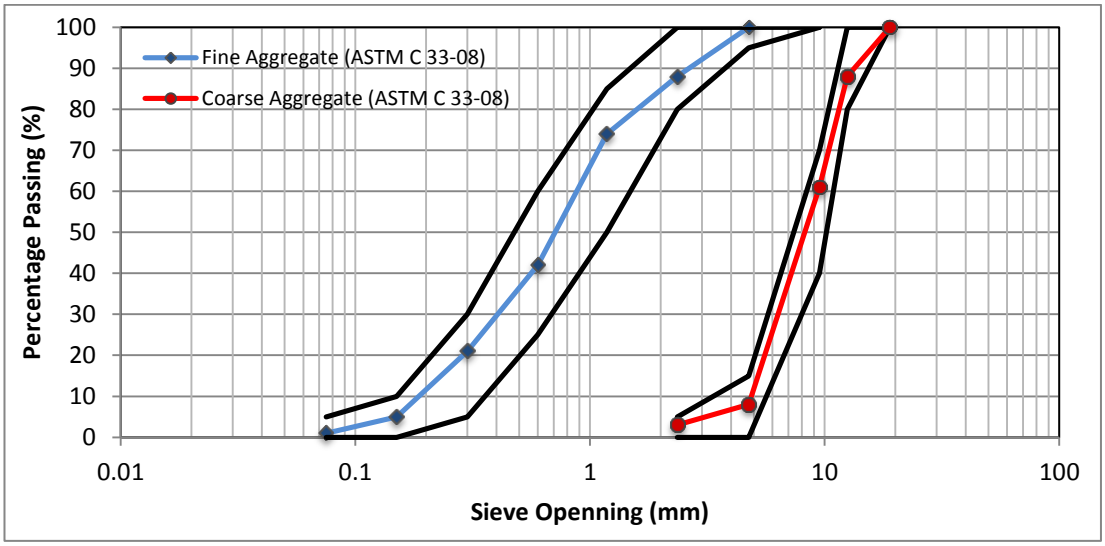

Figure 10: Particle size distribution of fine and coarse aggregates

3.2.3 Water

Drinking-quality water was used in all concrete mixes as the mixing water. The same water was used for curing the specimens.

3.2.4 Superplasticizer

To improve and maintain the workability of fresh concrete, a high range water reducing admixture (superplasticizer) (SIKA, 2006), which is commercially known

as Sika ViscoCrete Hi-Tech 32 was used. The properties of Sika ViscoCrete Hi-Tech 32 are shown in Table 9.

Table 9: The properties of Sika ViscoCrete Hi-Tech 32

Product Data	
Appearance / Color	Light brownish liquid
Storage Conditions /Shelf Life	12 months from date of production if stored properly in original and unopened packaging, in dry conditions at temperatures between 5°C and 35°C. Protect from direct sunlight and frost.
Technical Data	
Chemical Base	Modified polycarboxylate based polymer
Density	1.045-1.085 g/cm³, 20°C
pH Value	3 – 7
Viscosity	63 cp, 20°C
Freezing point	-4 °C
Total Chloride Ion Content	Max. 0,1%
Application Details	
Consumption / Dosage	For self-compacting concrete: 1.0 to 2.0% by weight of binder (1.0 - 2.0 kg for 100 kg cement).
Notes on Application / Limitations	When using Sika ViscoCrete Hi-Tech 32, a suitable mix design has been taken into account and local material sources should be trailed. - Sika ViscoCrete Hi-Tech 32 should not bedded to dry cement. - Sika ViscoCrete Hi-Tech 32should be added with the mixing water. - When using Sika ViscoCrete Hi-Tech 32 for the production of self-compacting concrete, suitable mix design must be taken into account.

Source: (SIKA, 2006)

3.2.5 Steel Fibers

Steel fibers used in this study were hooked-end bundled fibers with an aspect ratio (l/d = length over diameter ratio) of 60. The length and diameter of fibers were 30 mm and 0.5 mm respectively as it is shown in Photo 1 and Photo 2. Three different fiber amounts were added to each batch of concrete as 20, 30, and 40 kg/m^3.

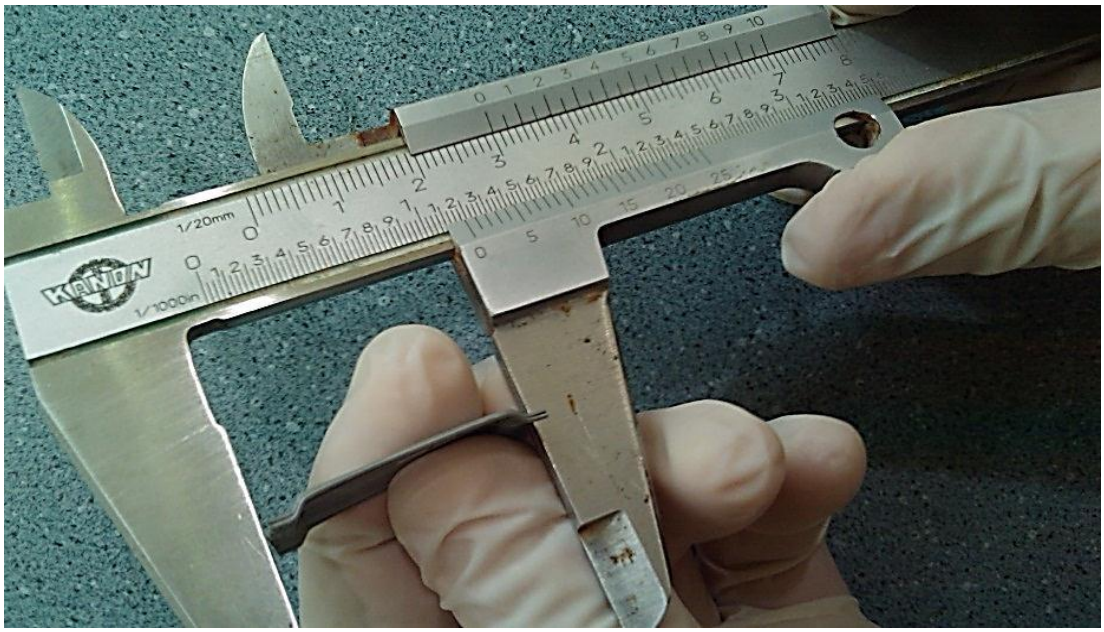

Photo 1: Hooked-end steel fibers with 30 mm length

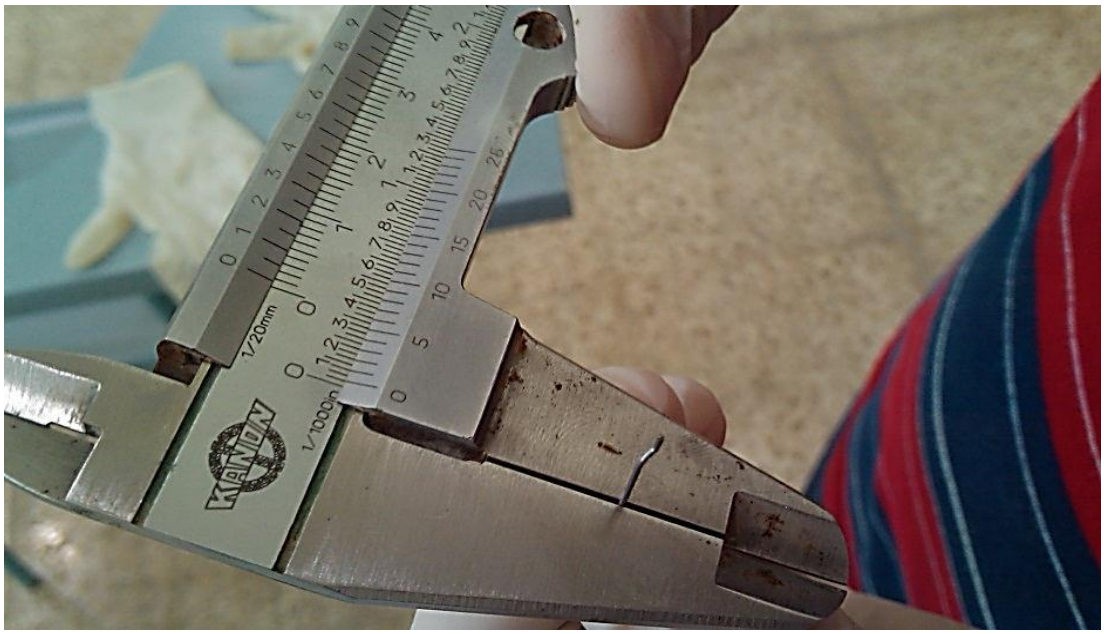

Photo 2: Hooked-end steel fiber with 0.5 mm diameter

3.3 Mix Details

The net water-cement ratio used for this study was 48.78%. Concretes were produced by using silica fume at percentage of 18.75 by weight of cement. The concrete mix proportions were designed in accordance with the standards (RILEM 174-SCC,

2000; ACI 237, 2007). The mix design proportioning for all mixes are detailed in Table 10.

Table 10: Mix design proportioning for all mixes used in this study

	kg/m^3			
Ingredient	**SCC**	**FR-SCC20**	**FR-SCC30**	**FR-SCC40**
Cement	400	400	400	400
Water	190	190	190	190
Silica Fume	75	75	75	75
Fine Aggregate	870	870	870	870
Coarse Aggregate	780	780	780	780
Steel Fiber	0	20	30	40
Superplasticizer	5.0	5.5	5.75	6.0

3.4 Mixing Procedure

For each mix, the ingredients were placed into the pan type laboratory mixer in the following order: coarse aggregate, medium aggregate, fine aggregate, cement, silica fume, steel fibers and (Water + superplasticizer). This procedure was adopted for all the mixes in order to minimize the risk of a possible disparity between the homogeneity of each mix.

Steel fibers were added after 30 seconds from the starting of mixing process while the ingredients were dry and after 15 seconds water started to be added gradually. The total mixing time was 4 minutes in order to ensure the uniformity. Addition of fibers was as shown in Photo 3.

3.5 Casting of SCC and FR-SCC Test Specimens

3.5.1 Casting of Compressive Strength Test Specimens

The size of standard cubic mold used for compressive strength test of SCC and FR-SCC was 150 x 150 x 150 mm. For each mix, twelve test cubes were casted in

accordance with the standards (BS EN 12390-3, 2002). All the specimens were cured according to the above mentioned procedures.

Photo 3: Addition of fibers to the mix from top of the mixer

3.5.2 Casting of Splitting Tensile Strength Test Specimens

The size of standard cylinder mold used for splitting tensile strength test of SCC and FR-SCC was 100 mm diameter and 200 mm length. For each mix, six test cylinders were casted. All the cylindrical test specimens were cured in curing tank until the testing age.

3.5.3 Casting of Flexural Strength Test Specimens

For each mix, three test beams (100 x 100 x 500 mm) were casted for flexural strength test. All the specimens were cured in curing tank until the testing age.

3.5.4 Casting of Impact Energy Test Specimens

For each mix, three cylinders of 150 mm diameter and 300 mm length were casted and then each cylinder was cut into smaller cylinders of 150 mm diameter and 60 mm length and the middle part of each cylinder was used for the test. Therefore for

each mix, 3 specimens were prepared for impact energy test at the age of 28 days. All the specimens were cured in curing tank until the testing age.

3.5.5 Casting of Depth of Water Penetration Test Specimens

The size of standard cubic mold used for depth of water penetration test of SCC and FR-SCC was 150 x 150 x 150 mm. For each mix, three test cubes were casted and cured in the curing tank until the testing age.

3.5.6 Casting of Density, Absorption and Voids Content Test Specimens

The size of standard cylinder mold used for density, absorption and voids content test of SCC and RC-SCC was 100 mm diameter and 200 mm length. For each mix, three test cylinders were casted and cured in the curing tank until the testing age.

3.5.7 Casting of Chloride Ion Penetration Test Specimens

For each mix, three cylinders of 100 mm diameter and 200 mm length were casted and then each cylinder was cut into smaller cylinders of 100 mm diameter and 52 mm length and the middle part of each cylinder was used for the test. Therefore for each mix, 3 specimens were prepared for chloride ion penetration test at the age of 28 days. All the specimens were cured in the curing tank until the testing age.

3.5.8 Casting of Surface Abrasion Test Specimens

For each mix, three cylinders of 150 mm diameter and 300 mm length were casted and then each cylinder was cut into smaller cylinders of 150 mm diameter and 60 mm length and the middle part of each cylinder was used for the test. Therefore for each mix, 3 specimens were prepared for surface abrasion test at the age of 28 days. All the specimens were cured in the curing tank until the testing age.

3.6 Curing Procedure

All the specimens on the hardened properties of SCC and FR-SCC were kept in their molds for the day after casting in moisture room as it is shown in Photo 4. After

about 24 hours of casting, the specimens were stripped and transferred to a standard curing tank and kept there throughout the curing period at a constant temperature of 22± 2 ºC for 28-day in accordance with the standards (BS EN 12390-2, 2000) as it is shown in Photo 5.

Photo 4: Specimens kept 24 hours in moisture room

3.7 Determination of the Properties of Fresh SCC and FR-SCC

For all the mixes, fresh properties for SCC and FR-SCC were checked to ensure the flowability, satiability, passing ability and segregation resistance of the mixes. Table 11 summarizes the testes that were done for the fresh properties of SCC and FR-SCC mixes.

Table 11: Fresh properties Tests of SCC and FR-SCC

Test name	**Used for**	**Relevant Standards**	**Shown in**
Slump Flow, VSI and T50	Flowing ability and stability	(ASTM C 1611, 2005; ACI 237, 2007)	Photos 6 and 7
J-ring	Passing ability	(ASTM 1621, 2006)	Photo 8
V-funnel	Flowing ability and passing ability	(De Schutter, 2005; Shetty, 2005)	Photo 9
Column segregation	Segregation resistance	(ASTM C 1610, 2006; ACI 237, 2007)	Photo 10

Photo 5: Curing of the specimens within the control tank

Photo 6: Sample under Slump Flow test

Photo 7: Sample under VSI test

Photo 8: Sample under J-ring test

Photo 9: V-funnel test apparatus

Photo 10: Sample under Column Segregation test

3.8 Determination of the Mechanical Properties of Hardened SCC and FR-SCC

3.8.1 Testing for Compressive Strength

The test was performed on 150 mm cubes according to the standards (BS EN 12390-3, 2002). The compressive strength was obtained at the ages of 7 and 28 days on water cured specimens by using a compressive strength testing machine, as shown in Photo 11.

Photo 11: Compressive Strength test machine

3.8.2 Testing for Splitting Tensile Strength

Splitting tensile strength test was performed according to the standards (ASTM C 496, 2004) on SCC and FR-SCC test specimens of size of 100 mm diameter and 200 mm length. The test specimens were tested for tensile splitting strength at an age of 28 days. The splitting tensile test specimen is shown in Photo 12 and Photo 13.

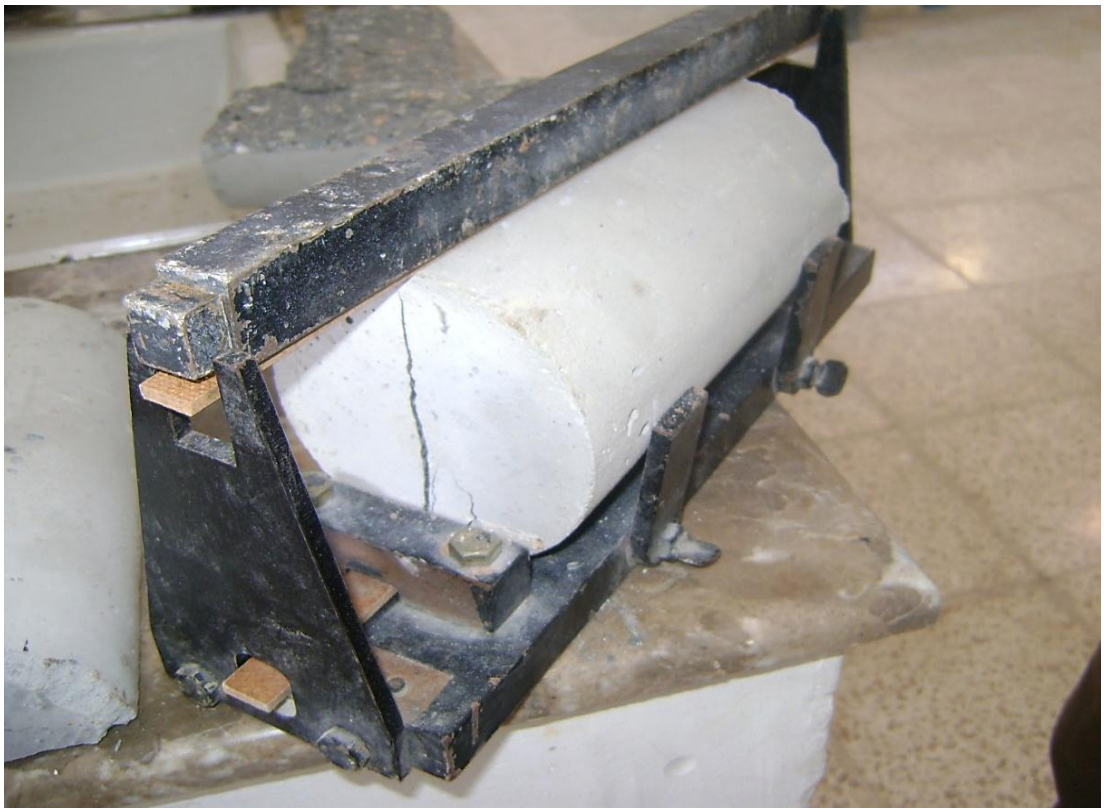

Photo 12: Splitting Tensile Strength test specimen

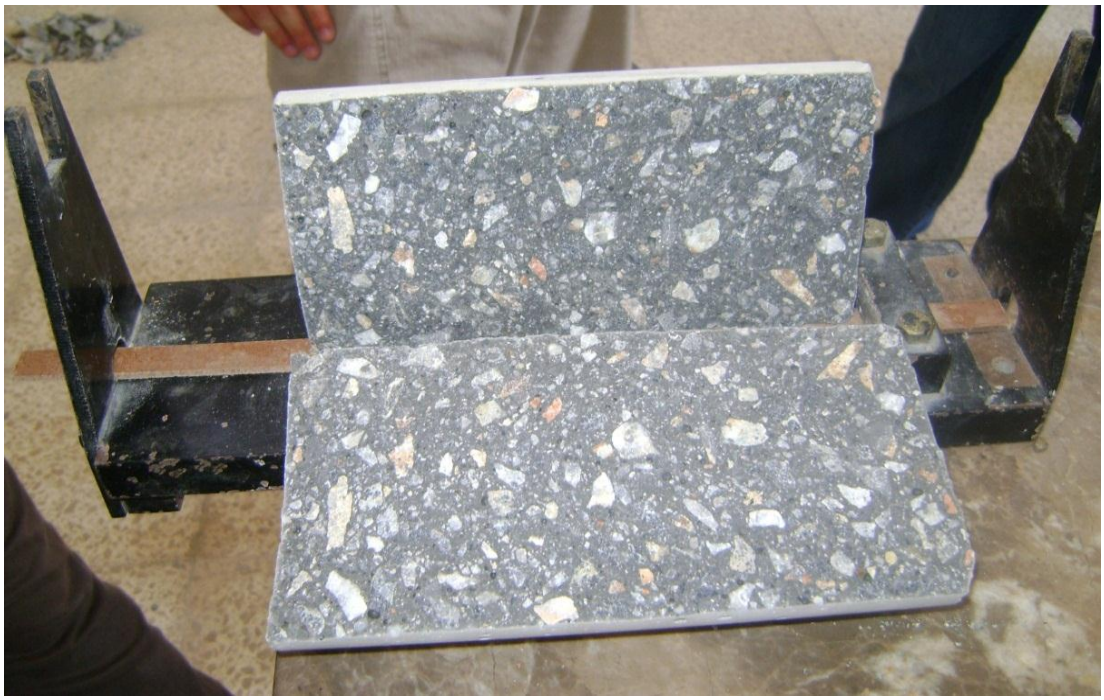

Photo 13: The specimen after Splitting Tensile Strength test

3.8.3 Testing for Flexural Strength

The flexural strength test was performed on SCC and FR-SCC beam test specimens of size 100 x 100 x 500 mm. The beams were subjected to a third-point loading in flexure at a constant deformation rate control of 0.05 mm/min in accordance with standards (ASTM C 1609, 2010). The span length of the beams tested was measured to be 39 cm. The mid-span deflections of the test beam were measured by using two LVDTs (one on each side), and the average of the measurements represents the true net mid-span deflections. A yoke was used in the flexural strength test in order to eliminate the extraneous settlements of the supports so as to record only the net beam specimen deflection. The arrangement of the flexural strength test apparatus is shown in Photo 14, while Photo 15 shows the specimen after failure.

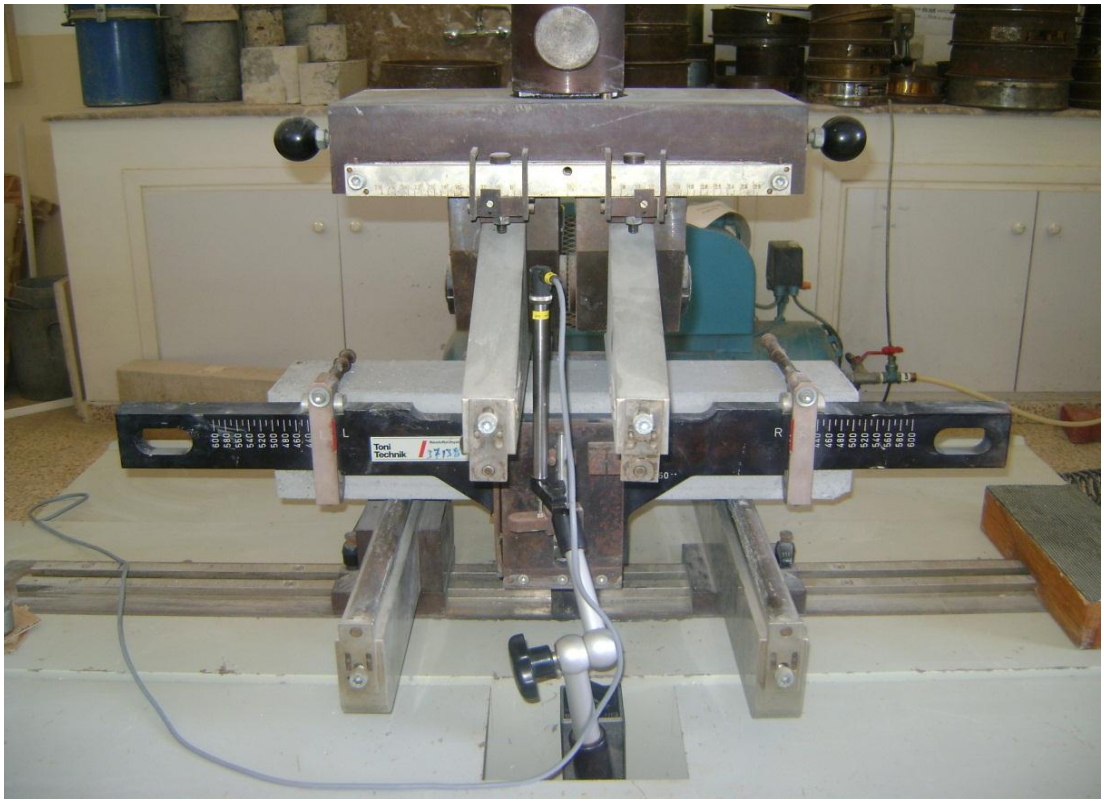

Photo 14: Flexural Strength test apparatus

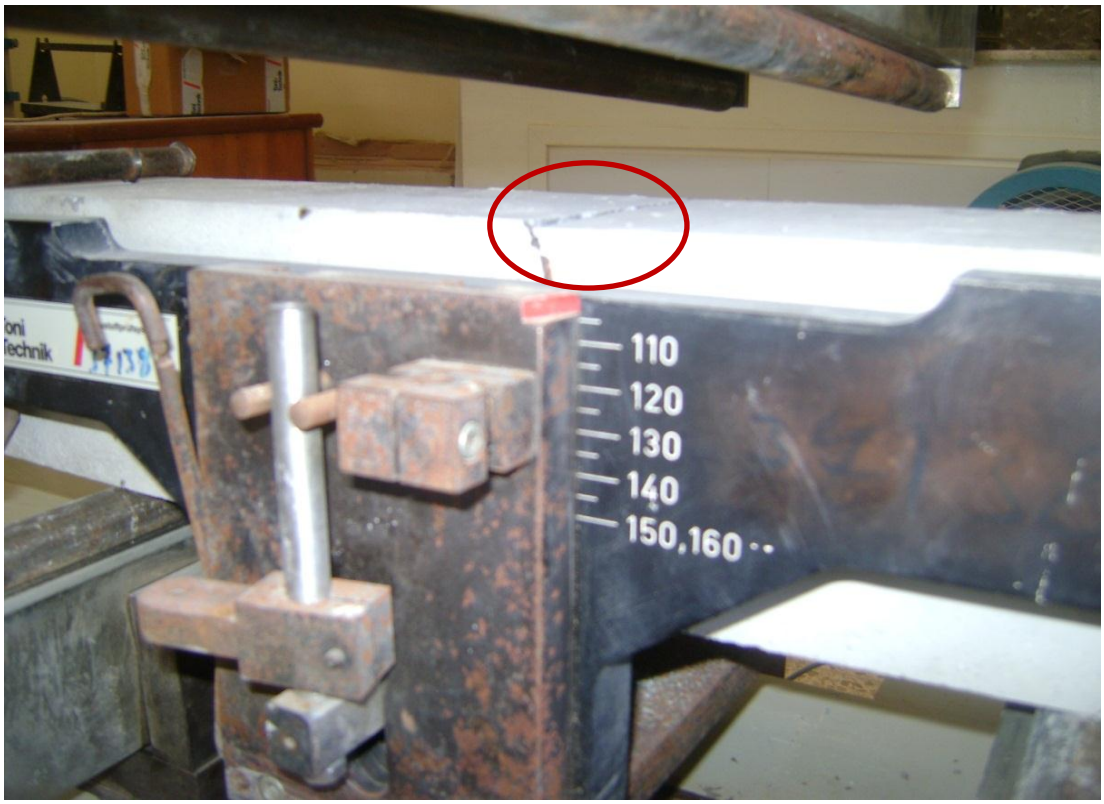

Photo 15: Specimen after failure due to Flexural Strength test

3.8.4 Testing for Impact Energy

The test was performed on 150 mm diameter and 60 mm length cylinders cut from 150 mm diameter and 300 mm length cylinders. The specimens were tested at the age of 28 days. Drop weight type impact test machine was used in accordance with method developed by Özgür Eren (1999). This machine was a combination of aggregate impact value test machine and drop weight type test apparatus recommended by the standards (ACI 544, 1978). This combination is as shown in Photo 16 and Figure 11. The drop hammer was weighing 13.5 kg, and it dropped from a height of 380 mm each time. Three cylinders were tested at 28 days age, and number of blows required to cause the first visible crack and ultimate failure was recorded. First crack is defined as the first visible crack. Ultimate failure is reached when the cracks have opened sufficiently to make the specimen touch each of the

four positioning lugs at the base plate (Eren, 1999). Photo 17 shows the specimens after failure by impact energy test.

The impact energy delivered to the specimen produced by each blow is calculated as follows (Marar, 2000):

$$E_I = \frac{1}{2} M V_I^2 N$$

Where,

E_I *= Impact energy (N.m),*

M = Mass of the drop hammer (kg),

V_I *= Impact velocity =1.8088 (m/s)* (Marar, 2000) , *and*

N = Number of blows.

Photo 16: Impact Energy test machine

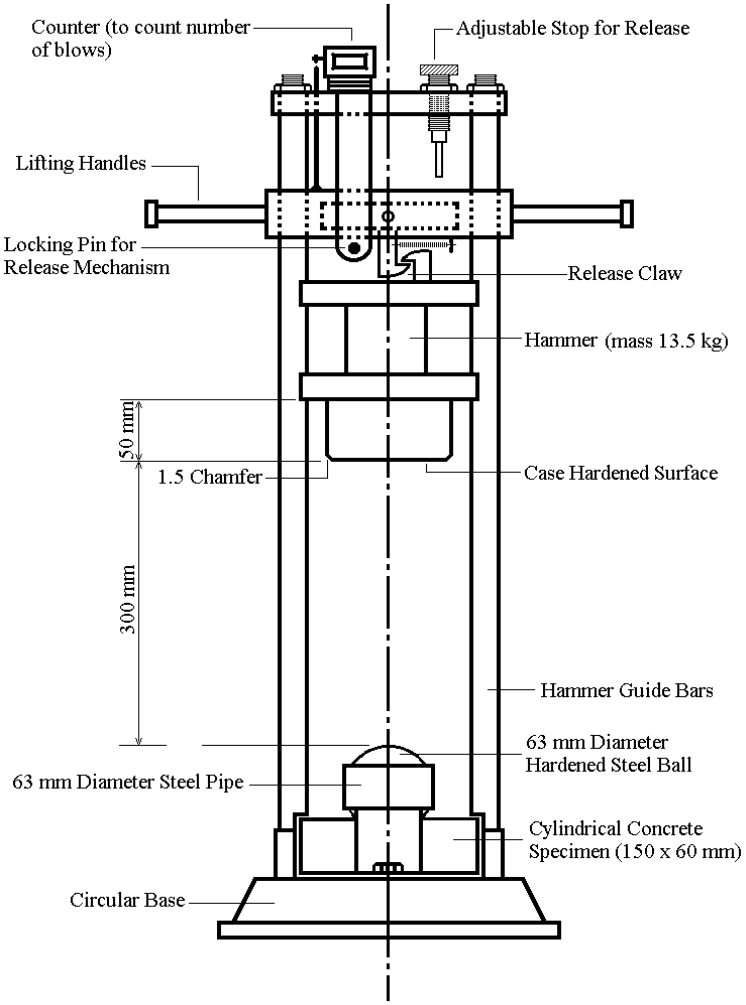

Figure 11: Repeated Drop-Weight Impact testing machine for SCC and FR-SCC
Source: (Eren, 1999)

3.8.5 Testing for Depth of Water Penetration

Three cubic specimens of size 150 X 150 X 150 mm were used. The testing age was 28 day for this experiment according with the standards (BS EN 12390-8, 2009). The test specimen inserted water impermeability testing apparatus cells with opposite direction of casting way. Testing specimen was left under water pressure of 500 ± 50 KPa with respect to the standards (BS EN 12390-8, 2009). This pressure was kept constant throughout the test. After the pressure was released, the specimen was removed and split down a center with the face, which was exposed to water facing down. When the split faces showed signs of drying (after about 5 to 10 minutes), the maximum depth of penetration was measured in mm (BS EN 12390-8, 2009). Photo

18 shows the water penetration testing apparatus and test specimens, while Photo 19 shows the depth of water penetration in the specimen.

Photo 17: The specimens after failure by Impact Energy Test

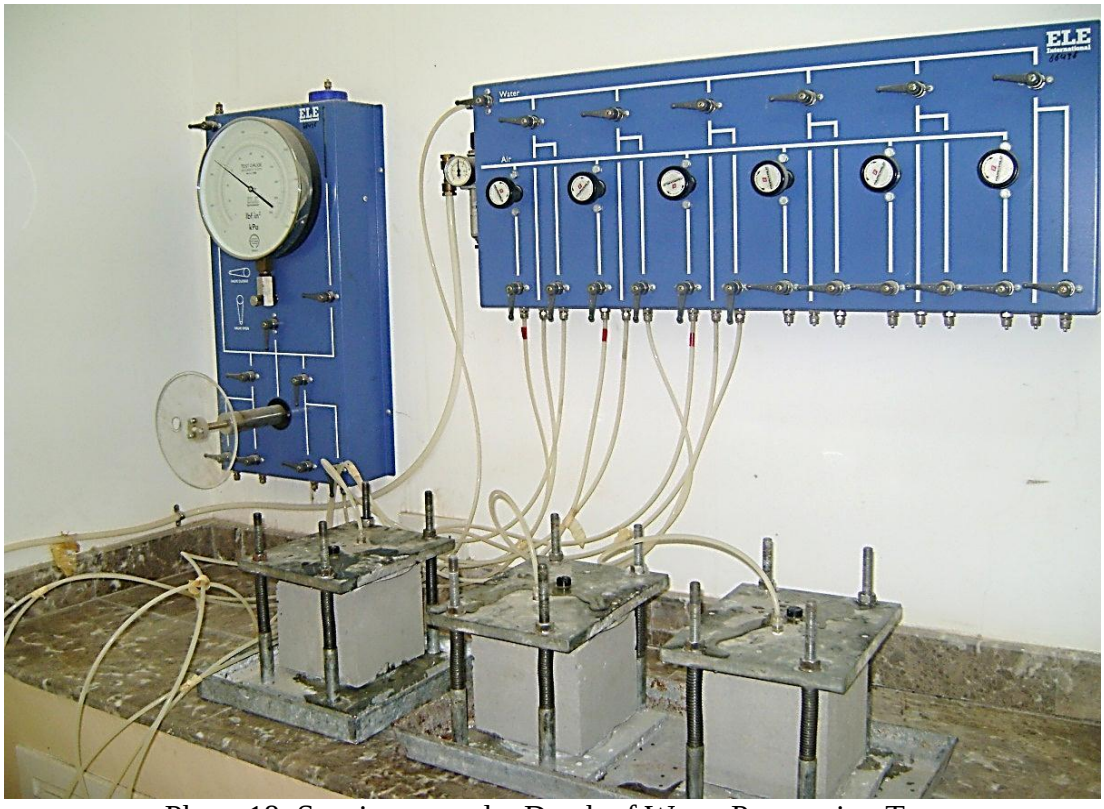

Photo 18: Specimens under Depth of Water Penetration Test

Photo 19: Depth of Water Penetration within the specimen

3.8.6 Testing for Density, Absorption and Voids Content

The test was performed on SCC and FR-SCC cylinder test specimens of 100 mm diameter 200 mm length. The test specimens were tested for density, absorption and voids content at an age of 28 day in accordance with the standards (ASTM C 642, 2006).

3.8.7 Testing for Chloride Ion Penetration

The test was performed on 100 mm diameter and 52 mm length cylinders cut from 100 mm diameter and 200 mm length cylinders. The specimens were tested at the age of 28 days in accordance with the standards (ASTM C 1202, 2010). Photo 20 shows the setup of chloride ion penetration test.

3.8.8 Testing for Surface Abrasion

The test was performed on 150 mm diameter 60 mm length cylinders cut from 150 mm diameter and 300 mm length cylinders. A surface abrasion testing machine was used in accordance with the method developed by Özgür Eren from a concrete

drilling machine as shown in Figure 12 and Photo 21. The free advance lever of the machine was removed and a pulley system was fixed in order to eliminate the difficulty in maintaining a constant load on the specimen. The load on the specimen was 19.62 N. Abrasion stone used was the one which is being used to complete the surface finishing of mosaics for floor tiles during their production. This stone which was about 120 mm in diameter and 75 mm thick was fixed at the edge of cylinder by using strong glue. The center of stone was left open in order to allow water-flow. In the beginning of the test, the abrasion stone was brought in contact with the surface of specimen to be tested and then the motor was started to work and abrasion continued for 75 seconds. A test period of 75 seconds was found to be sufficient to produce a significant wear on concrete surface. An electric motor with a gearbox system was used to rotate the abrasion stone with a speed of 311 rpm. Three concrete cylinders were tested at 28 days age to produce an average value. After each application of the abrasion test, the weight loss of the specimen was calculated in percentage by comparing its oven dried weight before and after the test (Eren, 1999).

Photo 20: Setup of Chloride Ion Penetration Test

Photo 21: Surface Abrasion Testing apparatus

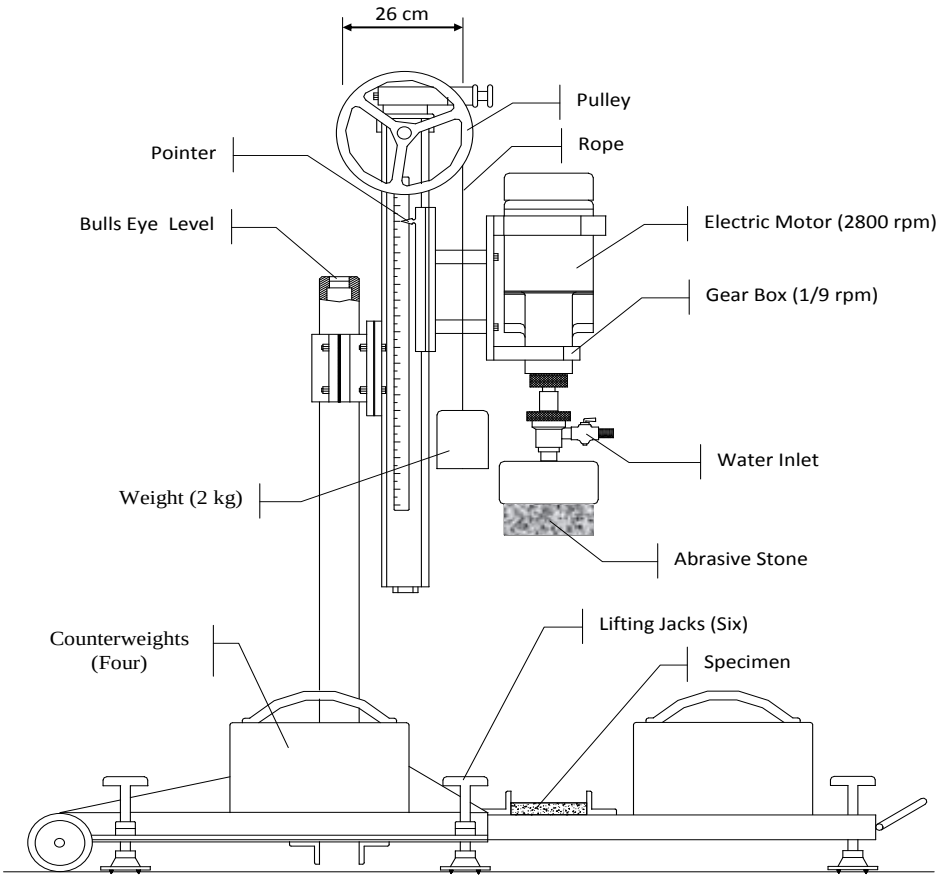

Figure 12: Abrasion test equipment

Source: (Eren, 1999)

3.8.9 Ultrasonic Pulse Velocity Test (UPV)

Ultrasonic pulse velocity test was performed on 150 mm cubes in accordance with the standards (ASTM C 597, 2009) as it is shown in Photo 22. Pulse velocity was determined by dividing the pulse time to length of path as shown in the following equation.

$$V = \frac{l}{t}$$

Where: *V = Velocity (km/sec),*

l = length of path (km) and

t = time (seconds)

Photo 22: The Pulse Velocity Test

Chapter 4

RESULTS AND DISCUSSIONS

4.1 Fresh properties of SCC and FR-SCC Mixes

The fresh properties (flowability, passingability, consistency, and segregation resistance) of SCC and FR-SCC mixes were evaluated using by slump flow tests (T50 and VSI), J-ring, V-funnel and column segregation test, respectively. It is known that using fibers within the concrete matrix will decrease the workability significantly. In this study; the workability and the consistency were maintained by gradually adjusting the chemical admixtures depending on the amount of steel fibers within the mixes. The results, given in Table 12, Figure 13, Figure 14 and Figure 15, show that, the SCC and FR-SCC mixes are complying with the requirements given in the literature.

By applying regression analysis through statistical approaches, it is observed that, there is a linear relation between the amount of fiber within the mixes and slump flow test results, J-ring test results, V-funnel test results and slump flow (T50) test results respectively as given in Figure 13 and Figure 14.

On the other hand a polynomial (2^{nd} order) regression relation was found between the column segregation test and fiber amount within the mixes as presented in Figure 15.

Table 12: Fresh properties results of SCC and FR-SCC mixes

Concrete Type	Slump Flow (mm)	T50 (sec)	VSI	J-Ring (mm)	V-Funnel (sec)	Column Segregation (%)
SCC	715	2.8	645	0	8.0	4.43
FR-SCC20	712	3.1	638	0	8.8	5.64
FR-SCC30	708	3.3	635	0	9.1	5.73
FR-SCC40	705	3.5	633	0	9.4	5.89

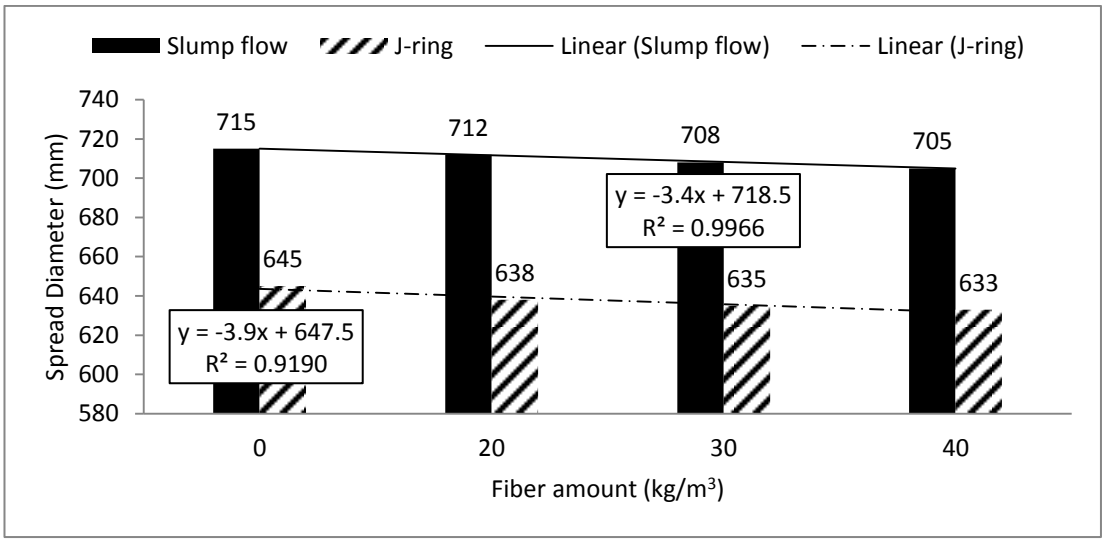

Figure 13: Slump flow test and J-ring test results

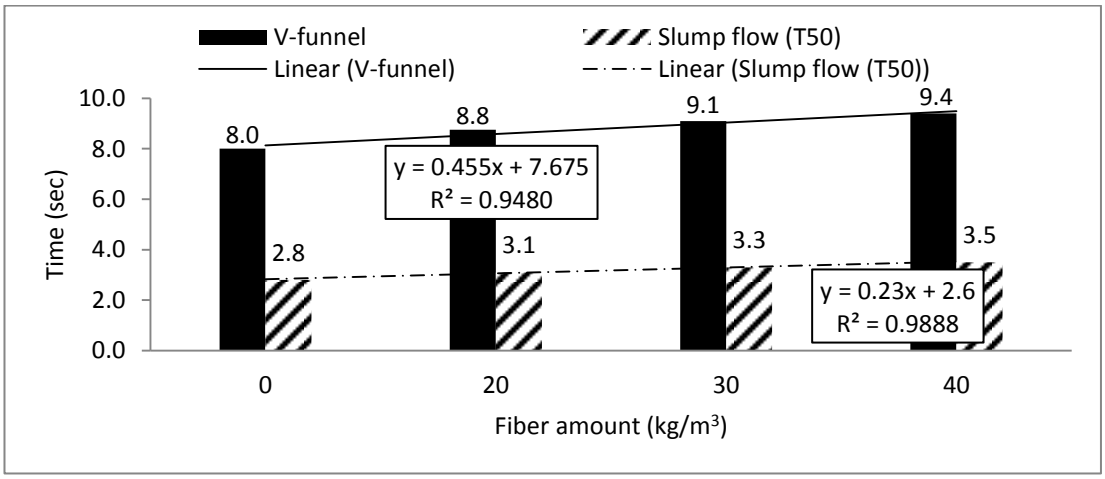

Figure 14: V-funnel test and Slump Flow (T50) test results

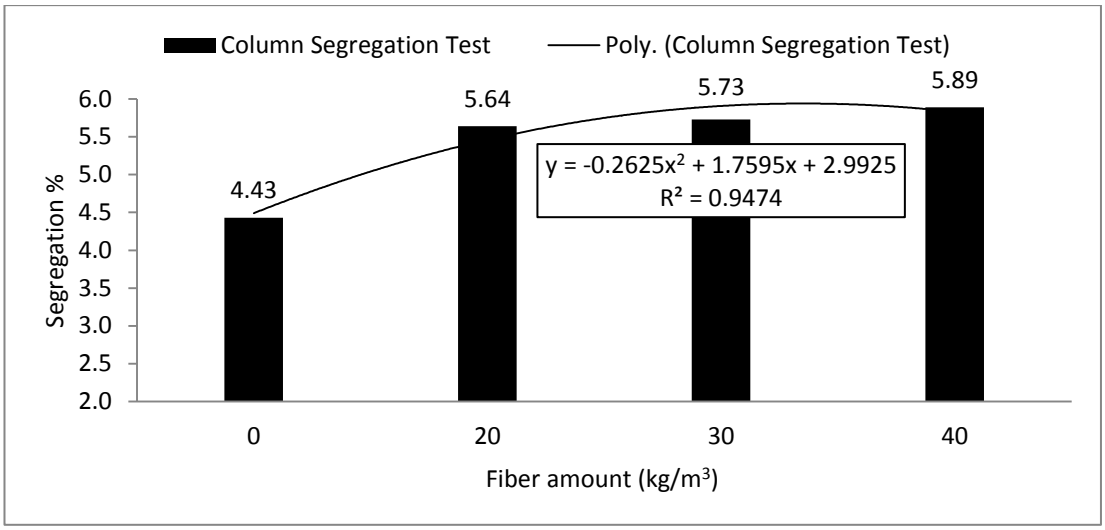

Figure 15: Column Segregation Test results

4.2 Compressive Strength Tests

The results of 7 and 28 days compressive strength tests of the mixes are given in Table 13 and Figure 16. It is observed that:

1. Due to the strength results over 60 MPa of SCC and FR-SCC mixes, these mixes can be considered as high strength concrete.
2. For 28 days compressive strength, fibers slightly improve the compressive strength of the mixes while for 7 days compressive strength; there is no clear effect of fibers on the compressive strength of the mixes. This may be due to the chemical structure of the cement type and silica fume which is directly related to the strength development, as well as the randomly distributed fibers that contain entrapped air voids could possibly affect the results. Similarly the amount of coarse aggregate, fine aggregate and silica fume together with the mix proportioning is a key factor that is directly affecting the overall strength and durability properties of concrete. Note that according to ACI, the strength is slightly affected by presence of fibers, hence to increasing its strength

between 0 to 15 percent with 1.5 percent by volume of fibers (ACI 544.1, 1996).

3. The highest 7 days compressive strength obtained is 48.22 MPa for FR-SCC40 with fiber content of 40 kg/m^3.
4. The compressive strength of mixes after 7 days are comparable to those obtained after 28 days. This was possible because of the use of silica fume, which usually tend to increase the early strength of concrete.
5. The highest 28 days compressive strength obtained is 65.12 MPa for FR-SCC40 with fiber content of 40 kg/m^3.
6. Figure 17 shows the percentage increase / decrease of 7 and 28 days compressive strength compared with SCC. This figure implies that:
   - Using fibers with different amount 20, 30 and 40 kg/m^3 respectively in the mixes improve the strength and the maximum improvement obtained is 8.14 % MPa from FR-SCC40 with fiber content of 40 kg/m^3.
   - Using 20 kg/m^3 and 30 kg/m^3 of steel fibers in FR-SCC20 reduced 7 days compressive strength by 6.76% and 6.63% respectively, compared to control mix SCC.
   - Using 40 kg/m^3 of steel fibers in FR-SCC20 increased 7 days compressive strength by 3.08% of the control mix SCC.

Table 13: The results of 7 and 28 days Compressive Strength Tests

Concrete Type	**The average (5 samples) results of 7 days compressive strength (MPa)**	**The average (5 samples) results of 28 days compressive strength (MPa)**
SCC	46.78	60.22
FR-SCC20	43.62	61.62
FR-SCC30	43.68	62.90
FR-SCC40	48.22	65.12

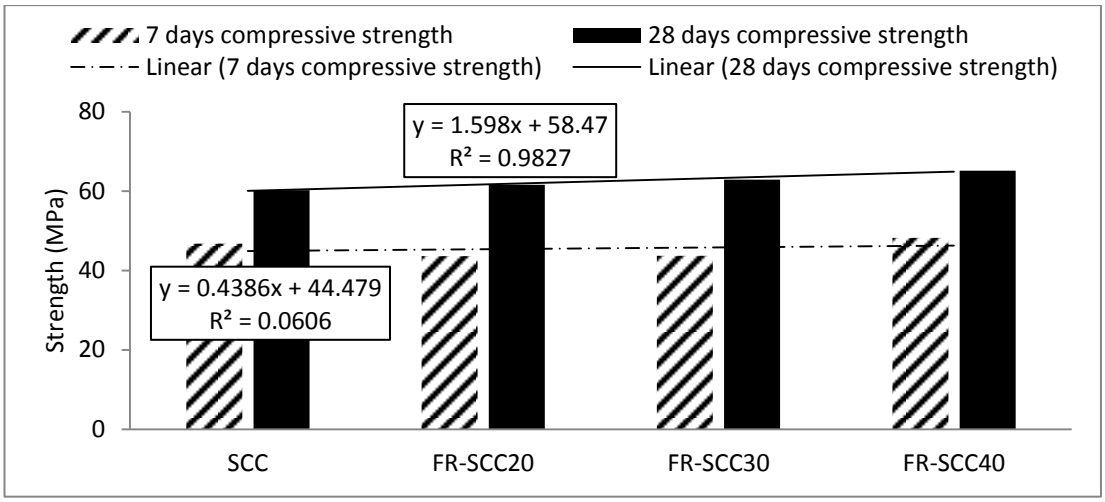

Figure 16: The average (5 samples) results of 7 and 28 days Compressive Strength

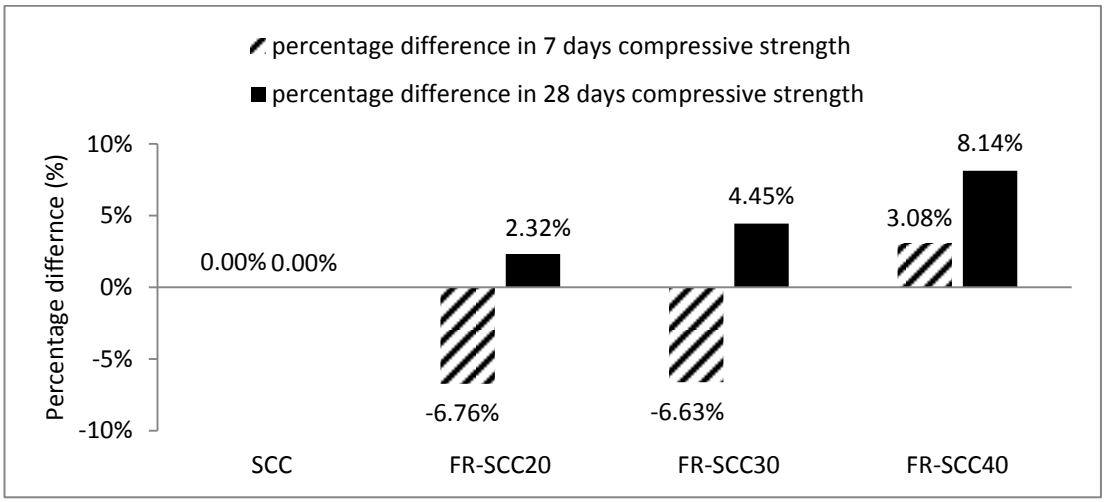

Figure 17: Percentage increase / decrease in Compressive Strength compared with control mix SCC

4.3 Splitting Tensile Strength Test

The results of splitting tensile strength test of the mixes are given in Table 14 and Figure 18 and it is found that:

1. Increasing the fiber contents increases the splitting tensile strength for all mixes. This in fact supports ACI which indicated that "the splitting tensile of mortar reinforced with steel fiber was reported to be about 2.5 times that of the unreinforced mortar when 3 percent fiber by volume was used and 2 times when 1.5 percent was used" (ACI 544.1, 1996).

2. The highest splitting tensile strength is 5.62 MPa from FR-SCC40 with fiber amount of 40 kg/m^3.
3. Figure 19 that shows the percentage increase / decrease of splitting tensile strength compared with control mix SCC and the highest increase is 13.26% from the mix FR-SCC40 with 40 kg/m^3.

Table 14: The average (5 samples) results of Splitting Tensile Strength Test

Concrete Type	**The average (5 samples) results of splitting tensile strength (MPa)**
SCC	4.96
FR-SCC20	4.99
FR-SCC30	5.54
FR-SCC40	5.62

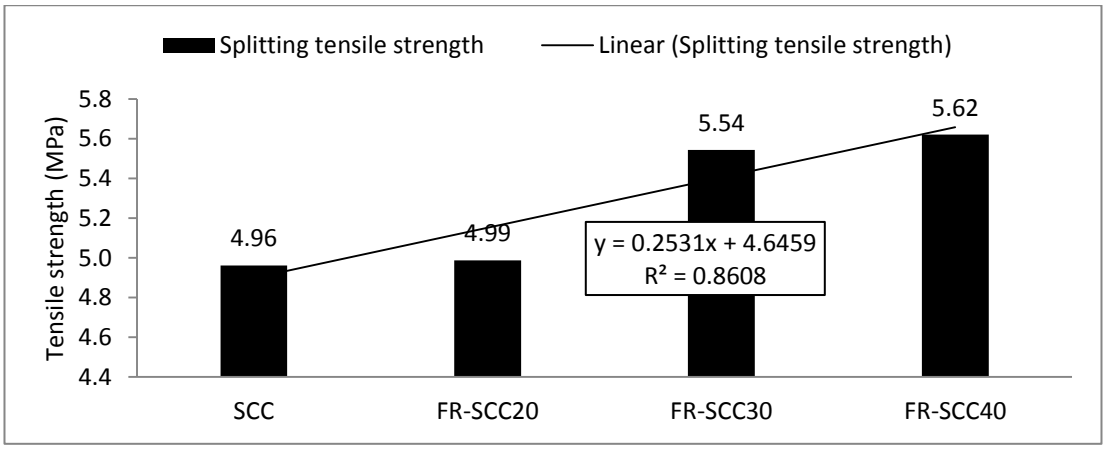

Figure 18: The average (5 samples) results of Splitting Tensile Strength

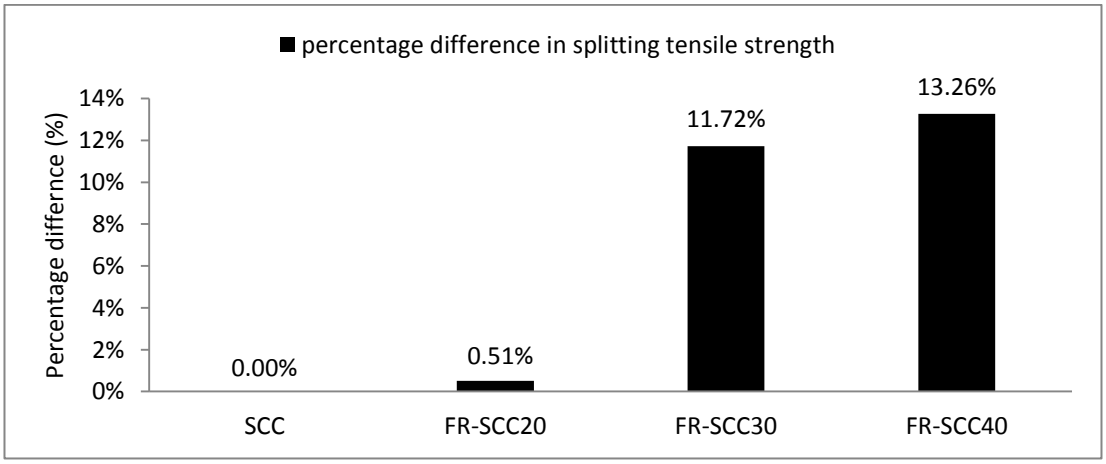

Figure 19: Percentage increase / decrease in Splitting Tensile Strength compared with control mix SCC

4.4 Flexural Strength Test

The results of flexural strength test of the mixes are given in Table 15 and Figure 20, and the followings can be concluded:

1. Although it is expected to see an increase in flexural strength of fiber reinforced concrete by increasing steel fibers, the flexural strength of control mix SCC is more than the flexural strength of fiber reinforced self-compacting concrete. The reason could be due to personal error during casing, sampling or testing or could be due to an error by the machine that was used for testing the flexural strength.
2. The highest flexural strength is obtained 7.05 MPa of SCC (plain concrete).

Table 15: The average (3 samples) results of Flexural Strength Test

Concrete Type	**The average (3 samples) results of flexural strength (MPa)**
SCC	7.05
FR-SCC20	6.69
FR-SCC30	6.67
FR-SCC40	6.92

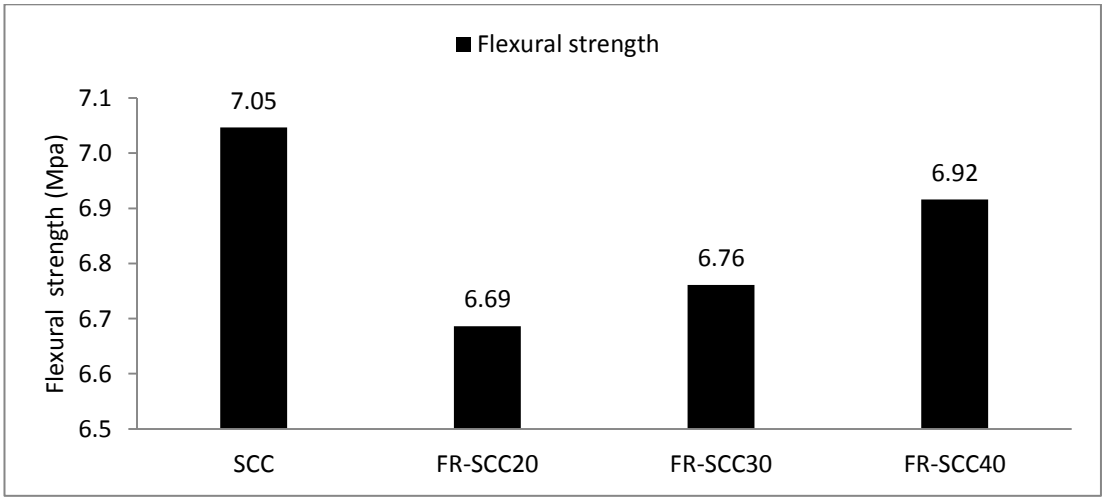

Figure 20: The average (3 samples) results of Flexural Strength Test

4.5 Impact Energy Test

The results of impact energy test at first crack and at complete failure are given in Table 16 and Figure 21, and the followings are concluded:

1. As the fiber volume fraction increases, impact energy at first crack and at complete failure increase for all the mixes. The reason could be due to the outstanding property of cement based fiber composite and crack control mechanism of the fibers. This directly relates to improvement in all other properties linked with cracking such as resistance to impact and energy absorption. Fibers prevent the total disintegration and shattering of concrete associated with shock loads. With explosive loading, the produced shock wave propagates as a compressional wave through a wall and is reflected on the opposite face of a tensile wave which causes spalling and disintegration of concrete. Steel fibers reduce the fragment velocity by 20% and even more important the fiber reinforcement enables the composite to retain its shape and integrity without being shattered into fragments (Eren, 1999).
2. From Figure 22, the maximum increase in impact energy at first crack is 700% compared with the impact energy of control mix SCC and it is obtained by FR-SCC40 which includes 40 kg/m^3 steel fibers.
3. Also from Figure 22, the maximum increase in impact energy at complete failure is 355.56% compared with the impact energy of control mix SCC and it is obtained by FR-SCC40 which includes 40 kg/m^3 steel fibers.

Table 16: The average (3 samples) results of Impact Energy Test

Concrete Type	The average results of Impact Energy at first crack (N.m)	The average (3 samples) results of Impact Energy at full failure (N.m)
SCC	12.21	36.63
FR-SCC20	52.91	81.40
FR-SCC30	77.33	138.37
FR-SCC40	97.68	166.86

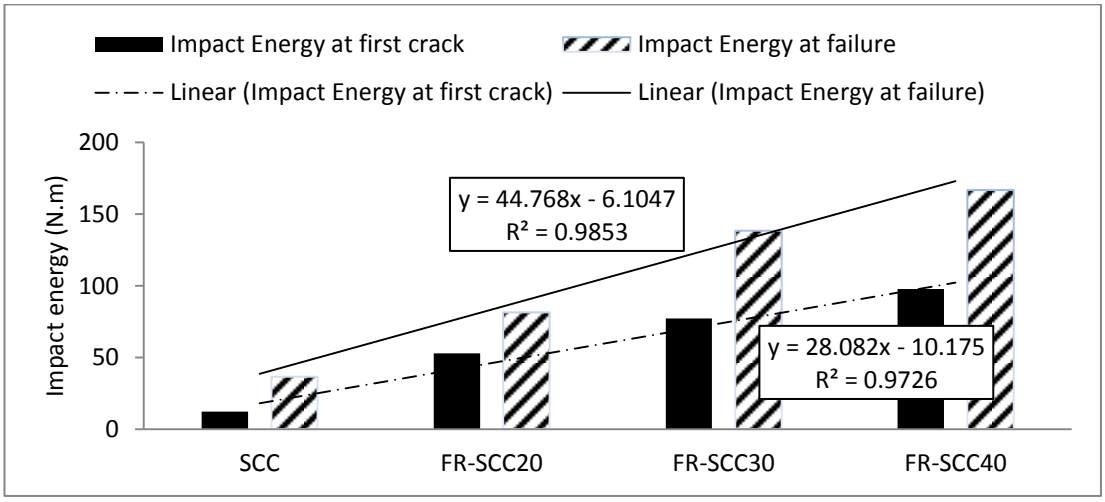

Figure 21: The average (3 samples) results of Impact Energy Test

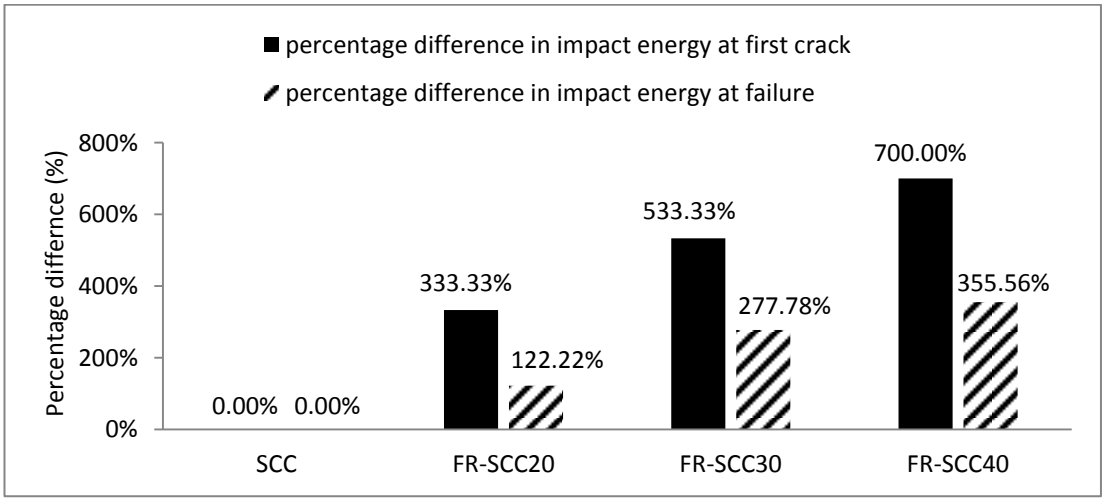

Figure 22: Percentage increase / decrease in Impact Energy compared with control mix SCC

4.6 Depth of Water Penetration Test

The results of depth of water penetration test of the mixes are given in Table 17 and Figure 23, and the followings can be said:

1. Using fibers increase the depth of water penetration of the concrete. The reason could be due to the voids content which is in fact more in the mixes with fibers than the voids content in the control mix SCC together with the randomly distribution of fibers in the mixes that will allow the water to penetrate more inside the concrete under the pressure.
2. The lowest water penetration resistance is obtained to be 14.50 mm from the FR-SCC 40 with 40 kg/m^3 of steel fibers. In order to accept the concrete resistant to the chemical attack, water should not penetrate to a depth of more than 50 mm in concrete likely to come in contact with slightly aggressive media and not more than 30 mm if concrete is likely to come in contact with aggressive media (Ozbay et al., 2009).
3. Figure 24 shows the percentage increase / decrease of water penetration compared with control mix SCC and the highest decrease is 73.72% from FR-SCC40 mix which contains 40 kg/m^3 fiber.

Table 17: The average (3 samples) results of Depth of Water Penetration Test

Concrete Type	**The average (3 samples) results of depth of water penetration (mm)**
SCC	8.35
FR-SCC20	9.00
FR-SCC30	11.00
FR-SCC40	14.50

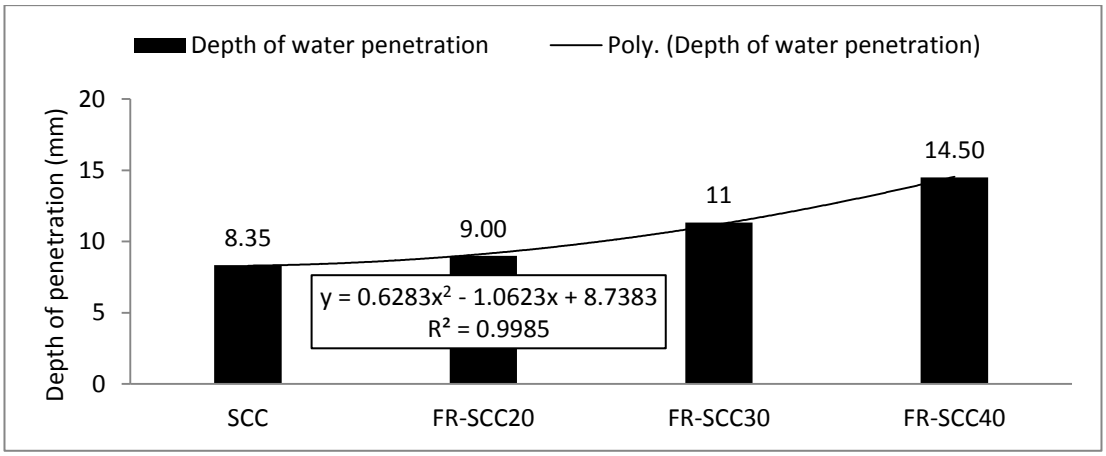

Figure 23: The average (3 samples) results of Depth of Water Penetration Test

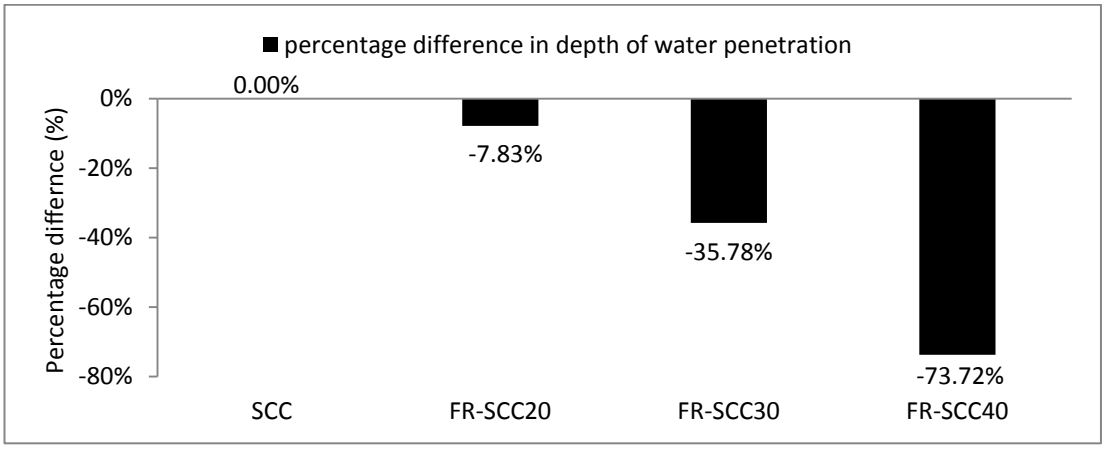

Figure 24: Percentage increase / decrease of Water Penetration compared with control mix SCC

4.7 Density, Absorption and Voids Content Tests

The results of density, absorption and voids content tests of the mixes are given in Table 18, Figure 25 and Figure 26, and the followings can be said:

1. Using 20 and 30 kg/m^3 of steel fibers, reduce the density of the concrete. Although it is expected to see an increase in density of fiber reinforced concrete by increasing steel fibers, no clear effect of fibers on the density is observed.

2. Although it is expected to see increases an in the absorption and voids content of fiber reinforced concrete by increasing steel fibers, no clear effect of fibers on the absorption and voids content is observed.

Table 18: The average (3 samples) results of Density, Absorption and Voids Tests

Concrete Name	Wet Density	Dry Density	Absorption %	Void content %
SCC	2.38	2.26	5.13	10.35
FR-SCC20	2.32	2.19	5.76	11.41
FR-SCC30	2.38	2.26	5.41	10.85
FR-SCC40	2.41	2.31	4.51	9.17

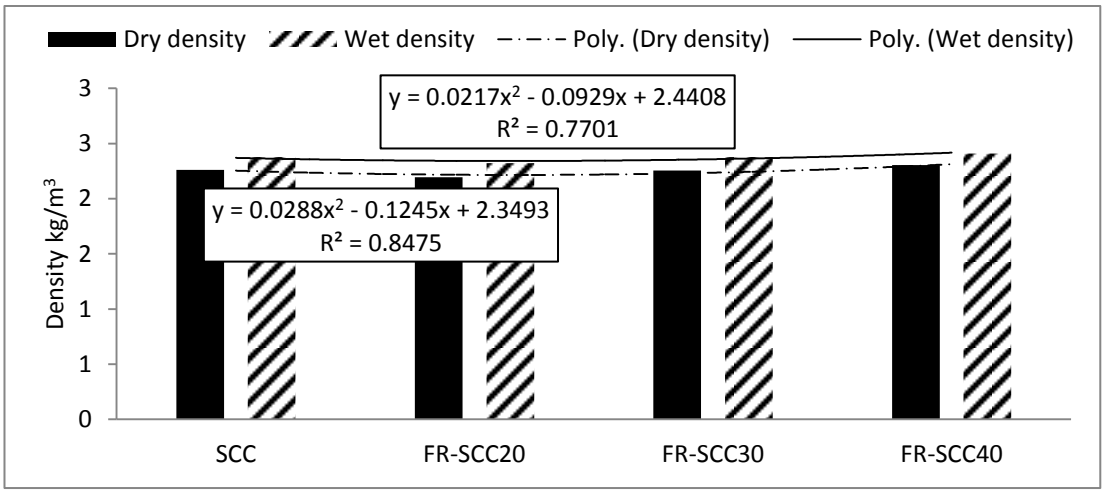

Figure 25: The average (3 samples) results of Wet Density and Dry Density

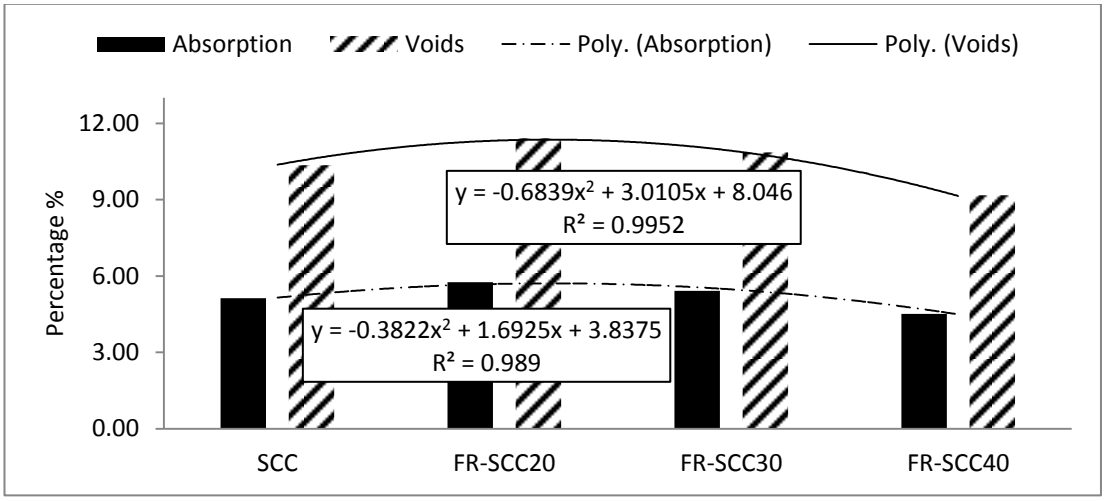

Figure 26: The average (3 samples) results of Absorption and Voids Tests

4.8 Chloride Ion Penetration Test

The results of chloride ion penetration test of the mixes are given in Table 19 and Figure 27, and the followings can be said:

1. Using fibers decrease the chloride ion penetration resistance of the concrete which supports the study that reports an increase in the total charge passing as the steel fiber volume fraction increases; this could be attributed to the electrical conductivity of the fibers (El-Dieb, 2009).
2. Table 20 shows the standard limits of chloride ion penetration according to ASTM. All chloride ion permeability values recorded indicate very low and negligible permeability according to standards classification (ASTM C 1202, 2010). Concrete electrical resistivity values support the findings in the RCPT. It should be noted that the resistivity values recorded for all mixes are very high which indicates very good protection to steel reinforcement against corrosion.
3. The highest chloride ion penetration resistance is 8 Coulombs obtained from the control mix SCC.
4. Figure 28 shows the percentage increase / decrease of chloride ion penetration compared with control mix SCC and the highest reduce in the chloride ion penetration resistance is 3740% obtained from FR-SCC40 with 40 kg/m3.

Table 19: The average (3 samples) results of Chloride Ion Penetration Test

Concrete Type	**The average (3 samples) results of chloride ion penetration (Coulombs)**
SCC	8
FR-SCC20	27
FR-SCC30	215
FR-SCC40	320

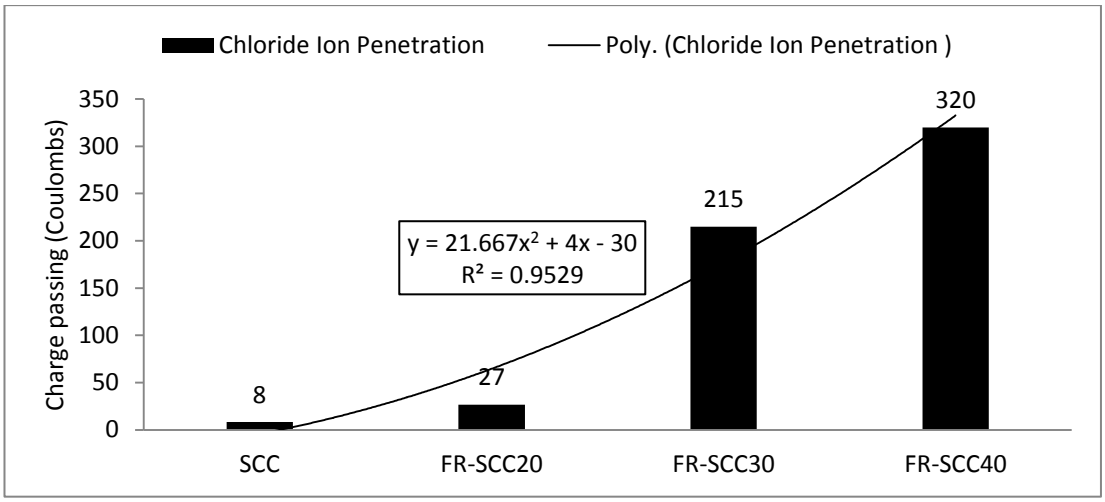

Figure 27: The average (3 samples) results of Chloride Ion Penetration Test

Table 20: Chloride Ion Penetrability Based on Charge Passed

Charge Passed (coulombs)	Chloride Ion Penetrability
> 4000	High
2000 - 4000	Moderate
1000 - 2000	Low
100 - 1000	Very Low
< 100	Negligible

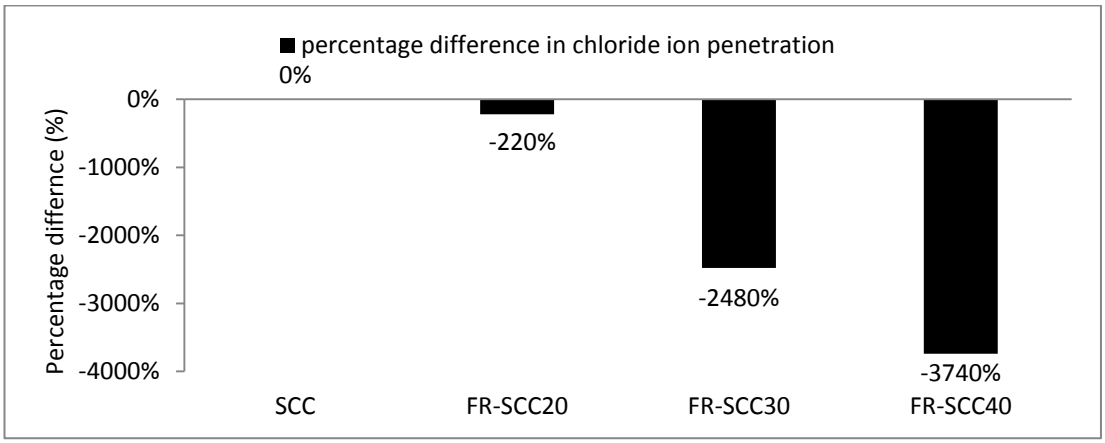

Figure 28: Percentage increase / decrease in chloride ion penetration compared with SCC

4.9 Surface Abrasion Test

The results of surface abrasion test of the mixes are given in Table 21, Figure 29 and Figure30. From the results the followings are deducted:

1. As it had been reported by Özgür Eren; using fibers slightly improve the surface abrasion resistance of the mixes (Eren, 1999).
2. The highest surface abrasion is obtained to be 3.99% (based on weight lost) from the control mix SCC. This is due to good bonding between fibers and cement matrix which makes it difficult for particles to be separated out from the concrete.
3. Figure 30 shows the percentage increase / decrease in surface abrasion compared with control mix SCC and the highest improvement is 9.40% obtained from FR-SCC40 which contains 40 kg/m^3 fiber.

Table 21: The average (3 samples) results of Surface Abrasion Test

Concrete Type	**Oven dry weight before the test (gr)**	**Oven dry weight after the test (gr)**	**Weight Loss (%)**
SCC	2156.27	2070.13	3.99
FR-SCC20	2255.67	2167.70	3.90
FR-SCC30	2458.73	2366.90	3.74
FR-SCC40	2396.50	2309.83	3.62

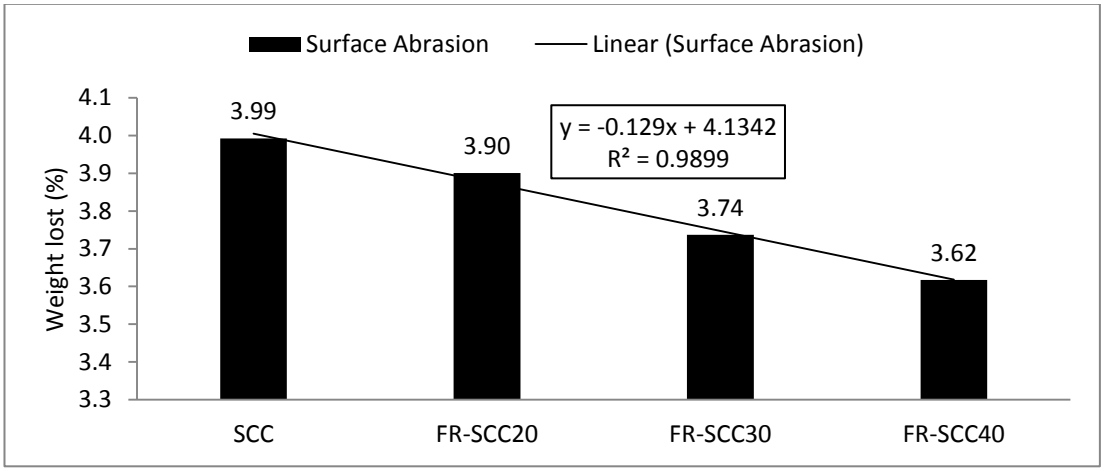

Figure 29: The average (3 samples) results of Surface Abrasion Test

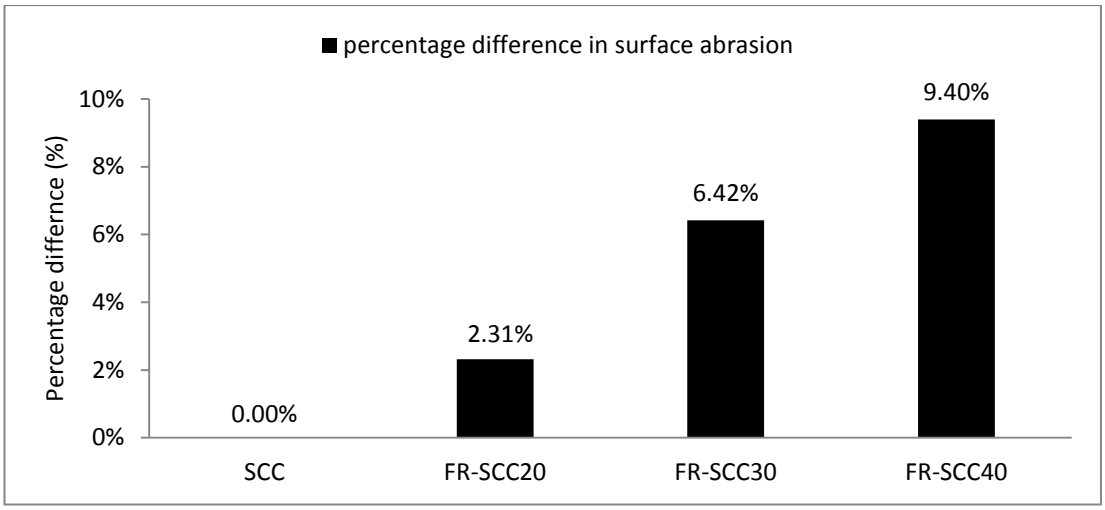

Figure 30: Percentage increase / decrease in Surface Abrasion compared with control mix SCC

4.10 Ultrasonic Pulse Velocity (UPV) Test

The results of ultrasonic pulse velocity test of the mixes are given in Table 22 and Figure 31, and the followings can be said:

1. Using fibers slightly increase the ultrasonic pulse velocity of the SCC mixes. The reason could be due to the availability of voids content in the mixes with fibers more than the voids content in the control mix SCC which will decrease the time needed for ultrasonic wave to pass, thus in directly proportional the velocity will be increased. Note that a general suggestion for the classification of quality of concrete by UPV technique for 2400 kg/m^3 density concretes. Concretes are classified as excellent, good, doubtful, poor, and very poor for 4.5 km/s and above, 3.50 – 4.50 km/s, 3.0 – 3.5 km/s, 2.0 – 3.0 km/s and 2.0 km/s and below UPV values, respectively (Whitehurst, 1951). The lower limit of good quality concrete is between 4.1 and 4.7 km/s UPV values. By using these proposed classification techniques, all produced concretes in this research are excellent quality (Jones & Gatfield, 1955).

2. The highest pulse velocity is 4.83 (km/s) obtained from the mix FR-SCC40 with 40 kg/m^3.

Table 22: The average (5 samples) results of Ultrasonic Pulse Velocity Test

Concrete Type	Time (mS)	Pulse velocity (km/s)
SCC	32.06	4.68
FR-SCC20	31.24	4.80
FR-SCC30	31.14	4.82
FR-SCC40	31.06	4.83

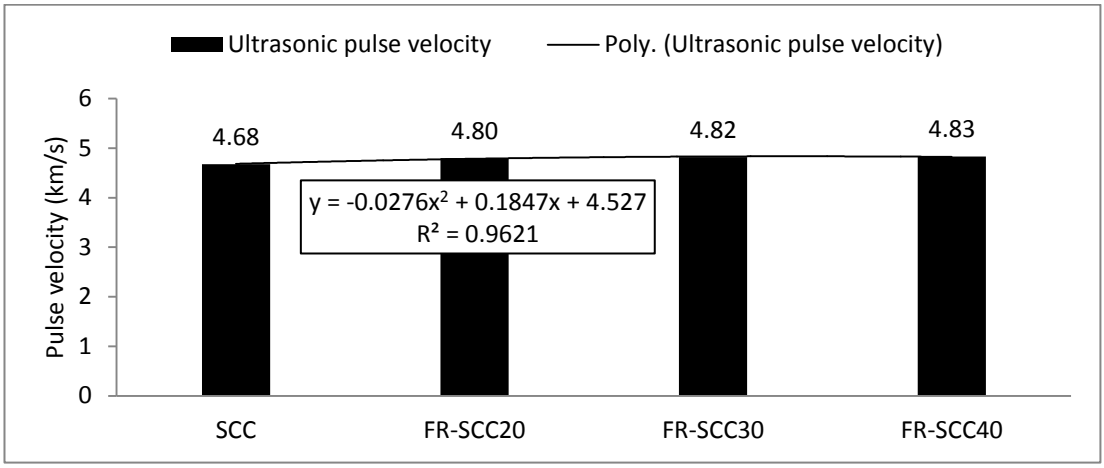

Figure 31: The average (5 samples) results of Ultrasonic Pulse Velocity Test

4.11 Statistical Analysis of the Results

The response data (results of SCC and FR-SCC tests) was analyzed using one-way analysis of variance (ANOVA for single factor - fixed effect model) technique using commercial software known as SPSS Statistics 17.0 at a 0.05 level of significance to examine the variation in the measured properties of the self-compacting and fiber reinforced self-compacting concretes. Steel fibers and Additives were selected as factors, whereas hardened properties of the concretes such as compressive strength, splitting tensile strength, flexural strength, impact energy, and depth of water penetration, density, absorption, voids content, chloride ion and ultrasonic pulse velocity tests were selected as dependent variables. A statistical analysis was performed to determine the statistically significant factors and data analysis are

presented in Table 23. The analysis of variance results of SCC and FR-SCC properties are presented in Table 24. The factor (steel fibers and additives) is considered to be significant if the level of significance in Table 24 is less than 0.05. Table 25 shows the multiple comparisons between the dependent variables. Standard deviation (sd) was also used to check the results in order to be sure that the values are not spread out too much and according to that value that spreading out of the standard deviation and the mean too much was eliminated, while regression analysis was done to study the relations between the models (see Appendix A and Appendix B).

Table 23: Statistical analysis of the results

Descriptive						
		N	**Mean**	**sd**	**Minimum**	**Maximum**
7 Days Compressive Strength (MPa)	0	5	46.780	1.018	45.70	47.90
	20	5	43.620	1.724	42.40	46.60
	30	5	43.680	0.444	43.30	44.40
	40	5	48.222	1.174	47.20	50.20
28 Days Compressive Strength (MPa)	0	5	60.220	4.249	56.00	66.50
	20	5	61.620	3.341	57.80	66.60
	30	5	62.900	2.184	60.40	65.20
	40	5	65.120	2.332	61.30	67.20
Ultrasonic pulse velocity km/s	0	5	4.678	0.032	4.64	4.72
	20	5	4.802	0.036	4.75	4.84
	30	5	4.816	0.018	4.79	4.84
	40	5	4.830	0.025	4.81	4.87
Splitting Tensile Strength (MPa)	0	5	4.962	0.240	4.63	5.22
	20	5	4.988	0.171	4.78	5.21
	30	5	5.544	0.124	5.41	5.75
	40	5	5.621	0.215	5.32	5.86
Flexural Strength (MPa)	0	3	7.047	0.055	6.99	7.10
	20	3	6.683	0.127	6.60	6.83
	30	3	6.763	0.199	6.62	6.99
	40	3	6.917	0.633	6.25	7.51
Chloride Ion Penetration (Coulombs)	0	3	8.333	1.528	7.00	10.00
	20	3	26.667	4.509	22.00	31.00
	30	3	215.000	7.000	207.00	220.00
	40	3	320.000	37.000	280.00	353.00

Depth of Water Penetration (mm)	0	3	8.347	1.845	6.70	10.34
	20	3	9.000	2.000	7.00	11.00
	30	3	11.333	1.528	10.00	13.00
	40	3	14.500	1.323	13.50	16.00
Impact Energy - first crack	0	3	12.210	0.000	12.21	12.21
	20	3	52.910	7.049	48.84	61.05
	30	3	77.330	14.099	61.05	85.47
	40	3	97.680	0.000	97.68	97.68
Impact Energy - full failure	0	3	36.630	0.000	36.63	36.63
	20	3	81.400	7.049	73.26	85.47
	30	3	138.370	7.049	134.30	146.51
	40	3	166.860	7.049	158.72	170.93
Surface Abrasion %	0	3	3.993	0.279	3.69	4.24
	20	3	3.900	0.030	3.87	3.93
	30	3	3.737	0.124	3.66	3.88
	40	3	3.617	0.304	3.28	3.87
Voids content %	0	3	10.350	0.446	9.89	10.78
	20	3	11.407	0.395	11.14	11.86
	30	3	10.850	0.479	10.30	11.18
	40	3	9.170	0.104	9.10	9.29
Absorption %	0	3	5.130	0.180	4.93	5.28
	20	3	5.757	0.246	5.60	6.04
	30	3	5.410	0.271	5.10	5.60
	40	3	4.517	0.035	4.48	4.55

Table 24: Analysis of variance results of SCC and FR-SCC properties

One-Way ANOVA						
		Sum of Squares	**df**	**Mean Square**	**F**	**Level of Significance**
7 Days Compressive Strength (MPa)	Between Groups	79.358	3	26.453	18.951	0.000
	Within Groups	22.334	16	1.396		
28 Days Compressive Strength (MPa)	Between Groups	64.961	3	21.654	2.197	0.128
	Within Groups	157.684	16	9.855		
Ultrasonic pulse velocity km/s	Between Groups	0.073	3	0.024	29.468	0.000
	Within Groups	0.013	16	0.001		
Splitting Tensile Strength (MPa)	Between Groups	1.861	3	0.620	16.734	0.000
	Within Groups	0.593	16	0.037		
Flexural	Between	0.235	3	0.078	0.682	0.587

Strength (MPa)	Groups					
	Within Groups	0.919	8	0.115		
Chloride Ion Penetration (Coulombs)	Between Groups	204541.667	3	68180.556	189.303	0.000
	Within Groups	2881.333	8	360.167		
Depth of Water Penetration (mm)	Between Groups	69.700	3	23.233	8.091	0.008
	Within Groups	22.972	8	2.871		
Impact Energy - first crack	Between Groups	12162.778	3	4054.259	65.267	0.000
	Within Groups	496.947	8	62.118		
Impact Energy - full failure	Between Groups	30506.930	3	10168.977	272.839	0.000
	Within Groups	298.168	8	37.271		
Surface Abrasion %	Between Groups	0.253	3	0.084	1.810	0.223
	Within Groups	0.373	8	0.047		
Voids content %	Between Groups	8.170	3	2.723	18.302	0.001
	Within Groups	1.190	8	0.149		
Absorption %	Between Groups	2.477	3	0.826	19.724	0.000
	Within Groups	0.335	8	0.042		

Table 25: Multiple comparisons between the dependent variables for SCC and FR-SCC mixes

Dependent Variable	**(I) Steel Fibers (kg/m^3)**	**(J) Steel Fibers (kg/m^3)**	**Mean Difference (I-J)**	**Level of Significance**	**Mean Ratio (J/I)**
7 Days Compressive Strength (MPa)	0	20	3.160*	0.001	0.932
		30	3.100*	0.001	0.934
		40	-1.442	0.072	1.031
	20	0	-3.160*	0.001	1.072
		30	-0.060	0.937	1.001
		40	-4.602*	0.000	1.106
	30	0	-3.100*	0.001	1.071
		20	0.060	0.937	0.999
		40	-4.542*	0.000	1.104
	40	0	1.442	0.072	0.970
		20	4.602*	0.000	0.905

		30	4.542*	0.000	0.906
28 Days Compressive Strength (MPa)	0	20	-1.400	0.491	1.023
		30	-2.680	0.196	1.045
		40	-4.900*	0.025	1.081
	20	0	1.400	0.491	0.977
		30	-1.280	0.528	1.021
		40	-3.500	0.097	1.057
	30	0	2.680	0.196	0.957
		20	1.280	0.528	0.980
		40	-2.220	0.280	1.035
	40	0	4.900*	0.025	0.925
		20	3.500	0.097	0.946
		30	2.220	0.280	0.966
Ultrasonic pulse velocity km/s	0	20	-0.124*	0.000	1.027
		30	-0.138*	0.000	1.029
		40	-0.152*	0.000	1.032
	20	0	0.124*	0.000	0.974
		30	-0.014	0.453	1.003
		40	-0.028	0.144	1.006
	30	0	0.138*	0.000	0.971
		20	0.014	0.453	0.997
		40	-0.014	0.453	1.003
	40	0	0.152*	0.000	0.969
		20	0.028	0.144	0.994
		30	0.014	0.453	0.997
Splitting Tensile Strength (MPa)	0	20	-0.025	0.839	1.005
		30	-0.582*	0.000	1.118
		40	-0.658*	0.000	1.133
	20	0	0.025	0.839	0.995
		30	-0.557*	0.000	1.112
		40	-0.633*	0.000	1.127
	30	0	0.582*	0.000	0.895
		20	0.557*	0.000	0.899
		40	-0.076	0.539	1.013
	40	0	0.658*	0.000	0.883
		20	0.633*	0.000	0.888
		30	0.076	0.539	0.987
Flexural Strength (MPa)	0	20	0.363	0.226	0.948
		30	0.283	0.336	0.960
		40	0.130	0.651	0.982
	20	0	-0.363	0.226	1.054
		30	-0.080	0.780	1.012
		40	-0.233	0.424	1.035
	30	0	-0.283	0.336	1.042
		20	0.080	0.780	0.988
		40	-0.153	0.595	1.023
	40	0	-0.130	0.651	1.019
		20	0.233	0.424	0.966

		30	0.153	0.595	0.978
Chloride Ion Penetration (Coulombs)	0	20	-18.333	0.271	3.200
		30	-206.667*	0.000	25.800
		40	-311.667*	0.000	38.400
	20	0	18.333	0.271	0.313
		30	-188.333*	0.000	8.063
		40	-293.333*	0.000	12.000
	30	0	206.667*	0.000	0.039
		20	188.333*	0.000	0.124
		40	-105.000*	0.000	1.488
	40	0	311.667*	0.000	0.026
		20	293.333*	0.000	0.083
		30	105.000*	0.000	0.672
Depth of Water Penetration (mm)	0	20	-0.653	0.649	1.078
		30	-2.987	0.063	1.358
		40	-6.153*	0.002	1.737
	20	0	0.653	0.649	0.927
		30	-2.333	0.130	1.259
		40	-5.500*	0.004	1.611
	30	0	2.987	0.063	0.736
		20	2.333	0.130	0.794
		40	-3.167	0.051	1.279
	40	0	6.153*	0.002	0.576
		20	5.500*	0.004	0.621
		30	3.167	0.051	0.782
Impact Energy - first crack	0	20	-40.700*	0.000	4.333
		30	-65.120*	0.000	6.333
		40	-85.470*	0.000	8.000
	20	0	40.700*	0.000	0.231
		30	-24.420*	0.005	1.462
		40	-44.770*	0.000	1.846
	30	0	65.120*	0.000	0.158
		20	24.420*	0.005	0.684
		40	-20.350*	0.013	1.263
	40	0	85.470*	0.000	0.125
		20	44.770*	0.000	0.542
		30	20.350*	0.013	0.792
Impact Energy - full failure	0	20	-44.770*	0.000	2.222
		30	-101.740*	0.000	3.778
		40	-130.230*	0.000	4.555
	20	0	44.770*	0.000	0.450
		30	-56.970*	0.000	1.700
		40	-85.460*	0.000	2.050
	30	0	101.740*	0.000	0.265
		20	56.970*	0.000	0.588
		40	-28.490*	0.000	1.206
	40	0	130.230*	0.000	0.220
		20	85.460*	0.000	0.488

		30	28.490*	0.000	0.829
Surface Abrasion %	0	20	0.093	0.611	0.977
		30	0.257	0.184	0.936
		40	0.377	0.065	0.906
	20	0	-0.093	0.611	1.024
		30	0.163	0.381	0.958
		40	0.283	0.147	0.927
	30	0	-0.257	0.184	1.069
		20	-0.163	0.381	1.044
		40	0.120	0.515	0.968
	40	0	-0.377	0.065	1.104
		20	-0.283	0.147	1.078
		30	-0.120	0.515	1.033
Voids content %	0	20	-1.057*	0.010	1.102
		30	-0.500	0.151	1.048
		40	1.180*	0.006	0.886
	20	0	1.057*	0.010	0.907
		30	0.557	0.115	0.951
		40	2.237*	0.000	0.804
	30	0	0.500	0.151	0.954
		20	-0.557	0.115	1.051
		40	1.680*	0.001	0.845
	40	0	-1.180*	0.006	1.129
		20	-2.237*	0.000	1.244
		30	-1.680*	0.001	1.183
Absorption %	0	20	-0.627*	0.006	1.122
		30	-0.280	0.132	1.055
		40	0.613*	0.006	0.880
	20	0	0.627*	0.006	0.891
		30	0.347	0.072	0.940
		40	1.240*	0.000	0.785
	30	0	0.280	0.132	0.948
		20	-0.347	0.072	1.064
		40	0.893*	0.001	0.835
	40	0	-0.613*	0.006	1.136
		20	-1.240*	0.000	1.275
		30	-0.893*	0.001	1.198
* The mean difference is significant at the 0.05 level					

4.11.1 Model Adequacy Checking

The decomposition of the variability in the observations through an analysis of variance identity is a purely algebraic relationship. However, the use of the partitioning to test formally for no differences in treatment means requires that

certain assumptions be satisfied. Specifically, these assumptions are that the residuals are normally distributed and the residuals are constant.

In practice, however, these assumptions will usually not hold exactly. Consequently, it is usually unwise to rely on the analysis of variance until the validity of these assumptions has been checked. Violations of the basic assumptions and model adequacy can be easily investigated by the examination of residuals. If the model is adequate, the residuals should be structureless; that is, they should contain no obvious patterns (Montgomery, 2001).

4.11.1.1 Normal Distribution Check for the Residuals

The residuals were checked for normally distribution using Probability-Probability (P-P) Plot.

The probability-probability (P-P) plot is constructed using the theoretical cumulative distribution function, F(x), of the specified model. The values in the sample of data, in order from smallest to largest, are denoted $x_{(1)}, x_{(2)}..., x_{(n)}$. For i = 1, 2..., n, $F(x_{(i)})$ is plotted against [pk = (k – ½)/n].

Where; *pk: Normal Probability*

k: Order label of observation

n: Number of observations

The (P-P) plots for the dependent variables are shown in the Figures (32 - 43) and from the figures it can be said that the residuals are structureless and contain no obvious patterns.

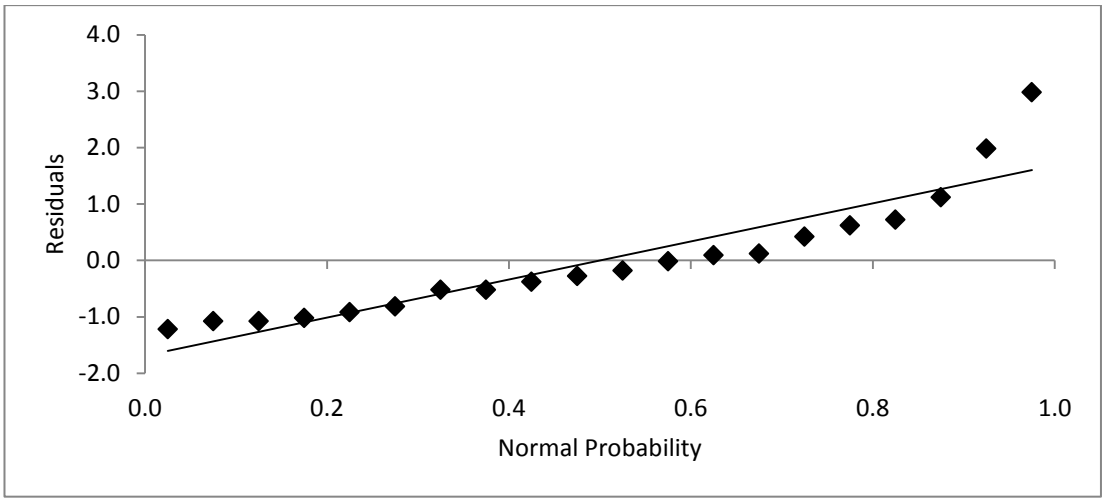

Figure 32: (P-P) Plot for 7 Days Compressive Strength Results

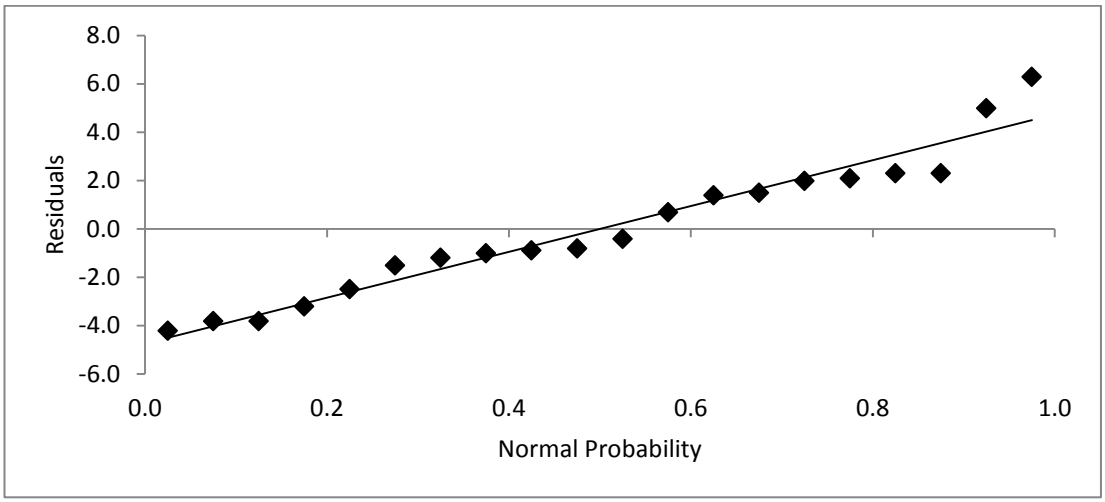

Figure 33: (P-P) Plot for 28 Days Compressive Strength Results

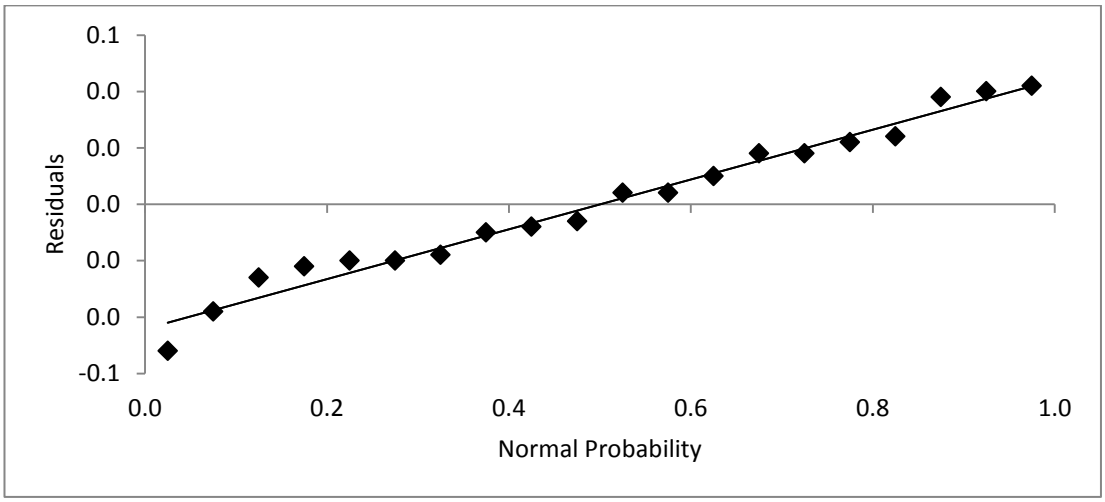

Figure 34: (P-P) Plot for Ultrasonic Results

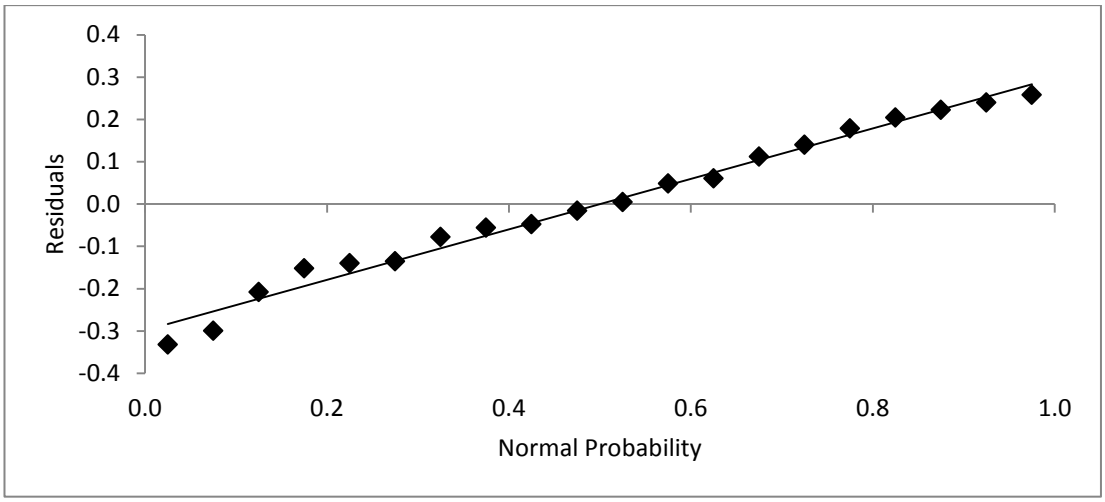

Figure 35: (P-P) Plot for Splitting Tensile Strength Results

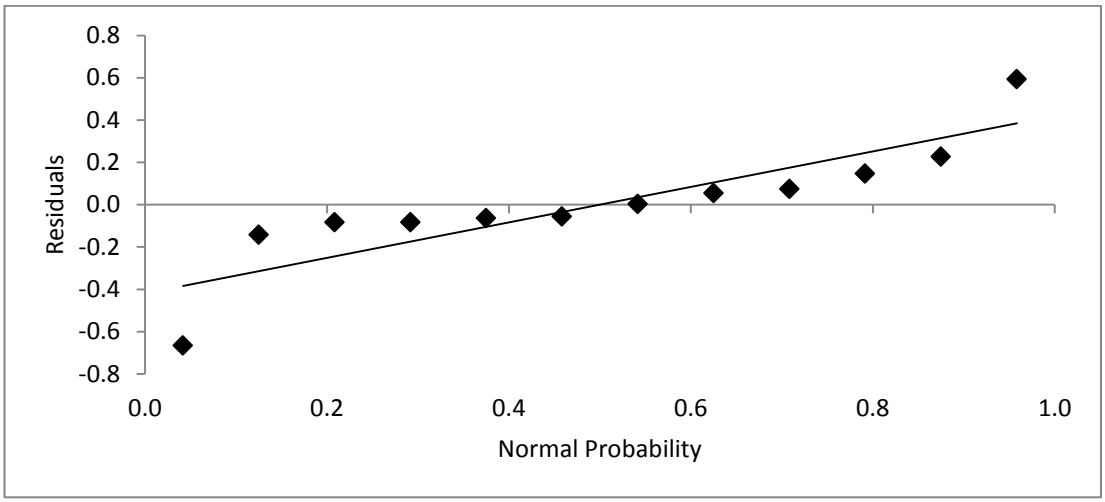

Figure 36: (P-P) Plot for Flexural Strength Results

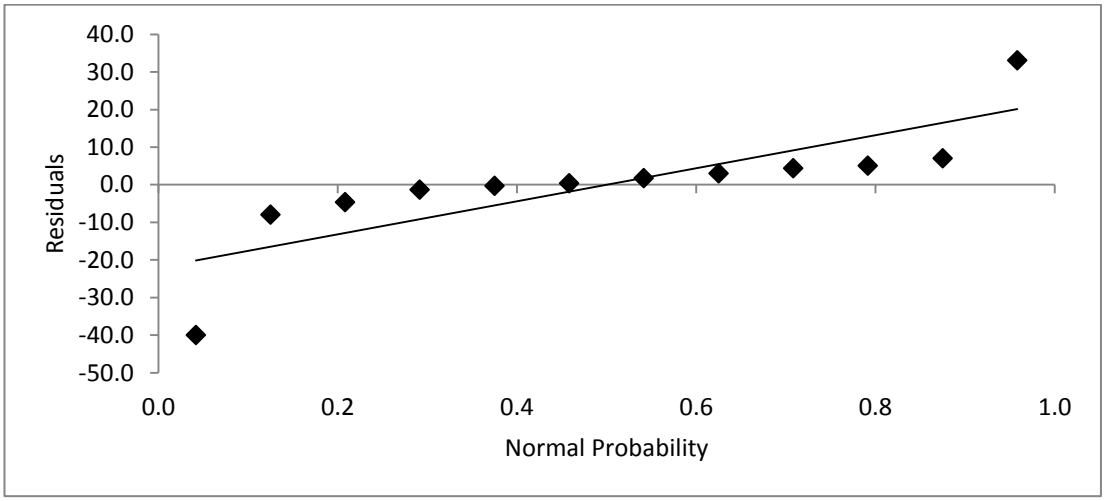

Figure 37: (P-P) Plot for Chloride Ion Penetration Results

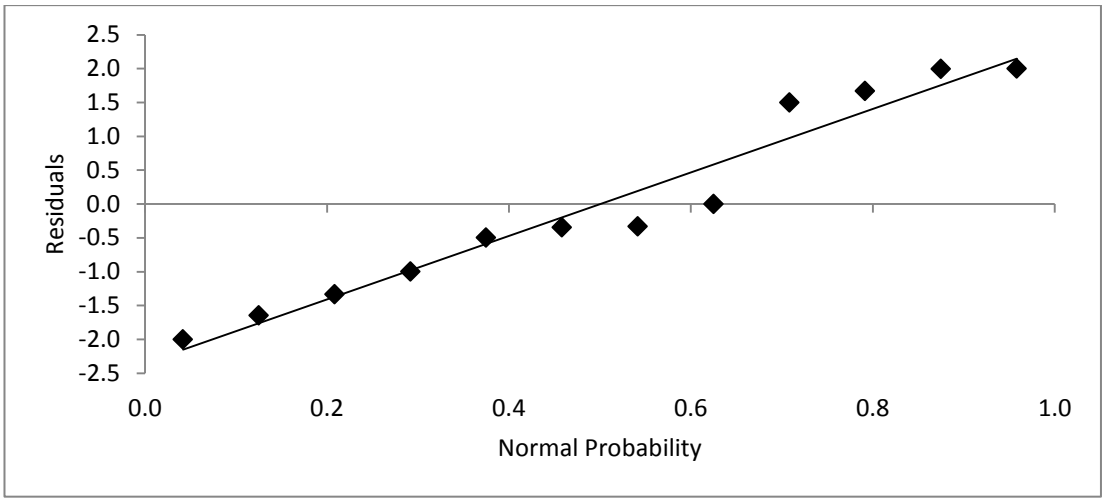

Figure 38: (P-P) Plot for Depth of Water Penetration Results

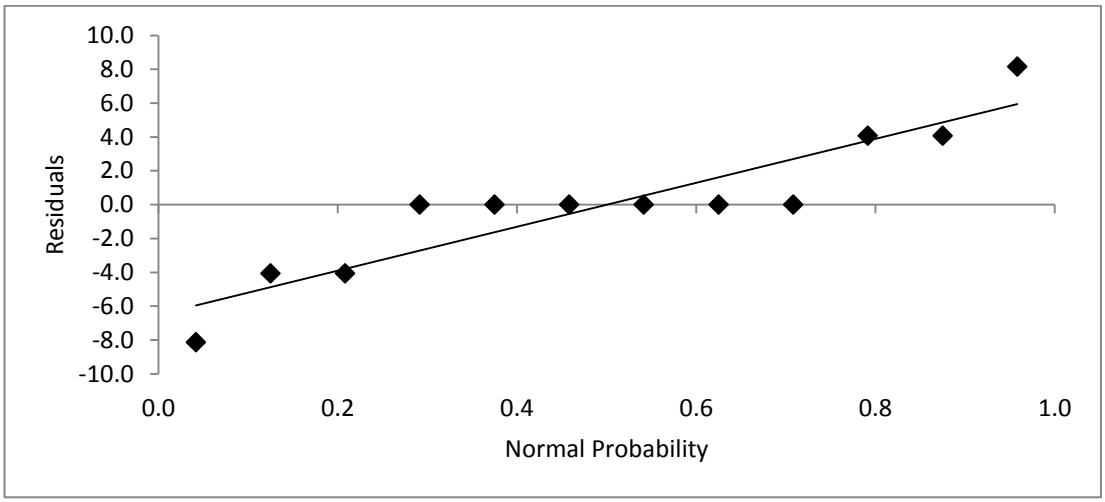

Figure 39: (P-P) Plot for Impact Energy (first crack) Results

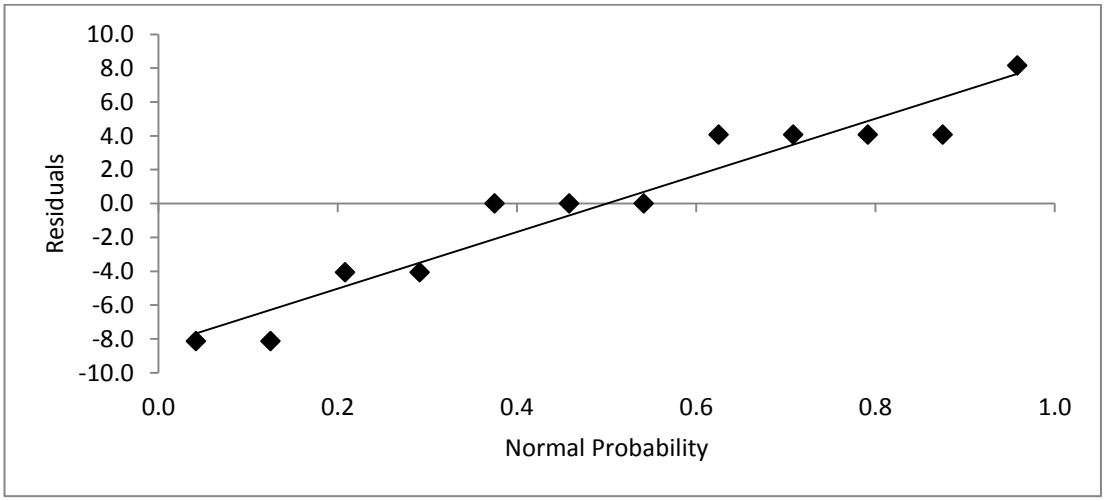

Figure 40: (P-P) Plot for Impact Energy (full failure) Results

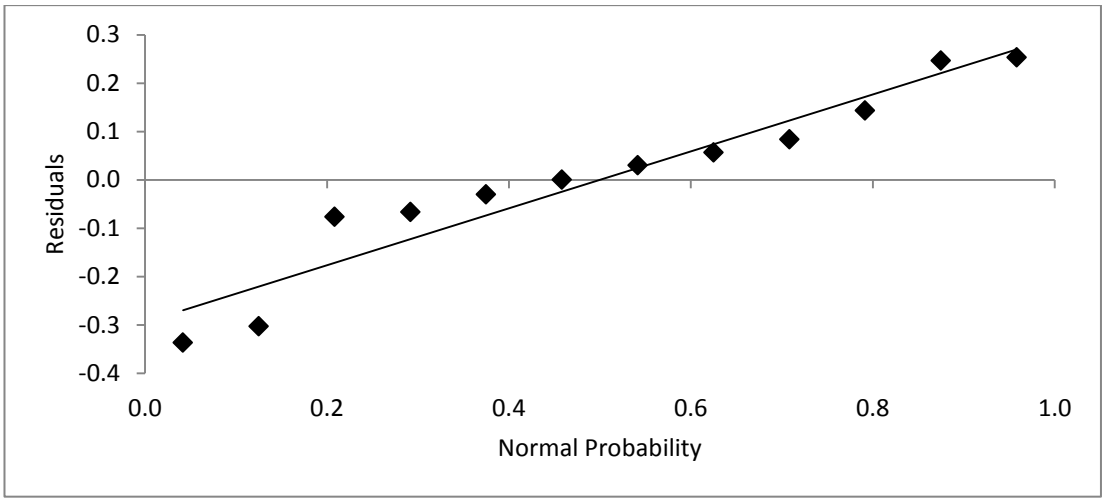

Figure 41: (P-P) Plot for Surface Abrasion Results

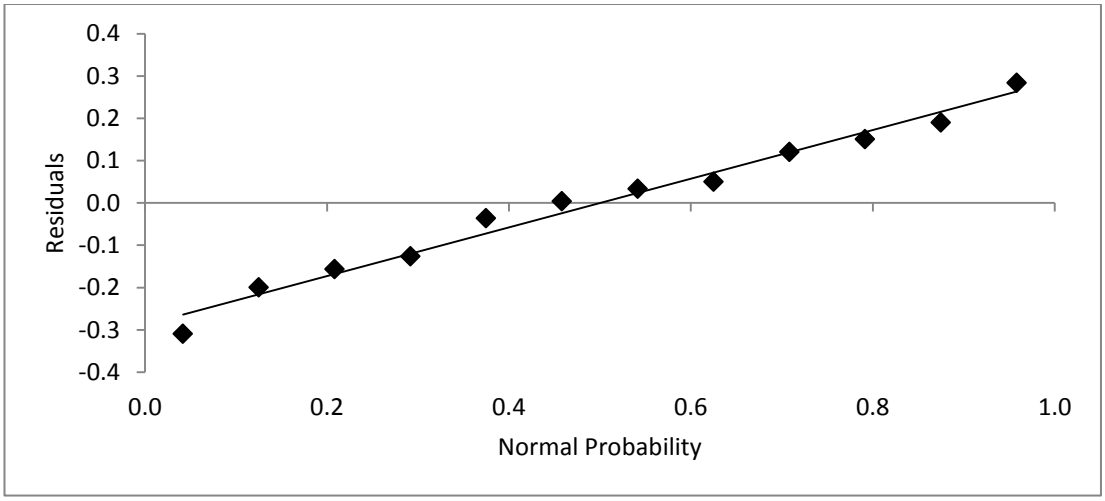

Figure 42: (P-P) Plot for Absorption Results

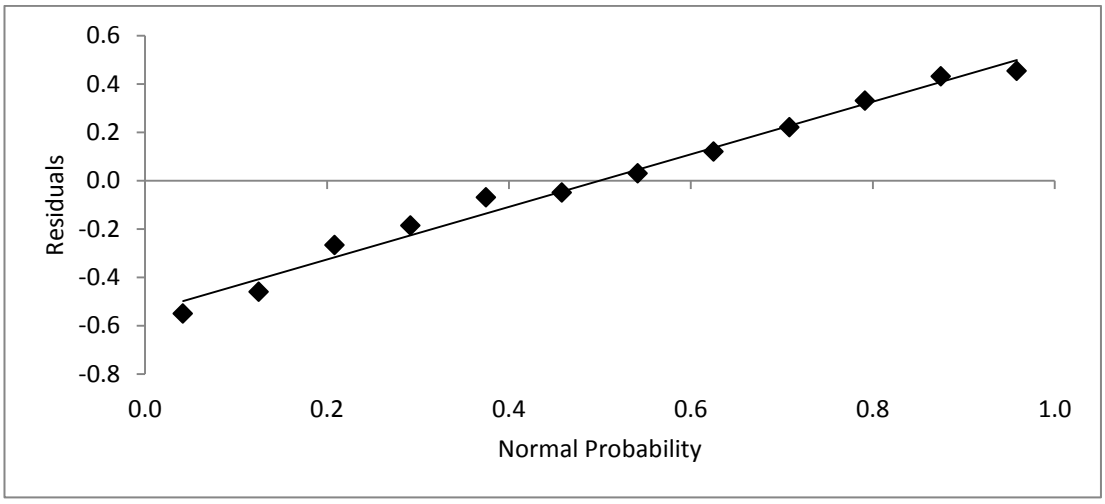

Figure 43: (P-P) Plot for Voids Contents Results

4.11.1.2 Constancy Check for the Residuals

Since the model is balanced model (equal sample sizes in all treatments) fixed effect model the constancy test is only slightly affected although the constancy is violated. However, in unbalanced designs or in cases where one variance is very much larger than the others, the problem is more serious (Montgomery, 2001).

4.12 Relationships between the Test Results

In order to find the relations between the results; different regression types were applied to each model with the correlation factor R^2. Depending on the correlation factor R^2; best regression type is selected.

4.12.1 Relationship between Compressive Strength and Splitting Tensile Strength

In order to quantify the variation of splitting tensile strength of the concrete mixes as a function of 28 days compressive strength; different regression types were applied to the model with the correlation factor R^2 as it is presented in Table 26, from the table it is observed that it is not a very strong correlation. Figure 44 shows the variation of splitting tensile strength with the 28 days compressive strength for the concrete mixes; from the figure, a linear relation with directly proportional relation can be seen. As compressive strength increases, splitting tensile strength increases respectively.

Table 26: Different regression types for the relation between Splitting Tensile Strength and 28 days Compressive Strength

Regression Type	**Equation**	**R^2**
Exponential	$y = 0.8702e^{0.0288x}$	0.8079
Linear	$y = 0.1523x - 4.2373$	0.8102
Logarithmic	$y = 9.565\ln(x) - 34.265$	0.8126
Polynomial (2^{nd} order)	$y = -0.0131x^2 + 1.7938x - 55.679$	0.8239
Power	$y = 0.003x^{1.8105}$	0.8103

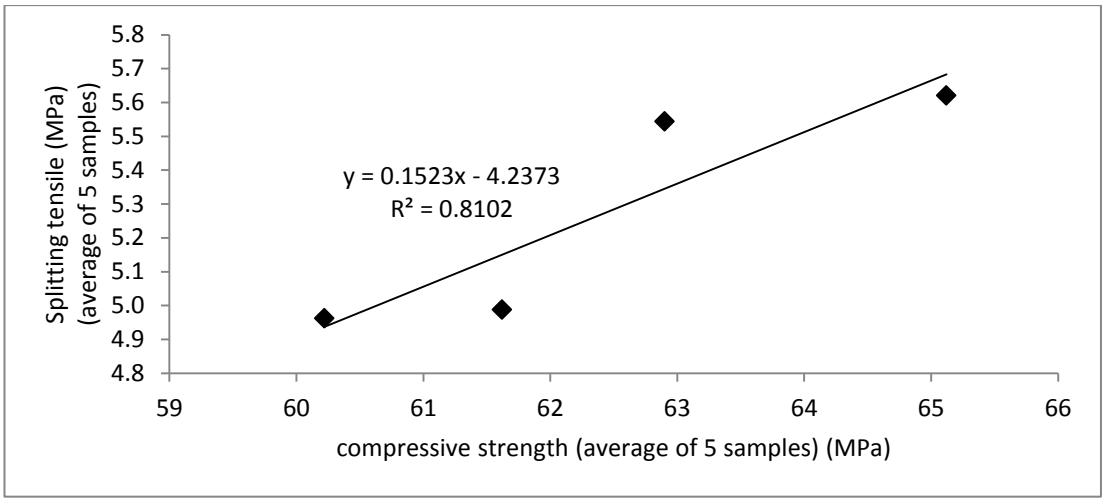

Figure 44: Variation of Splitting Tensile Strength with the 28 days Compressive Strength for the concrete mixes

4.12.2 Relationship between Compressive Strength and Depth of Water Penetration

In order to quantify the variation of depth of water penetration of the concrete mixes as a function of 28 days compressive strength; a linear regression analysis is chosen from Table 27 depending on R^2. Since there is no big difference between the regression types; a linear regression analysis is chosen since it clearly represents the relation between the results. Figure 45 shows the variation of depth of water penetration with the 28 days compressive strength for the concrete mixes; from the figure, a directly proportional relation can be seen. As compressive strength increases, depth of water penetration increases respectively.

Table 27: Different regression types for the relation between Depth of Water Penetration and 28 days Compressive Strength

Regression Type	**Equation**	**R^2**
Exponential	$y = 0.0066e^{0.1182x}$	0.9739
Linear	y = 1.315x - 71.343	0.9669
Logarithmic	y = 9.565ln(x) - 34.265	0.9635
Polynomial (2^{nd} order)	y = 0.1192x2 - 13.639x + 397.3	0.9852
Power	$y = 5E\text{-}13x^{7.4038}$	0.9721

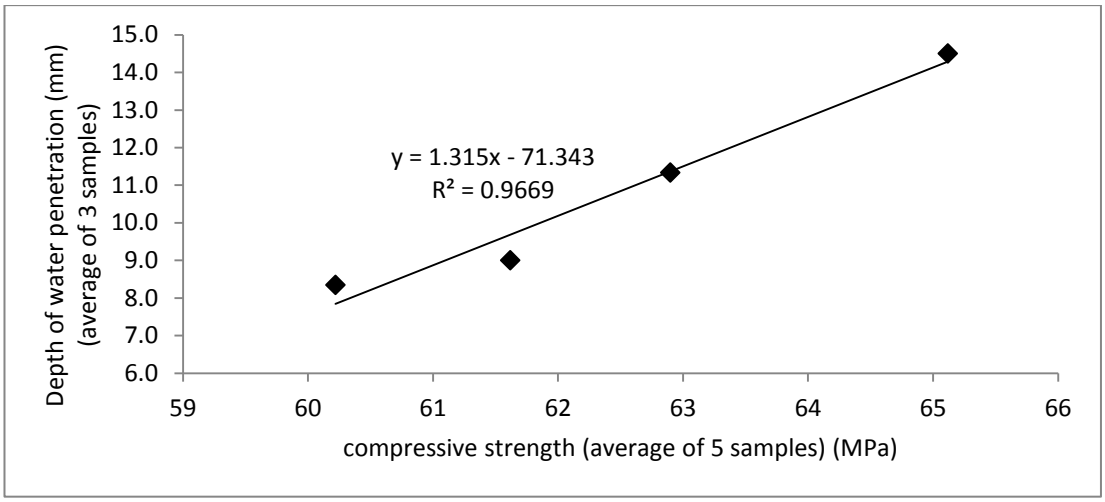

Figure 45: Variation of Depth of Water Penetration with the 28 days Compressive Strength for the concrete mixes

4.12.3 Relationship between Compressive Strength and Ultrasonic Pulse Velocity

In order to quantify the variation of ultrasonic pulse velocity of the concrete mixes as a function of 28 days compressive strength; A polynomial (2^{nd} order) regression analysis is chosen from Table 28 depending on R^2. Figure 46 shows the variation of ultrasonic pulse velocity with the 28 days compressive strength for the concrete mixes; from the figure, a directly proportional relation can be seen. As compressive strength increases, ultrasonic pulse velocity increases respectively. On the other hand a linear relation was suggested by Neville and Brooks. The reason could be due to the presence of moisture content or the presence of steel fibers which are affecting the relation (Neville & Brooks, 2008).

Table 28: Different regression types for the relation between Ultrasonic Pulse Velocity and 28 days Compressive Strength

Regression Type	**Equation**	**R^2**
Exponential	$y = 3.3363e^{0.0058x}$	0.6707
Linear	$y = 0.0274x + 3.0699$	0.6728
Logarithmic	$y = 1.7316\ln(x) - 2.377$	0.6833
Polynomial (2^{nd} order)	$y = -0.0117x^2 + 1.5015x - 43.126$	0.9564
Power	$y = 1.0615x^{0.364}$	0.6813

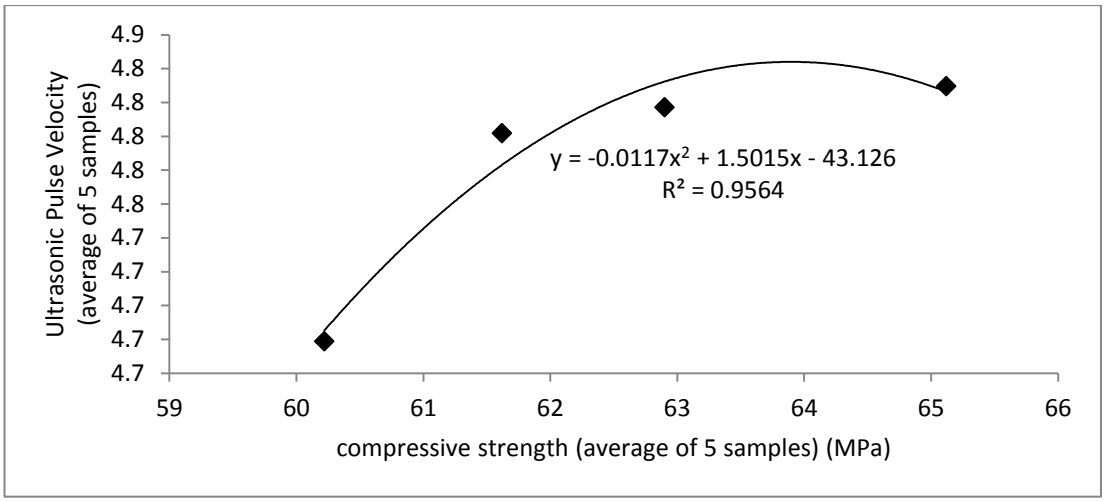

Figure 46: Variation of Ultrasonic Pulse Velocity with the 28 days Compressive Strength for the concrete mixes

4.12.4 Relationship between Compressive Strength and Absorption

In order to quantify the variation of absorption of the concrete mixes as a function of 28 days compressive strength; A polynomial (2^{nd} order) regression analysis is chosen from Table 29 depending on R^2. Figure 47 shows the variation of absorption with the 28 days compressive strength for the concrete mixes.

Table 29: Different regression types for the relation between Absorption and 28 days Compressive Strength

Regression Type	**Equation**	**R^2**
Exponential	$y = 37.647e^{-0.032x}$	0.4074
Linear	$y = -0.1567x + 14.991$	0.3835
Logarithmic	$y = -9.68\ln(x) + 45.22$	0.3723
Polynomial (2^{nd} order)	$y = -0.1249x^2 + 15.514x - 476.09$	0.9423
Power	$y = 17279x^{-1.962}$	0.3959

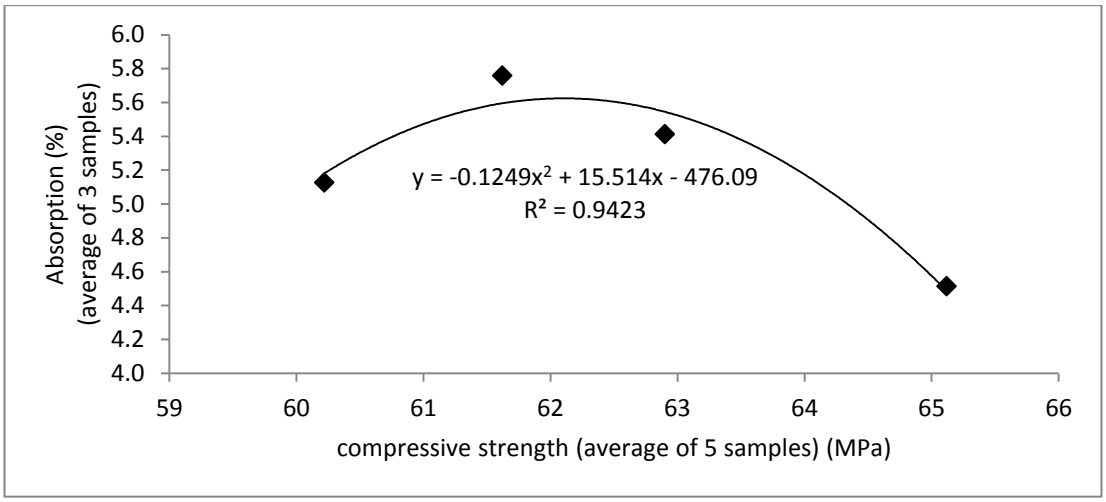

Figure 47: Variation of Absorption with the 28 days Compressive Strength for the concrete mixes

4.12.5 Relationship between Compressive Strength and Voids Content

In order to quantify the variation of voids content of the concrete mixes as a function of 28 days compressive strength; A polynomial (2^{nd} order) regression analysis is chosen from Table 30 depending on R^2. Figure 48 shows the variation of voids content with the 28 days compressive strength for the concrete mixes.

Table 30: Different regression types for the relation between Voids Content and 28 days Compressive Strength

Regression Type	**Equation**	**R^2**
Exponential	$y = 65.45e^{-0.029x}$	0.4303
Linear	$y = -0.2927x + 28.725$	0.4091
Logarithmic	$y = -18.09\ln(x) + 85.229$	0.3976
Polynomial (2^{nd} order)	$y = -0.2239x^2 + 27.799x - 851.62$	0.9581
Power	$y = 19294x^{-1.82}$	0.4186

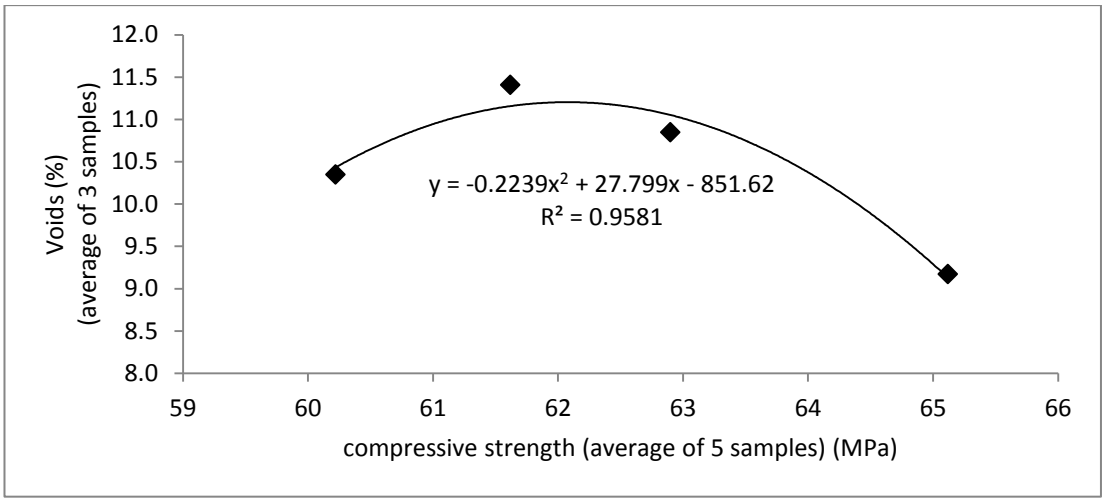

Figure 48: Variation of Voids Content with the 28 days Compressive Strength for the concrete mixes

4.12.6 Relationship between Compressive Strength and Impact Energy

In order to quantify the variation of impact energy (full failure) of the concrete mixes as a function of 28 days compressive strength; a linear regression analysis is chosen from Table 31 depending on R^2. Since there is no big difference between the regression types; a linear regression analysis is chosen since it clearly represents the relation between the results. Figure 49 shows the variation of impact energy (full failure) with the 28 days compressive strength for the concrete mixes; from the figure, a directly proportional relation can be seen. As compressive strength increases, impact energy for full failure increases respectively. On the other hand, it was reported that as compressive increases; the impact resistant decreases (Eren, 1999).

Table 31: Different regression types for the relation between Impact Energy and 28 days Compressive Strength

Regression Type	**Equation**	**R^2**
Exponential	$y = 6E\text{-}07e^{0.3024x}$	0.8587
Linear	$y = 27.108x - 1587.5$	0.9388
Logarithmic	$y = 1703.9\ln(x) - 6938.5$	0.9436
Polynomial (2^{nd} order)	$y = -3.8982x^2 + 516.17x - 16914$	0.9833
Power	$y = 6E\text{-}33x^{19.053}$	0.8670

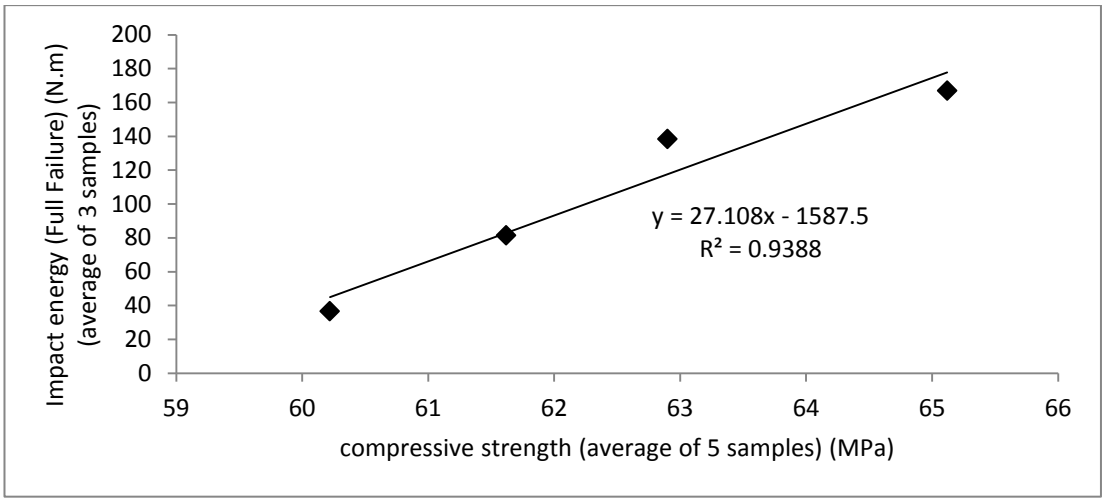

Figure 49: Variation of Impact Energy (full failure) with the 28 days Compressive Strength for the concrete mixes

4.12.7 Relationship between Compressive Strength and Surface Abrasion

Researchers considered the compressive strength as one of the most important factors that are responsible for the abrasion resistance for concrete (Eren, 1999).

In order to quantify the variation of surface abrasion of the concrete mixes as a function of 28 days compressive strength; a linear regression analysis is chosen from Table 32 depending on R^2. Since there is no big difference between the regression types; a linear regression analysis is chosen since it clearly represents the relation between the results. Figure 50 shows the variation of surface abrasion resistance with the 28 days compressive strength for the concrete mixes; from the figure, an inverse relation can be seen. As compressive strength increases, surface abrasion resistance increases respectively. This supports the relation found by Özgür Eren (1999).

Table 32: Different regression types for the relation between Surface Abrasion Resistace and 28 days Compressive Strength

Regression Type	**Equation**	**R^2**
Exponential	$y = 14.028e^{-0.021x}$	0.9736
Linear	$y = -0.0793x + 8.7631$	0.9716
Logarithmic	$y = -4.974\ln(x) + 24.377$	0.9734
Polynomial (2^{nd} order)	$y = 0.0046x^2 - 0.6536x + 26.763$	0.9790
Power	$y = 855.16x^{-1.31}$	0.9752

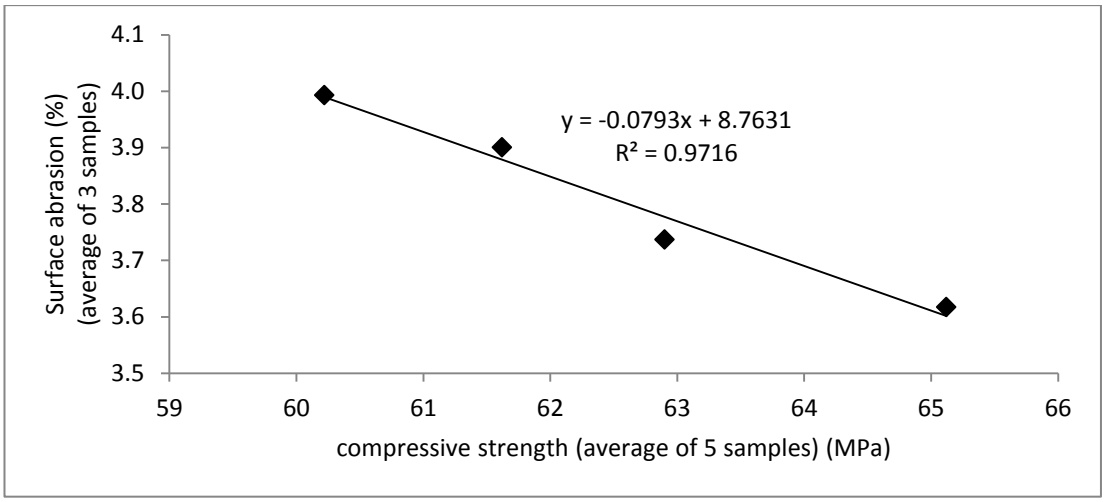

Figure 50: Variation of Surface Abrasion Resistace with the 28 days Compressive Strength for the concrete mixes

4.12.8 Relationship between Chloride Ion Penetration and Depth of Water Penetration

In order to quantify the variation of surface chloride ion penetration of the concrete mixes as a function of depth of water penetration; a linear regression analysis is chosen from Table 33 depending on R^2. A linear regression analysis is chosen since it clearly represents the relation between the results. Figure 51 shows the variation of surface chloride ion penetration of the concrete mixes as a function of depth of water penetration for the concrete mixes; from the figure, a directly proportional relation can be seen.

Table 33: Different regression types for the relation between Chloride Ion Penetration and Depth of Water Penetation

Regression Type	**Equation**	**R^2**
Exponential	$y = 8.3499e^{0.0016x}$	0.9779
Linear	$y = 0.0181x + 8.2178$	0.9599
Logarithmic	$y = 1.4677\ln(x) + 4.7253$	0.8325
Polynomial (2^{nd} order)	$y = 5E\text{-}05x^2 + 0.0024x + 8.5902$	0.9925
Power	$y = 6.0226x^{0.1353}$	0.8824

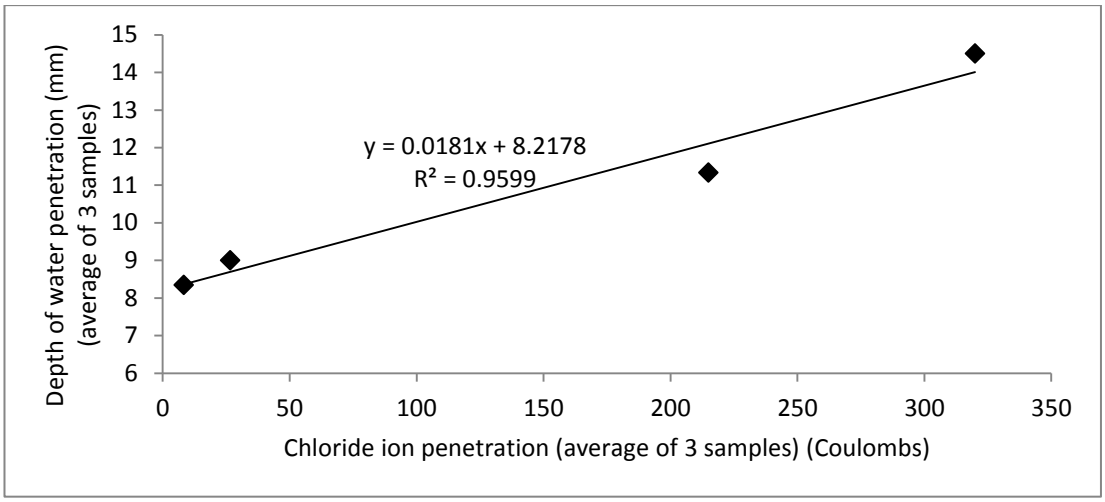

Figure 51: Variation of Chloride Ion Penetration with Depth of Water Penetation for the concrete mixes

4.12.9 Relationship between Chloride Ion Penetration and Absorption

The variation of chloride ion penetration of the concrete mixes as a function of absorption is presented in Table 34 and Figure 52. Since R^2 is not close to 1, which means that the model is not a useful model as it is obvious from the Table 33, it can be said that there is no strong correlation between chloride ion and absorption. Figure 52 shows the variation of chloride ion penetration with absorption for the concrete mixes.

Table 34: Different regression types for the relation between Chloride Ion Penetration and Absorption

Regression Type	**Equation**	**R^2**
Exponential	$y = 5.5416e^{-5E-04x}$	0.4708
Linear	$y = -0.0024x + 5.5393$	0.4582
Logarithmic	$y = -0.132\ln(x) + 5.7488$	0.1884
Polynomial (2^{nd} order)	$y = -3E-05x^2 + 0.0078x + 5.2994$	0.8364
Power	$y = 5.7874x^{-0.027}$	0.1995

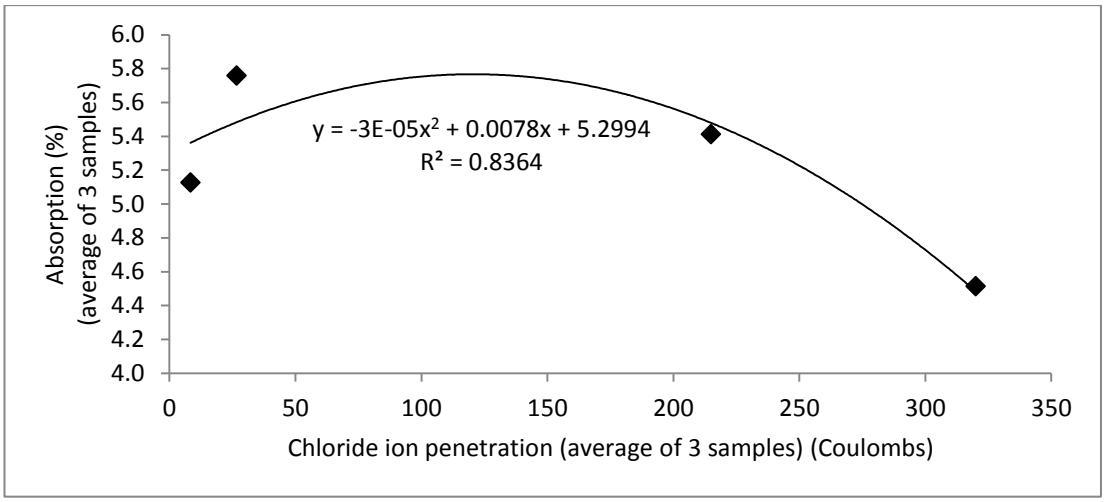

Figure 52: Variation of Chloride Ion Penetration with Absorption for the concrete mixes

4.12.10 Relationship between Chloride Ion Penetration and Voids Content

The variation of chloride ion penetration of the concrete mixes as a function of voids content is presented in Table 35; Since R^2 is not close to 1, which means that the model is not a useful model as it is obvious from the Table 34, it can be said that there is no strong correlation between chloride ion and voids content. Figure 53 shows the variation of chloride ion penetration with voids content for the concrete mixes.

Table 35: Different regression types for the relation between Chloride Ion Penetration and Voids Content

Regression Type	**Equation**	**R^2**
Exponential	$y = 11.067e^{-4E-04x}$	0.4817
Linear	$y = -0.0043x + 11.06$	0.4707
Logarithmic	$y = -0.246\ln(x) + 11.46$	0.1997
Polynomial (2^{nd} order)	$y = -6E-05x^2 + 0.0144x + 10.617$	0.8657
Power	$y = 11.53x^{-0.025}$	0.2099

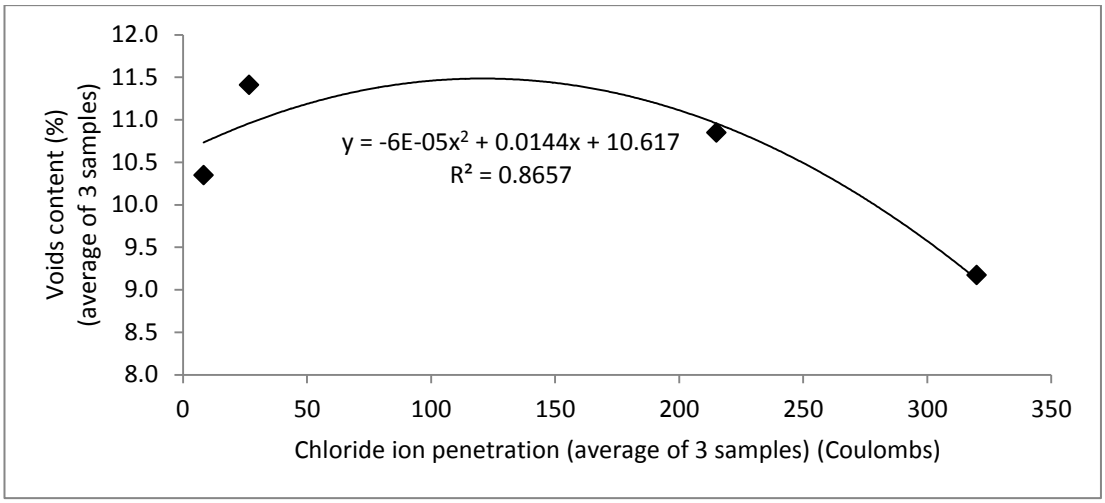

Figure 53: Variation of Chloride Ion Penetration with Voids Content for the concrete mixes

4.12.11 Relationship between Depth of Water Penetration and Absorption

The variation of depth of water penetration of the concrete mixes as a function of absorption is presented in Table 36. Since R^2 is not close to 1, which means that the model is not a useful model as it is obvious from the Table 35, it can be said that there is no correlation between depth of water penetration and absorption. Figure 54 shows the variation of depth of water penetration with absorption for the concrete mixes.

Table 36: Different regression types for the relation between Depth of Water Penetration and Absorption

Regression Type	**Equation**	**R^2**
Exponential	$y = 58.653e^{-0.33x}$	0.4858
Linear	$y = -3.9061x + 31.116$	0.5463
Logarithmic	$y = -20.25\ln(x) + 44.106$	0.5672
Polynomial (2^{nd} order)	$y = 5.2045x^2 - 57.143x + 166.13$	0.6898
Power	$= 176.07x^{-1.711}$	0.5051

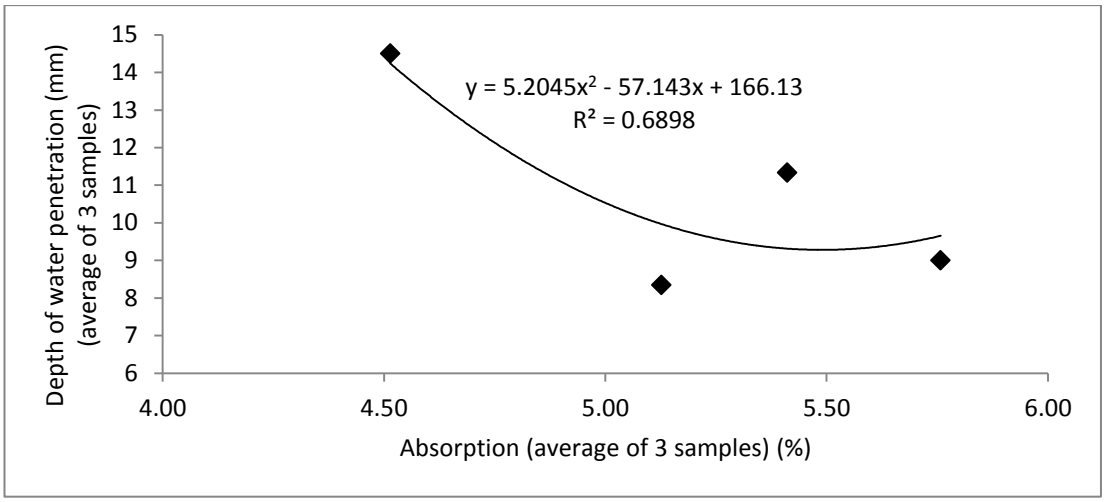

Figure 54: Variation of Depth of Water Penetration with Absorption for the concrete mixes

4.12.12 Relationship between Depth of Water Penetration and Voids Content

The variation of depth of water penetration of the concrete mixes as a function of absorption is presented in Table 37. Since R^2 is not close to 1, which means that the model is not a useful model as it is obvious from the Table 35, it can be said that there is no correlation between depth of water penetration and voids content. Figure 55 shows the variation of depth of water penetration with absorption for the concrete mixes.

Table 37: Different regression types for the relation between Depth of Water Penetration and Voids Content

Regression Type	**Equation**	**R^2**
Exponential	$y = 73.674e^{-0.186x}$	0.5060
Linear	$y = -2.203x + 33.801$	0.5683
Logarithmic	$y = -22.82\ln(x) + 64.255$	0.5863
Polynomial (2^{nd} order)	$y = 1.6198x^2 - 35.382x + 202.53$	0.7060
Power	$y = 969.9x^{-1.93}$	0.5229

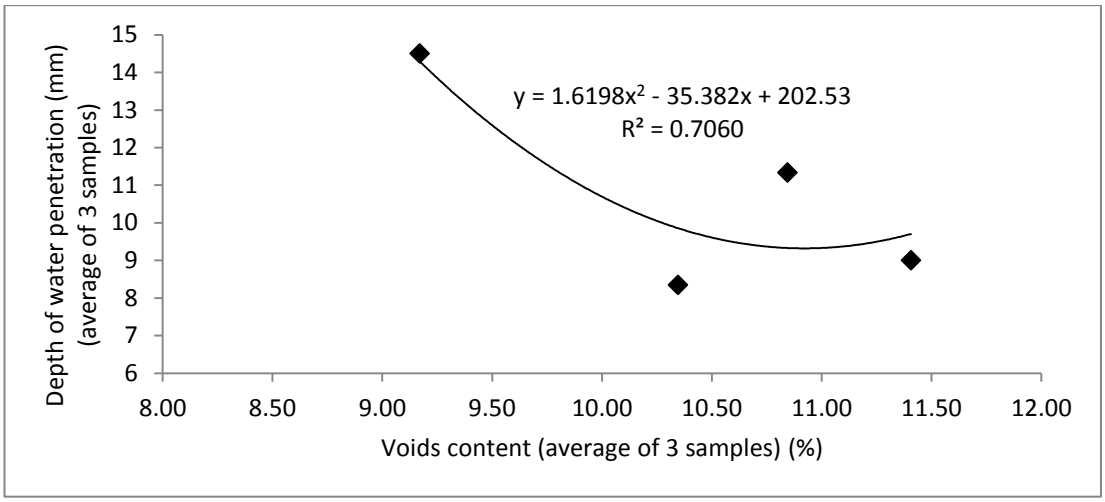

Figure 55: Variation of Depth of Water Penetration with Voids Content for the concrete mixes

4.12.13 Relationship between Voids Content and Absorption

In order to quantify the variation of voids content of the concrete mixes as a function of absorption; a linear regression analysis is chosen from Table 38 depending on R^2. A linear regression analysis is chosen since it clearly represents the relation between the results. Figure 56 shows the variation of voids content of the concrete mixes as a function of absorption for the concrete mixes; from the figure, a directly proportional relation can be seen. As voids content increases, the absorption increases respectively.

Table 38: Different regression types for the relation between Voids Content and Absorption

Regression Type	**Equation**	**R^2**
Exponential	$y = 1.6654e^{0.1087x}$	1.0000
Linear	$y = 0.5525x - 0.5671$	0.9983
Logarithmic	$y = 5.624\ln(x) - 7.9728$	0.9946
Polynomial (2^{nd} order)	$y = 0.0342x^2 - 0.1477x + 2.9939$	1.0000
Power	$y = 0.3868x^{1.1077}$	0.9987

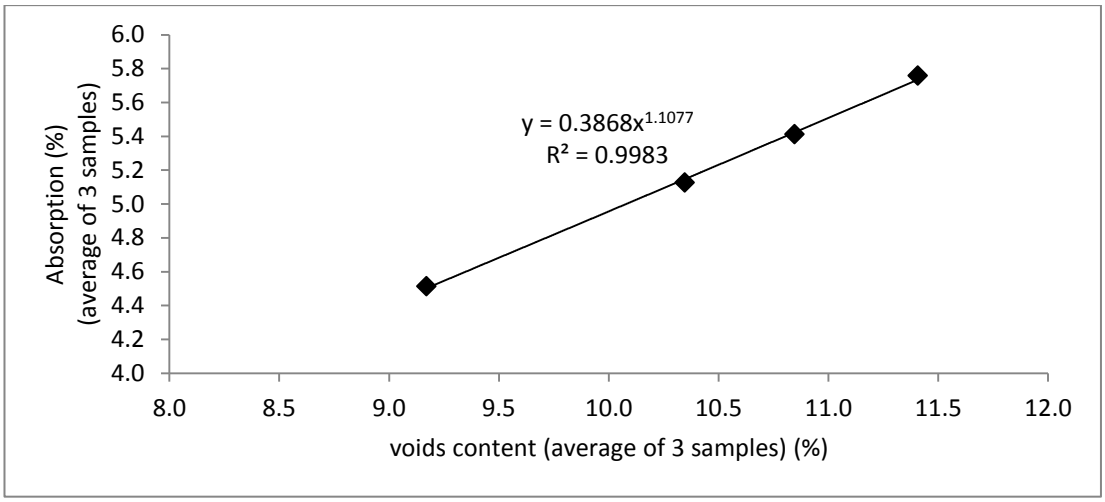

Figure 56: Variation of Voids Content with Absorption for the concrete mixes

4.12.14 Relationship between Surface Abrasion and Impact Energy

In order to quantify the variation of surface abrasion of the concrete mixes as a function of impact energy; a linear regression analysis is chosen from Table 39 depending on R^2. A linear regression analysis is chosen since it clearly represents the relation between the results. Figure 57 shows the variation of surface abrasion of the concrete mixes as a function of impact energy for the concrete mixes; from the figure, an inverse relationship can be seen. As surface abrasion increases, the impact energy decreases respectively.

Table 39: Different regression types for the relation between Surface Abrasion and Impact Energy

Regression Type	**Equation**	**R^2**
Exponential	$y = 2E+08e^{-3.855x}$	0.9024
Linear	$y = -345.1x + 1421.3$	0.9840
Logarithmic	$y = -1310\ln(x) + 1857.5$	0.9806
Polynomial (2^{nd} order)	$y = -446.14x^2 + 3050x - 5028.4$	0.9999
Power	$y = 3E+10x^{-14.6}$	0.8950

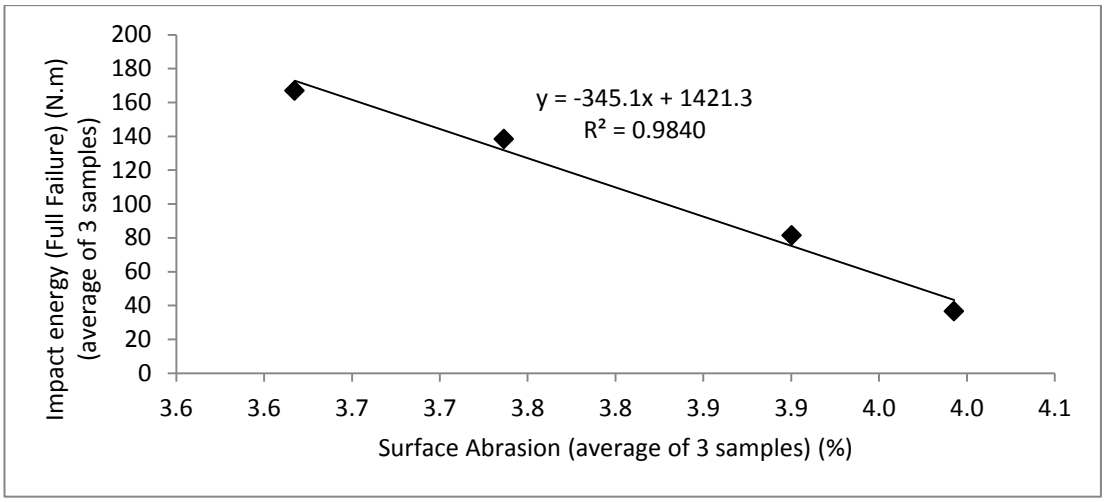

Figure 57: Variation of Surface Abrasion with Impact Energy for the mixes

Chapter 5

CONCLUSION AND RECOMNDATIONS

5.1 Conclusions

In this study various proportions of steel fibers were used to produce fiber reinforced self-compacting concrete. The effect of various proportions of steel fibers on fresh properties such as slump flow, J-ring L-box, V-funnel and column segregation, and on hardened properties such as compressive strength, splitting tensile strength, flexural strength, impact energy, and depth of water penetration, density, absorption, voids content, chloride ion penetration, surface abrasion resistance and ultrasonic pulse velocity tests were examined.

The following conclusions have been reached in the scope of study:

1. For fresh properties: using steel fibers with different proportions decreased the workability such as flowability, passingability. While the use of steel fibers slightly decrease the segregation resistance.
2. For hardened properties: addition of steel fibers improves the compressive strength, splitting tensile strength, impact energy and surface abrasion resistance however there is no clear effect on flexural strength, density, absorption and voids content. On the other hand the addition of fibers increases the depth of water penetration and reduces the chloride ion

resistance. The optimum fiber fraction is 40 kg/m^3 for compressive strength, splitting tensile strength and impact energy tests.

3. A correlation among the results were statistically studied and the followings were found:
    - There is a directly proportional linear regression relationship between compressive strength and splitting tensile Strength.
    - There is a directly proportional linear regression relationship between compressive strength and depth of water penetration.
    - There is a polynomial (2^{nd} order) regression relationship between compressive strength and ultrasonic pulse velocity.
    - There is a polynomial (2^{nd} order) regression relationship between compressive strength and absorption.
    - There is a polynomial (2^{nd} order) regression relationship between compressive strength and voids content.
    - There is a directly proportional linear regression relationship between compressive strength and impact energy.
    - There is an inverse linear regression relationship between compressive strength and surface abrasion resistance.
    - There is a directly proportional relationship between chloride ion penetration and depth of water penetration.
    - There is a directly proportional linear regression relationship between voids content and absorption.
    - There is an inverse linear regression relationship between surface abrasion and impact energy.

5.2 Recommendations

Following parameters are recommended for producing SCC using local aggregates:

Cement:	400 kg/m^3
Silica fume content:	75 kg/m^3
Water/Powder ratio:	0.40
Fine/Coarse aggregates ratio:	1.12
Superplasticizer:	1.25% of cement content

In order to produce FR-SCC; the amount of superplasticizer must be adjusted to achieve the self-compactability properties.

5.3 Suggestions for Future Research

1. This research was done for a maximum of 28 days age for all mechanical properties. Long term properties could be done also.
2. In this study, the w/c ratio was kept constant. In order to see the effect of w/c ratio on fresh and hardened properties on self-compacting concrete and fiber reinforced self-compacting concrete, different w/c ratios could be tried.
3. In this study, silica fume was kept constant. In order to see the effect of silica fume on fresh and hardened properties on self-compacting concrete and fiber reinforced self-compacting concrete, different silica fume amounts could be tried.
4. Other fiber types (carbon, polymer, etc.) could be used for other studies.
5. For further studies such as fire resistance, freeze-thaw resistance and corrosion of steel fibers with different steel fibers percentages and different

silica fume replacement level could be studied for different engineering applications such as highway and dam construction.

6. Supplementary materials such as silica fume, fly ash, slug and limestone dust with different replacement levels can be used to produce SCC to study the affection of these materials on fresh properties, hardened and durability properties.

REFERENCES

ACI 211.1, 1991. *Standard Practice for Selecting Proportions for Normal, Heavyweight and Mass Concrete. Farmington Hills, Michigan*. ACI Committee.

ACI 237, 2007. ACI 237R-07 *Self-Consolidating Concrete*. Farmington Hills: American Concrete Institute.

ACI 544.1, 1996. *Fiber Reinforced Concrete*. ACI Committee.

ACI 544.4, 1988. *Design Consideration for Steel Fiber Reinforced Concrete*. ACI Committee.

ACI 544, 1978. Measurement of Properties of Fiber Reinforced Concrete. *ACI Journal*, pp.283 - 289.

Aggarwal, P., Siddique, R., Aggarwal, Y. & Gupta, S.M., 2008. Self-compacting concrete - procedure for Mix Design. *Leonardo Electronic Journal of Practices and Technologies*, pp.15-24.

Association Francaise de Genie Civil, 2000. *Betons Auto-Placants-Recommandations Provisoires*. France.

ASTM 1621, 2006. *Passing Ability of Self-Consolidating Concrete by J-Ring*. West Conshohocken, USA: ASTM International.

ASTM C 117, 2004. *Materials finer than (No. 200) sieve in mineral aggregates by washing*. American Society for Testing and Materials.

ASTM C 1202, 2010. *Electrical Indication of Concrete's Ability to Resist Chloride Ion Penetration*. American Society for Testing and Materials.

ASTM C 127, 2007. *Density, Relative Density (Specific Gravity), and Absorption of Coarse Aggregate*. American Society for Testing and Materials.

ASTM C 128, 2007. *Density, Relative Density (Specific Gravity), and Absorption of Fine Aggregate*. American Society for Testing and Materials.

ASTM C 1609, 2010. *Flexural Performance of Fiber-Reinforced Concrete (Using Beam With Third-Point Loading)*. American Society for Testing and Materials.

ASTM C 1610, 2006. *Static Segregation of Self-Consolidating Concrete using column technique*. West Conshohocken: ASTM Intenational.

ASTM C 1611, 2005. *Slump Flow of Self-Consolidating Concrete*. West Conshohocken, USA: ASTM International.

ASTM C 33, 2008. *Concrete Aggregates*. American Society for Testing and Materials.

ASTM C 496, 2004. *Splitting Tensile Strength of Cylindrical Concrete Specimens*. American Society for Testing and Materials.

ASTM C 597, 2009. *Pulse Velocity Through Concrete*. American Society for Testing and Materials.

ASTM C 642, 2006. *Density, Absorption, and Voids in Hardened Concrete*. American Society for Testing and Materials.

Bartos, P.J.M., Sonebi, M. & A.K., T., 2002. *Workability and rheology of Fresh Concrete: Compendium of Tests*. Paris: RILEM Committee TS-145-WSM.

BE96-3801, 1996. *Rational Production and Improved Working Environment Through Using Self-Compacting Concrete*. European Union, DG XII.

BE96-3801, 2000. *Quality Control Report on SCC*. European Union, DG XII.

BE96-3801, 2000. *Rational Production and Improved Working Environment Through Using Self-Compacting Concrete*. European Union, DG XII.

BS EN 12390-2, 2000. *Testing hardened concrete - Part 2: Making and curing specimens for strength tests*. British European Standards.

BS EN 12390-3, 2002. *Testing hardened concrete - Part 3: Compressive strength of test specimens*. British European Standards.

BS EN 12390-8, 2009. *Testing hardened concrete - Part 8 : Depth of penetration of water under pressure*. British European Standards.

Bui Khanh, V. & Montgomery, D., 1999. Drying shrinkage of self compacting concrete containing milled limeston. In *The 1st international RILEM Symposum on self compacting concrete*. Stockholm, Sweden, 1999. RILEM.

Byun, K.J., Kim, J.K. & Song, H.W., 1998. Self-Compacting Concrete in Korea. In *International Workshop on Self-Compacting Concrete*. Kochi, Japan, 1998.

Chanh, N.V., 2005. *Steel Fiber Reinforced Concrete*. Japan: Japan Society of Civil Engineers.

Chih-Ta, T., Lung-Sheng, L., Chien-Chih, C. & Chao-Lung Hwang, 2009. *Durability Design and Application of Steel Fiber Reinforced Concrete in Taiwan*, 34(1B).

Collepardi, M., 2003. Self-Compacting Concrete: What is New? In *The 7th Canmet/ACI International Conference on Superplastisizers and Other Chemical Admixtures in Concrete*. Berlin, Germany, 2003.

Cunha, V.M.C.F., Barros, J.A.O. & Sena-Cruz, J., 2008. Modelling the influence of age of steel fibre reinforced self-compacting concrete on its compressive behaviour. *Materials and Structures, vol. 41,* pp.465 - 478.

Daczko, J.A. & Kurtz, M.A., 2001. Development of high-volume coarse aggregate SCC. In *The 2nd international symposium on SCC*. Tokyo, Japan, 2001.

Daczko, J.A. & Vachon, M., 2006. Self-Consolidating Concrete. pp.637-45.

De Schutter, G., 2005. *Guidelines for testing fresh self-compacting concrete*. European Research Center (Testing SCC).

EFNARC, 2002. *Specifications and Guidelines for Self-Compacting Concrete*. Surrey, UK.

El-Dieb, A.S., 2009. Mechanical, durability and microstructural characteristics of ultra-high-strength self-compacting concrete incorporating steel fibers. *Materials and Design,* pp.4286 - 4292.

Eren, O., 1999. *PhD Thesis, Various Properties of High Strength Fiber Reinforced Concrete*. Gazimagusa: EMU.

Felekoğlu, Türkela, S. & Baradana, B., 2007. Effect of water/cement ratio on the fresh and hardened properties of self-compacting concrete. *Building and Environment, vol. 42,* pp.1795-802.

Ferrara, L., Park, Y.-D. & Shah, S.P., 2007. A method for mix-design of fiber-reinforced self-compacting concrete. *Cement and Concrete Research*, pp.957 - 971.

Gaimster, R. & Dixon, N., 2003. Self compacting concrete. In Newman, J. & Choo, B.S. *Advanced Concrete Technology*. Great Britaine: Butterworth-Heinemann. pp.9/1 - 9/23.

Gambhir, M.L., 1990. *Concrete Technology*. New Delhi: TATA McGrow Hill Ltd.

Grünewald, S. & Walraven, J.C., 2001. Parameter-study on the influence of steel fibers and coarse aggregate content on the fresh properties of self-compacting concrete. *Cement and Concrete Research*, pp.1793-98.

Hannant, D.J., 1978. *Fiber Cements and Fiber Concretes*. Chichester, United Kingdom: John Wiley and Sons Ltd.

Illston, J.M. & Domone, P.L.J., eds., 2001. *Construction Materials*. London: Spon Press.

Jacobs, F. & Hunkeler, F., 2001. SCC for the Rehabilitation of a Tunnel in Zurich / Switzerland. In Ozawa, K. & Ouchi, M., eds. *The 2nd International Symposium on SCC*., 2001.

Jones , R. & Gatfield, E., 1955. Testing concrete by an ultrasonic pulse technique. *DSIR Road Research Technical Paper No. 34 (London, H.M.S.O)*.

Jones, J., 2010. *One-Way ANOVA*. [Online] Available at: http://people.richland.edu/james/lecture/m170/ch13-1wy.html [Accessed 01 August 2010].

Khayat, K.H. & Aitcin, P.C., 1998. In *Use of Self-Consolidating in Canada - Present Situation and Perspectives*. Kochi, Japan, 1998. International Workshop on Self-Compacting Concrete.

Khayat, K.H. & Morin, R., 2002. In *Performance of Self-Consolidating Concrete Used to Repare Parapet Wall in Montreal*. Chicago, 2002. The 1st North-American Conference on the Design and Use of the SCC.

Kordts, S. & Grube, H., 2003. Controlling the workability properties of self compacting concrete used as ready-mixed concrete. *Beton*, pp.103-12.

Marar, K., 2000. *PhD Thesis, The Effect of Steel Fibers on Some Properties of Normal and High Strength Concrete*. gazimagusa: EMU.

Miao, B., Chern, J.-C. & Yang, C.-A., 2003. Influences of Fiber Content on Properties of Self-Compacting Steel Fiber Reinforced Concrete. *Journal of the Chinese Institute of Engineers*, 26(4), pp.523 - 530.

Montgomery, D.C., 2001. *Design and Analysis of Experiments*. New York: John Wiley & Sons, INC.

Neville, A.M. & Brooks, J.J., 2008. *Concrete Technology*. Pearson.

Okamura & Ouchi, 1999. Self-Compacting Concrete Development, Present Use and Future. In *1st International RILEM Symposium on self-compacting concrete*. Paris, 1999. RILEM.

Okamura, H. & Ouchi, M., 2003. Self-Compacting Concrete. *Journal of Advanced Concrete Technology*, pp.5-15.

Ouchi, M., 1998. History of Development and Applications of Self-Compacting Concrete in Japan. In *International Workshop on Self-Compacting Concrete*. Kochi, 1998.

Ouchi, M., Hibino, M., Ozawa, K. & Okamura, H., 1998. A ratonal mix design method for mortar in self compacting concrete. In *The sixth South-East Asia Pasific Confrence of Structural Engineering and Construction*. Taipie, Taiwan, 1998.

Ozawa, K., Maekawa, K., Kunishima, M. & Okamura, H., 1989. Development of High Performance Concrete Based on the Durability Design of Concrete Structures. In *The 2nd East-Asia and Pacific Conference on Structural Engineering and Constuction (EASEC2)*. Chiang-Mai, 1989.

Ozbay, E., Oztas, A., Baykasoglu, A. & Ozbebek, H., 2009. Investigating mix proportions of high strength self compacting concrete by using Taguchi method. *Construction and Building Materials*, p.694–702.

RILEM 174-SCC, 2000. *Self-Compacting Concrete*. France: RILEM Publlications.

Rougeau, P., Maillard, J.L. & Mary-Dippe, C., 1999. Comparative study on properties of sels compacting and high performance concrete used in precast construction. In *The 1st international RILEM Symposum on self compacting concrete*. Paris, 1999. RILEM.

Sengul, C., Akkaya, Y. & Tasdemir, M.A., 2006. Fracture Behavior of High Performance Fiber Reinforced Self Compacting Concrete. *Measuring, Monitoring and Modeling Concrete Properties*, pp.171 - 177.

Shetty, M.S., 2005. *Concrete technology - theory and practice*. New Delhi, India: Chand & company Ltd.

SIKA, 2006. *Sika ViscoCrete Hi-Tech 32*. [Online] Available at: www.sika.com.tr [Accessed 10 May 2010].

Skarendahl, A., 1998. Self-Compacting Concrete in Sweden. Research and Application. In *International Workshop on Self-Compacting Concrete*. Kochi, Japan, 1998.

Somayaji, S., 2001. *Civil Engineering Materials*. New Jersey: Prentice Hall.

Sonebi, M. & Batros, P.J.M., 1999. Hardened SCC and its bond with reinforcement. In *The 1st International Symposium of SCC*. Stockholm, 1999. RILEM.

Swamy, N.R., 1975. *Fiber Reinforced of Cement and Concrete*.

Swamy, R.N. & Stavrides, H., 1979. *Influence of Fiber Reinforced on Restrained Shrinkage and Cracking*, 76(3), pp.443 - 460.

Tang, L., Andalen, A., Johnsson, J.O. & Hjelm, S., 1999. Chloride diffusivity of self compacting concrete. In *The 1st international RILEM Symposum on self compacting concrete*. Paris, 1999. RILEM.

Tangtermsirikul, S., 1998. Design and Construction of Self-Compacting Concrete in Thiland. In *International Workshop on Self-Compacting Concrete*. Kochi, Japan, 1998.

Taylor, G.D., 1991. *Construction Materials*. Singapore: Longman Sientific & Technical.

Torrijos, Barragán, B.E. & Zerbino, R.L., 2007. Physical–mechanical properties, and mesostructure of plain and fibre reinforced self-compacting concrete. *Construction and Building Materials*, pp.1780 - 1788.

Vachon, M. & Daczko, J., 2002. U.S. Regulatory Work on SCC. In *First North American Conference on the Design and Use of Self-Consolidating Concrete*. Evanston, 2002.

Walraven, J., 1998. The Development of Self-Compacting Concrete in Netherlands. In *International Workshop on Self-Compacting Concrete*. Kochi, Japan, 1998.

Walraven, 2003. Structural aspects of self-compacting concrete. In *The 3rd International Symposium on SCC*. Reykjavik, Iceland, 2003.

Whitehurst, 1951. Soniscope tests concrete structures. *J Am Concrete Inst 443–4*..

APPENDICES

Appendix A: One-way ANOVA

A One-Way Analysis of Variance is a way to test the equality of three or more means at one time by using variances.

Assumptions

- The populations from which the samples were obtained must be normally or approximately normally distributed.
- The samples must be independent.
- The variances of the populations must be equal.

Hypotheses

The null hypothesis will be that all population means are equal; the alternative hypothesis is that at least one mean is different.

In the following, lower case letters apply to the individual samples and capital letters apply to the entire set collectively. That is, n is one of many sample sizes, but N is the total sample size.

Grand Mean

The grand mean of a set of samples is the total of all the data values divided by the total sample size. This requires that to have all of the sample data available, which is usually the case, but not always. It turns out that all that is necessary to find perform a one-way analysis of variance are the number of samples, the sample means, the sample variances, and the sample sizes.

$$\bar{X}_{GM} = \frac{\sum x}{N}$$

Another way to find the grand mean is to find the weighted average of the sample means. The weight applied is the sample size.

$$\bar{X}_{GM} = \frac{\sum n\bar{x}}{\sum n}$$

Total Variation

The total variation (not variance) is comprised the sum of the squares of the differences of each mean with the grand mean.

$$SS(T) = \sum (x - \bar{X}_{GM})^2$$

There is the between group variation and the within group variation. The whole idea behind the analysis of variance is to compare the ratio of between group variance to within group variance. If the variance caused by the interaction between the samples is much larger when compared to the variance that appears within each group, then it is because the means are not the same.

Between Group Variation

The variation due to the interaction between the samples is denoted SS (B) for Sum of Squares Between groups. If the sample means are close to each other (and therefore the Grand Mean) this will be small. There are k samples involved with one data value for each sample (the sample mean), so there are k-1 degrees of freedom.

$$SS(B) = \sum n(\bar{x} - \bar{X}_{GM})^2$$

The variance due to the interaction between the samples is denoted MS (B) for Mean Square Between groups. This is the between group variation divided by its degrees of freedom. It is also denoted by S_B^2.

Within Group Variation

The variation due to differences within individual samples denoted SS (W) for Sum of Squares Within groups. Each sample is considered independently, no interaction between samples is involved. The degree of freedom is equal to the sum of the individual degrees of freedom for each sample. Since each sample has degrees of freedom equal to one less than their sample sizes, and there are k samples, the total degrees of freedom is k less than the total sample size: df = N - k.

$$SS(w) = \sum df.s^2$$

The variance due to the differences within individual samples is denoted MS (W) for Mean Square Within groups. This is the within group variation divided by its degrees of freedom. It is also denoted by S_w^2. It is the weighted average of the variances (weighted with the degrees of freedom).

F test statistic

Recall that an F variable is the ratio of two independent chi-square variables divided by their respective degrees of freedom. Also recall that the F test statistic is the ratio of two sample variances, well, it turns out that's exactly what we have here. The F test statistic is found by dividing the between group variance by the within group variance. The degrees of freedom for the numerator are the degrees of freedom for the between group (k-1) and the degrees of freedom for the denominator are the degrees of freedom for the within group (N-k).

$$F = \frac{S_b^2}{S_w^2}$$

Summary Table

Table 40: Summary of ANOVA

	SS	**df**	**MS**	**F**
Between	SS(B)	k-1	$\frac{SS(B)}{k-1}$	$\frac{MS(B)}{MS(W)}$
Within	SS(W)	N-k	$\frac{SS(W)}{N-k}$	.

Notice that each Mean Square is just the Sum of Squares divided by its degrees of freedom, and the F value is the ratio of the mean squares. Largest variance cannot be used in the numerator, always divide the between variance by the within variance. If the between variance is smaller than the within variance, then the means are really close to each other and then it is not possible to reject the claim that they are all

equal. The degrees of freedom of the F-test are in the same order they appear in Table 40.

Decision Rule

The decision will be to reject the null hypothesis if the test statistic from the table is greater than the F critical value with k-1 numerator and N-k denominator degrees of freedom.

If the decision is to reject the null, then at least one of the means is different. However, the ANOVA does not tell where the difference lies.

Source: (Jones, 2010)

Appendix B: Statistical Measures

Regression analysis investigates the relations between two or more quantitative statistical attributes. Regression analysis is statistical procedure can be used to develop a mathematical equation showing how variable are related. The symbol used for regression analysis is R^2 (where $0 \leq R^2 \leq 1$). R^2 values close to 1 would imply that the model is explaining most of the variation in the depended variable and may be a very useful model. R^2 values close to 0 would imply that the model is explaining little of the variation in the depended variable and may not be a very useful model.

Standard deviation (sd) measures the spread of the data about the mean value. It is useful in comparing sets of data which may have the same mean but a different range. For example, the mean of the following two is the same: 15, 15, 15, 14, 16 and 2, 7, 14, 22, 30. However, the second is clearly more spread out. If a set has a low standard deviation, the values are not spread out too much.

Mean, in statistics, is the mathematical simple average of a set of numbers. The simple average is calculated by adding up two or more scores and dividing the total by the number of scores. Consider the following number set: 2, 4, 6, 9, and 12. The average is calculated in the following manner: 2 + 4 + 6 + 9 + 12 = 33 / 5 = 6.6. So the average of the number set is 6.6.